

# SHARP ILL-POSEDNESS OF THE EULER EQUATIONS IN LORENTZ SPACES

JEAHEANG BANG AND ALEXEY CHESKIDOV

**ABSTRACT.** We study vortex stretching for the three-dimensional axisymmetric Euler equations without swirl in vorticity formulation. Danchin [Dan07a] established global existence and uniqueness for bounded vorticity  $\omega_0$  provided  $\omega_0/r$  lies in the endpoint Lorentz space  $L^{3,1}(\mathbb{R}^3)$  (together with a decay assumption on  $\omega_0$ ). We prove that this  $L^{3,1}$  endpoint is sharp: for every Lorentz exponent  $q > 1$ , we construct multi-ring data  $\omega_0 \in L^\infty(\mathbb{R}^3)$  with  $\omega_0/r \in L^{3,q}(\mathbb{R}^3)$  that produce  $L^\infty$ -norm inflation of the vorticity; moreover, within the same class, we obtain instantaneous blow-up from data with infinitely many rings.

Our initial data are inspired by the Kim–Jeong dyadic ring superposition [KJ22], but we crucially generalize it by allowing flexible conical support geometry for the ring profile. In the regime where outer rings are dominant—a multiscale viewpoint appearing in recent works including [KJ22, CMZ25]—we obtain a forward-in-time ODE cascade for ring amplitudes and aspect ratios in which vortex stretching weakens its own future forcing: as a ring amplifies, incompressibility flattens it, the aspect ratio collapses, and the induced stretching coefficient is geometrically depleted. A key new ingredient is a profile-localization argument that freezes the relevant Biot–Savart kernel and makes this depletion explicit, enabling us to exploit a monotone “productive window” (controlled by the cone slope) together with an exact cascade identity. This propagates stretching across scales and gives a robust lower bound on cumulative stretching, yielding ill-posedness in the full range  $q > 1$ .

## CONTENTS

1. Introduction	2
1.1. A Global Estimate in Lorentz Spaces	3
1.2. Worst-Case Singular Geometry in $L^{3,q}$	4
1.3. Ill-Posedness Beyond Danchin’s Regime	5
1.4. Geometric Self-Slowdown Mechanism	6
1.5. Kim–Jeong’s Ill-Posedness for Large $q$	7
1.6. Initial Data and Main Results	8
1.7. Framework: Dominant Outer-Rings and ODE Reduction	12
1.8. Main Idea: Evolution of the Stretching Rate $S_k$ and Front-Migration	14
1.9. Scale Separation and Stability of the Profiles	22
1.10. Instantaneous Blow-Up	23
1.11. Comparison with the Córdoba–Martinez–Zoroa–Zheng Construction	25
1.12. Hölder Spaces	30
1.13. Notation Conventions	31
1.14. Outline of the Paper	32
2. Cone-Free Outer-Region Dominance	33
3. Norm Inflation	39
3.1. Initial Data and Ansatz	39

3.2. Roadmap of a Bootstrap Argument	41
3.3. Cauchy Formula and Freezing the Profiles	42
3.4. Study of ODEs	44
3.5. A bootstrap Argument	52
3.6. Norm inflation and Proof of Theorem 1.1	57
4. Instantaneous blow-up	58
4.1. Preliminary Lemmas for Instantaneous Blow-Up	58
4.2. Proof of Theorem 1.2-(1)	66
4.3. Proof of Theorem 1.2-(2)	76
Appendix A. Proof of the Danskin-type lemma and the Cauchy formula	82
Appendix B. ODE Models	89
B.1. Sharp Dichotomy for the Flattened-Coefficient ODEs	90
B.2. Frozen-Profile ODEs	91
Appendix C. List of notation	93
Acknowledgements	97
References	97

## 1. INTRODUCTION

Consider the initial value problem of the incompressible Euler equations in  $\mathbb{R}^3$ :

$$\begin{cases} \partial_t u + u \cdot \nabla u + \nabla p = 0, & \operatorname{div} u = 0 \\ u(x, 0) = u_0(x). \end{cases} \quad (1)$$

Equivalently, one can also consider its vorticity formulation:

$$\begin{cases} \partial_t \omega + u \cdot \nabla \omega = \omega \cdot \nabla u, \\ \omega(x, 0) = \omega_0(x) \end{cases} \quad (2)$$

Here,  $u$  is determined by the Biot–Savart law:  $u = (-\Delta)^{-1} \operatorname{curl} \omega$ , that is,

$$u(x) = \frac{1}{4\pi} \int_{\mathbb{R}^3} \frac{\omega(y) \times (x - y)}{|x - y|^3} dy. \quad (3)$$

See our sign convention related to the Biot–Savart law in Appendix C.

Well-posedness and ill-posedness of the Euler equations have long been central topics in mathematical fluid mechanics. Advection tends to mix the flow, while the vortex stretching mechanism can amplify vorticity. The interplay between these two effects plays a crucial role in the analysis of well-posedness and ill-posedness.

In two dimensions, vortex stretching is absent, and the vorticity is purely transported along particle trajectories. As a consequence, the  $L^\infty$  norm of the vorticity is conserved in time. Although the condition  $\omega \in L^\infty$  only yields log-Lipschitz continuity of the velocity field  $u$ , this regularity is sufficient to define the Lagrangian flow map  $Y(x, t)$  through

$$\frac{\partial}{\partial t} Y(x, t) = u(Y(x, t), t), \quad Y(x, 0) = x.$$

This observation underlies Yudovich theory [Yud63], which establishes global existence and uniqueness of solutions for initial vorticity  $\omega_0 \in L^\infty(\mathbb{R}^2)$  under a mild decay condition at infinity.

This global result shows that, although the formation of small scales is not excluded—since no assumption is imposed on the vorticity gradient—the sole boundedness of the initial vorticity is sufficient to ensure global well-defined Lagrangian dynamics.

On the other hand, in three dimensions, the presence of vortex stretching fundamentally alters the dynamics and renders the extension of Yudovich theory highly nontrivial. In general, the amplification of vorticity induced by stretching may lead to loss of regularity, even for initially smooth flows. However, in the special class of axisymmetric flows without swirl, the structure of the vorticity equation simplifies significantly:

$$\partial_t \omega + u^r \partial_r \omega + u^z \partial_z \omega = \omega \frac{u^r}{r}. \quad (4)$$

By abuse of notation, here  $\omega$  still denotes a scalar quantity defined by

$$\operatorname{curl} u = \omega e_\theta,$$

where  $e_\theta = e_z \times e_r$ , and  $\theta$  denotes the angular variable in cylindrical coordinates.

In addition, we will identify meridional  $(r, z)$ -functions, such as  $\omega(r, z)$ , with their axisymmetric lifts to  $\mathbb{R}^3$ . The axisymmetric Biot–Savart law reads as follows.

$$\begin{aligned} u^r(x) &= \frac{1}{4\pi} \int_{\mathbb{R}^3} \frac{(z_x - z_y) \cos(\theta_x - \theta_y)}{|x - y|^3} \omega(y) dy, \\ u^z(x) &= -\frac{1}{4\pi} \int_{\mathbb{R}^3} \frac{r_x \cos(\theta_x - \theta_y) - r_y}{|x - y|^3} \omega(y) dy, \end{aligned} \quad (5)$$

where  $(r_x, \theta_x, z_x)$  denotes cylindrical coordinates of  $x$ . We call  $u^r/r$ , that appears on the right-hand side of the equation, *vortex stretching rate*. See our sign convention related to the Biot–Savart law in Appendix C.

**1.1. A Global Estimate in Lorentz Spaces.** For the axisymmetric flows without swirl, the vorticity equation (4) can be re-written as

$$\partial_t \left( \frac{\omega}{r} \right) + u^r \partial_r \left( \frac{\omega}{r} \right) + u^z \partial_z \left( \frac{\omega}{r} \right) = 0. \quad (6)$$

Hence, the so-called relative vorticity  $\omega/r$  is transported along particle trajectories. This partial suppression of vortex stretching makes the axisymmetric, no-swirl case the closest three-dimensional analogue of the two-dimensional case.

Motivated by Yudovich theory, one may attempt to establish a *global* well-posedness result in this setting under a minimal additional assumption controlling vortex stretching. Since  $\omega/r$  is conserved along the flow, it is natural to impose an assumption on the initial quantity  $\omega_0/r$ . From a scaling perspective, the condition  $\omega_0/r \in L^{3,q}(\mathbb{R}^3)$  for  $q \geq 1$  has the same homogeneity as the main assumption  $\omega_0 \in L^\infty(\mathbb{R}^3)$ .

Moreover, like the  $L^\infty$  condition in Yudovich theory, such a Lorentz-space assumption does not impose any explicit Sobolev or Hölder regularity on the vorticity. While the condition  $\omega_0/r \in L^{3,q}$  in fact does enforce a mild constraint near the symmetry axis, it remains a borderline assumption that does not directly control vorticity gradients. (A detailed discussion about possible singular behaviors in this class can be found in the next section 1.2.) Thus, the family of Lorentz spaces  $L^{3,q}$  provides a natural class in which to seek a Yudovich-type global result. Now, the central question is whether such a condition is sufficient to control the vortex stretching rate  $u^r/r$ .

To answer this question, one observes that  $\omega/r$  and  $u^r/r$  behave as if they are related by the singular kernel  $|x|^{-2}$ . Since this kernel belongs to the Lorentz space  $L^{\frac{3}{2},\infty}(\mathbb{R}^3)$ , one obtains the

estimate

$$\left\| \frac{u^r}{r} \right\|_{L^\infty(\mathbb{R}^3)} \leq C \left\| \frac{\omega}{r} \right\|_{L^{3,1}(\mathbb{R}^3)} \left\| \frac{1}{|x|^2} \right\|_{L^{\frac{3}{2},\infty}(\mathbb{R}^3)} \leq C \left\| \frac{\omega}{r} \right\|_{L^{3,1}(\mathbb{R}^3)}. \quad (7)$$

Here, among the Lorentz spaces  $L^{3,q}$ ,  $q \geq 1$ , the space  $L^{3,1}$  arises naturally from duality, since  $(L^{3,1})^* = L^{\frac{3}{2},\infty}$ .

If  $\omega_0/r \in L^{3,1}(\mathbb{R}^3)$ , then the Lorentz norm of  $\omega/r$  is conserved in time, and the estimate (7) yields a uniform-in-time bound on the vortex stretching rate  $u^r/r$ . This observation explains the main heuristic behind Danchin's global existence result. More precisely, Danchin proved global existence and uniqueness of solutions under the assumptions

$$\omega_0 \in L^\infty(\mathbb{R}^3) \cap L^{3,1}(\mathbb{R}^3), \quad \frac{\omega_0}{r} \in L^{3,1}(\mathbb{R}^3). \quad (8)$$

The additional condition  $\omega_0 \in L^{3,1}(\mathbb{R}^3)$  ensures sufficient decay at infinity; see [Ser95, SR01, SY94, AHK10] for related results in various settings.

In contrast to the two-dimensional case, the additional Lorentz condition  $\omega_0/r \in L^{3,1}(\mathbb{R}^3)$  in (8) is needed to control the stretching mechanism. However, the assumption  $\omega_0/r \in L^{3,1}(\mathbb{R}^3)$  is weak in the sense that it has the same scaling as the primary boundedness condition  $\omega_0 \in L^\infty(\mathbb{R}^3)$ . Moreover, the main estimate (7) fails if  $L^{3,1}$  is replaced by  $L^{3,q}$  for any  $q > 1$ . For this reason, Danchin's result is regarded as a sharp extension of Yudovich theory to the three-dimensional axisymmetric no-swirl setting.

**1.2. Worst-Case Singular Geometry in  $L^{3,q}$ .** More precisely, Danchin's result is expected to be sharp in the sense that if one instead considers Lorentz spaces  $L^{3,q}(\mathbb{R}^3)$  for any  $q > 1$  in (8), then ill-posedness might occur; see [LJ25, p. 32, footnote 3].

To investigate this ill-posedness, let us consider a worst-case scenario in the class

$$\omega_0 \in L^\infty(\mathbb{R}^3), \quad \frac{\omega_0}{r} \in L^{3,q}(\mathbb{R}^3),$$

for a fixed  $q > 1$  (together with a decay condition at infinity).

First, any potentially singular behavior is strongest when it is concentrated on the  $z$ -axis. Otherwise, it does not contribute to amplifying the vortex stretching in view of Danchin's result. In addition, if the singularity is uniformly distributed along the  $z$ -axis, then the Lorentz condition in (8) forces  $\omega$  to be Hölder continuous along the axis; in that case one has a classical local well-posedness theory (explained below). Hence, it is natural to consider a *singularity concentrated at a point* on the axis, say the origin  $(r, z) = (0, 0)$ .

In addition, since  $\omega/r$  is conserved along particle trajectories, outward radial motion of a fluid particle amplifies the vorticity. This suggests considering flows that are *odd in  $z$*  such that

$$\omega(r, z) \leq 0 \quad \text{when } z > 0.$$

In this case,  $\omega_0/r$  should behave like a typical example of a singular function that barely belongs to  $L_{\text{loc}}^{3,q}(\mathbb{R}^3)$ :

$$\frac{\omega_0}{r} \sim -\frac{1}{|x|} \frac{1}{\log^\alpha(1/|x|)} \text{sgn}(z), \quad \text{that is,} \quad \omega_0 \sim -\frac{r}{|x|} \frac{1}{\log^\alpha(1/|x|)} \text{sgn}(z),$$

where  $\alpha q > 1$ .

Near the origin, one expects  $u_0^r(r, z) \approx r \partial_r u_0^r(0, 0)$  (using that  $u_0^r(0, 0) = 0$  and  $\partial_z u_0^r(0, 0) = 0$  due to the axisymmetry). Therefore, one can approximate the initial vortex stretching rate  $u_0^r/r$

via the Biot–Savart law as follows:

$$\begin{aligned} \frac{u_0^r(r, z)}{r} &\approx \partial_r u_0^r(0, 0) = C \iint \frac{r^2 z}{(r^2 + z^2)^{5/2}} (-\omega_0(r, z)) dr dz \\ &\sim C \iint_{r \sim |z|} \frac{r^2 z}{(r^2 + z^2)^{5/2}} (-\omega_0(r, z)) dr dz \geq 0. \end{aligned} \quad (9)$$

Here, the kernel carries factors  $r^2$  and  $z$ , so the dominant contribution near the origin comes from the region where  $r$  and  $|z|$  are comparable. Restricting to  $r \sim |z|$  therefore still captures the worst singular behavior.

Consequently, we focus on the region  $r \sim |z|$ , in which

$$\omega_0 \sim -\frac{1}{\log^\alpha(1/|x|)} \operatorname{sgn}(z). \quad (10)$$

This provides a simple worst-case scenario in the class  $\omega_0/r \in L^{3,q}(\mathbb{R}^3)$ . Note that if  $q > 1$  is close to 1, then one may take  $\alpha < 1$  arbitrarily close to 1 while still having  $\alpha q > 1$ .

**1.3. Ill-Posedness Beyond Danchin’s Regime.** To study ill-posedness beyond Danchin’s regime, we will focus on norm inflation or instantaneous blow-up and use the worst-case scenario (10) as a model for that.

One of the main motivations behind ill-posedness is that for any  $q > 1$  (equivalently, for any  $\alpha < 1$  in (10)), the initial vortex stretching rate  $u_0^r/r$  near the singular point can become very large.

A first (too naive) heuristic is to insert (10) into (9) and obtain that for small  $x$ ,

$$\frac{u_0^r(x)}{r} \sim C \int_{\substack{|y| \leq C, \\ r_y \sim |z_y|, \\ z_y \geq 0}} \frac{-\omega_0(y)}{|y|^3} dy \sim C \int_{\substack{|y| \leq C, \\ r_y \sim |z_y|}} \frac{1}{|y|^3 \log^\alpha(1/|y|)} dy = \infty$$

for any  $\alpha < 1$  (indeed, this integral diverges even for  $\alpha = 1$ ). Hence the stretching rate becomes very large near the singular point.

However, this heuristic does not take into account the competition between the blow-up of vortex stretching rate  $u^r/r$  and decay of the initial data  $\omega_0$ , which occurs as one approaches the singular point  $(r, z) = (0, 0)$ . More precisely, the vorticity equation (4) can be re-written via the Lagrangian flow map  $Y$  as

$$\omega(Y(r, z; t), t) = \omega_0(r, z) \exp \left( \int_0^t \frac{u^r(Y(r, z; s), s)}{Y^r(r, z; s)} ds \right). \quad (11)$$

As  $|x| \rightarrow 0$ , the initial data  $\omega_0$  on the right-hand side decays to 0 while the vortex stretching factor blows up.

To account for this competition,

$$\left| \frac{u_0^r(x)}{r} \right| \leq C \int_{\substack{r_y \sim |z_y|, \\ |y| \leq 1/2}} \frac{1}{|x - y|^2 \log^\alpha(1/|y|)} dy \sim \log^{1-\alpha}(1/|x|) \quad (12)$$

where  $x$  is also in a region where  $r \sim |z|$ . Indeed, we decompose the domain of integration into the outer region:  $|y| \geq 2|x|$  and the remaining region  $|y| \leq 2|x|$  and denote each integral by  $I_{\text{out}}, I_{\text{rem}}$ . Then

$$I_{\text{out}} \sim \int_{2|x| \leq |y| \leq 1/2} \frac{1}{|y|^2 \log^\alpha(1/|y|)} dy \sim \log^{1-\alpha} \left( \frac{1}{|x|} \right), \quad I_{\text{rem}} \sim \frac{1}{\log^\alpha(1/|x|)}.$$

Hence the claim (12) follows, and note that the main contribution arises from the outer region  $|y| \geq 2|x|$ .

Moreover, if  $\omega_0$  is odd in  $z$  and  $\omega_0 \leq 0$  for  $z > 0$ , then the dominant contribution to the Biot–Savart integral has a definite sign. In particular, the outer-region contribution yields a genuine lower bound for  $u_0^r(x)/r$  of order  $\log^{1-\alpha}(1/|x|)$ .

By contrast, in the borderline case  $\alpha = 1$  one instead has  $\frac{u_0^r(x)}{r} \sim \log \log \left( \frac{1}{|x|} \right)$ .

With this in mind, for very short times, the trajectory has not moved far, and we may heuristically approximate the stretching factor by its initial value, obtaining from (11) that for  $z > 0$ ,

$$\omega(Y(r, z; t), t) \sim \omega_0(r, z) \exp\left(Ct \frac{u_0^r(x)}{r}\right) \sim -\frac{1}{\log^\alpha \frac{1}{|x|}} \exp\left(Ct \log^{1-\alpha} \frac{1}{|x|}\right) \rightarrow -\infty \quad \text{as } |x| \rightarrow 0,$$

for any fixed  $t > 0$  provided  $\alpha < 1$ .

Thus the initial vortex stretching rate is strong enough to overwhelm the initial decay of  $\omega_0$  near the singular point for every  $\alpha < 1$  (i.e. for every  $q > 1$ ). In contrast, when  $\alpha = 1$  the growth of  $\frac{u_0^r(x)}{r}$  is only of size  $\log \log \frac{1}{|x|}$ , and the above short-time heuristic does not force instantaneous blow-up of  $\omega$ .

**1.4. Geometric Self-Slowdown Mechanism.** Although the approximation by the initial stretching rate  $u_0^r/r$  in Subsection 1.3 suggests ill-posedness, there is another important mechanism that competes with strong vortex stretching and can significantly weaken it over time. We refer to this effect as the *geometric self-slowdown mechanism*. This is also referred to as squeezing of vorticity; see [KJ22, p. 8].

We begin with a qualitative explanation that does not rely on any detailed kernel computation. Consider a portion of vorticity concentrated in a region where  $r \sim R$ ,  $z \sim \pm H$ , more precisely  $|r - R| \leq cR$ ,  $|z \pm H| \leq cH$ . (In a general distribution of vorticity, we decompose the vorticity into small regions like this.) As the flow evolves, vortex stretching tends to increase the radial scale  $R$  of this region. Since the flow is incompressible, this radial expansion must be accompanied by a collapse of the vorticity support toward the mid-plane  $z = 0$ , so that the vertical scale  $H$  decreases in time. Consequently, the aspect ratio  $H/R$  becomes smaller as vortex stretching proceeds.

The key observation is that the Biot–Savart law governing the vortex stretching rate  $u^r/r$  is essentially homogeneous and introduces no preferred length scale. As a result, the contribution of a vortex packet to the stretching rate  $u^r/r$  depends primarily on the *shape* of the vorticity distribution rather than its absolute size. In particular, for a vortex packet that becomes increasingly flattened in the  $z$ -direction, the contribution to the stretching rate is suppressed as  $H/R$  decreases.

This suppression has a simple geometric origin. Since the relevant kernel is odd in  $z$ , the leading contribution is controlled by a vertical moment,  $\int z \omega dz$ , of the vorticity distribution. As the support collapses toward  $z = 0$ , this moment decreases, and so does the induced vortex stretching. Thus, vortex stretching deforms the vorticity support in a way that weakens further stretching.

To illustrate this slowdown mechanism more concretely, we now present a representative heuristic computation based on the structure of the axisymmetric Biot–Savart law. Suppose that  $\omega$  is essentially supported in a region where  $r \sim R$  and  $z \sim \pm H$ , and consider a point  $x$  located much closer to the origin than to the support of  $\omega$ . Using (9), we estimate

$$\frac{u^r(x)}{r} \sim \|\omega\|_{L^\infty} \iint_{\substack{r \sim R, \\ z \sim H}} \frac{r^2 z}{(r^2 + z^2)^{5/2}} dr dz.$$

Since  $r \sim R$  on the support of  $\omega$ , the kernel contributes a factor of order  $R^{-2}$  as  $H/R$  becomes small. Then we obtain

$$\frac{u^r(x)}{r} \sim \frac{\|\omega\|_{L^\infty}}{R^2} \int_{z \sim H} z \, dz \sim \|\omega\|_{L^\infty} \frac{H^2}{R^2}.$$

This computation shows explicitly that the stretching rate decreases as the aspect ratio  $H/R$  becomes small.

In summary, strong initial vortex stretching does not by itself guarantee ill-posedness. One must instead analyze the competition between the initial amplification of the stretching rate  $u^r/r$  and its subsequent suppression due to the self-slowdown mechanism.

**1.5. Kim–Jeong’s Ill-Posedness for Large  $q$ .** The heuristic analysis in Subsection 1.3 shows that, for the worst-case scenario (10), the dominant contribution to the initial vortex stretching rate arises from an *outer region* of the Biot–Savart integral. Kim and Jeong [KJ22] exploit this same mechanism in a multiscale setting and show that, for sufficiently large  $q \gg 1$ , the outer-region stretching can be made effective on suitable time scales before the slowdown mechanism plays a role, leading to norm inflation.

Motivated by (10), Kim–Jeong replace the continuous logarithmic profile by a dyadic superposition of localized vortex rings. More precisely, they consider initial data of the form

$$\omega_0^{(m)}(r, z) = \sum_{k=n_0}^m \omega_{0,k}(r, z), \quad \omega_{0,k}(r, z) = \frac{1}{k^\alpha} \phi\left(\frac{r}{(1/8)^{k-1}}, \frac{z}{(1/8)^k}\right), \quad \frac{1}{q} < \alpha < 1. \quad (13)$$

where  $\phi$  is a fixed profile that is odd in  $z$ , nonpositive for  $z > 0$ , and supported near  $(r, z) = (1, \pm 1)$ . Each  $\omega_{0,k}$  represents a vortex ring localized at spatial scale  $1/8^k$ , and the amplitude  $k^{-\alpha}$  reflects the logarithmic decay in (10). In particular,  $\omega_0^{(m)}/r \in L^{3,q}(\mathbb{R}^3)$  since  $1/q < \alpha < 1$ . See our sign convention related to the Biot–Savart law in Appendix C.

Kim–Jeong’s key lemma turns the outer-region mechanism in the Biot–Savart law into an estimate usable for short times after  $t = 0$ : it writes the stretching rate  $u^r(x, t)/r$  as a sign-definite outer-region integral up to controllable errors. When  $x$  is associated with the  $k$ -th ring and the rings remain well-separated, the main term depends essentially only on vorticity at larger scales  $n < k$ .

A further issue in using the strong initial stretching is that the outer-region contribution could, in principle, weaken due to geometric flattening (self-slowdown). Kim–Jeong overcame this difficulty by combining the key lemma with a scale-dependent *stability* statement for the outer rings: on a scale-dependent time interval, each outer ring remains localized in a comparable annulus, so that the contributions by the outer rings stay comparable to its initial value. Summing these stable outer-ring contributions yields a robust lower bound on the time-integrated stretching rate felt by the  $k$ -th ring.

The assumption that  $q$  is large (equivalently, that  $\alpha$  is small) is crucial here, since it ensures that the amplitudes of the outer rings decay slowly with scale, allowing the outer-ring contributions to accumulate before the self-slowdown mechanism becomes effective.

Although the construction replaces the continuous worst-case profile (10) by a dyadic superposition of localized rings, this still captures the strong initial vortex stretching rate  $u_0^r/r$ . In addition, the dyadic superposition provides a *scale-by-scale decomposition* of the outer-region contribution, and the contribution of each outer ring can be tracked (for a short, scale-dependent time) before geometric self-slowdown degrades its effect.

Kim–Jeong show that outer-region forcing can produce norm inflation when  $q$  is sufficiently large because the dyadic amplitudes decay slowly enough for cumulative stretching to build up before geometric flattening suppresses the Biot–Savart coefficient. The main difficulty in the present paper is to recover this mechanism for every  $q > 1$ , where the amplitudes decay much faster. Our key new idea is to allow a flexible conical geometry for the rings and to localize the relevant Biot–Savart kernel, which isolates a monotone productive window and yields an effective ODE cascade even near the endpoint  $q = 1$ .

**1.6. Initial Data and Main Results.** Motivated by (13), we use generalized data in the following form:

$$\omega_0^{(m)}(r, z) = \sum_{k=1}^m \omega_{0,k}(r, z), \quad \omega_{0,k}(r, z) = \frac{\varepsilon}{k^\alpha} \phi\left(\frac{r}{d^k}, \frac{z}{d^k}\right), \quad d := 10^{-2} \quad (14)$$

where  $\phi$  is a fixed smooth profile satisfying

$$\begin{cases} \text{(i) } \phi \text{ is odd in } z, \\ \text{(ii) } \phi \leq 0 \text{ for } z > 0, \\ \text{(iii) } \|\phi\|_{L^\infty(\mathbb{R}^3)} \geq 1, \\ \text{(iv) } \text{supp}\phi \cap \{z > 0\} \subset [(1-\eta)r_0, (1+\eta)r_0] \times [(1-\eta)z_0, (1+\eta)z_0], \end{cases} \quad (15)$$

where

$$r_0 := 1, \quad \eta := 1/4, \quad L := z_0/r_0 > 0.$$

We call  $L$  the *cone-slope* parameter,  $\alpha$  the *logarithmic decay exponent*, and  $\eta$  the *localization* parameter. The specific choice of  $d, r_0, \eta$  is not necessary.

A schematic evolution of two consecutive vortex-ring supports is drawn in Figure 1.

For more details on the choice of parameters  $r_0, \eta, d, \dots$ , see the list of notation at the end of the paper.

First of all, similar to Kim–Jeong’s data (13), one can show our data (14) with (15) also satisfies  $\omega_0^{(m)}/r \in L^{3,q}(\mathbb{R}^3)$ ,  $q > 1$ , for  $\alpha \in (1/q, 1)$ .

Compared with (13), this class of data (14) is more general because the geometry of  $\text{supp}\phi$  is more flexible. Especially, the cone slope parameter  $L$  is not fixed for (14). This difference plays a critical role in our result. The other differences do not seem to be essential. In particular, the condition on the  $L^\infty$  norm of  $\phi$  and the specific choice of  $r_0, \eta, d$  are made just for convenience. See § 1.13 for more details about this choice.

Using this data (14) and tuning the cone-slope parameter  $L$ , we prove norm inflation as follows:

**Theorem 1.1** (Norm inflation). *Fix any  $q > 1$ . For any  $\tilde{\varepsilon}, \delta, A > 0$ , there exists an axisymmetric initial datum  $\omega_0 \in C_c^\infty(\mathbb{R}^3)$  such that*

$$\|\omega_0\|_{L^\infty \cap L^1(\mathbb{R}^3)} + \left\| \frac{\omega_0}{r} \right\|_{L^{3,q}(\mathbb{R}^3)} \leq \tilde{\varepsilon}$$

*and the unique global-in-time solution  $\omega(x, t)$  to the vorticity equation (4) with the initial condition  $\omega|_{t=0} = \omega_0$  satisfies*

$$\sup_{0 \leq t \leq \delta} \|\omega(\cdot, t)\|_{L^\infty(\mathbb{R}^3)} \geq A.$$

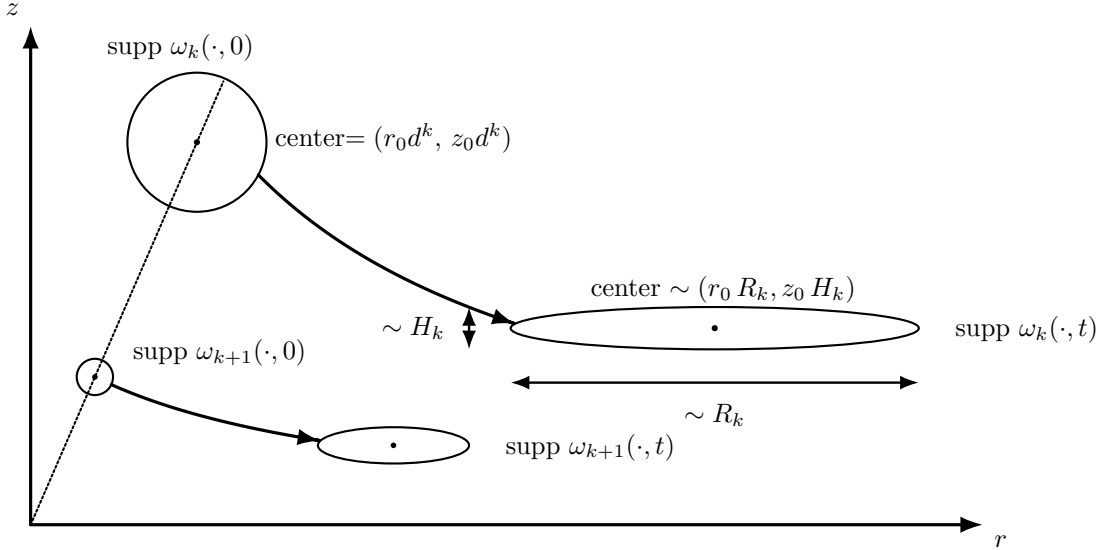


FIGURE 1. Schematic evolution of two consecutive vortex-ring supports in the upper half-plane. The left pair represents the initial supports  $\text{supp } \omega_k(\cdot, 0)$  and  $\text{supp } \omega_{k+1}(\cdot, 0)$ , whose centers lie on the same cone  $z = (z_0/r_0)r$ . The right pair represents the corresponding supports at a common later time  $t > 0$ : the  $k$ -th ring has moved outward and flattened into an ellipse with center  $\sim (r_0 R_k, z_0 H_k)$ , while the  $(k + 1)$ -th ring remains in a smaller inner annulus. The picture is schematic and not to scale; its purpose is only to indicate the common initial cone, the qualitative outward transport and flattening, and the outer/inner annular ordering at later time. In particular, the arrows represent qualitative transport and deformation rather than exact trajectories, and the relative placement of supports belonging to different indices and different times is not intended to encode any further quantitative relation. Only the upper half-plane is shown; the reflected lower half-plane is omitted.

**Remark 1.1.** *To elaborate on how the cone-slope parameter  $L$  plays a role in our proof for norm inflation (Theorem 1.1) and thus for instantaneous blow-up (Theorem 1.2 below), given any  $q > 1$ , we choose a large cone-slope parameter  $L = L_q > 0$  such that*

$$\frac{1}{q} < \frac{\log(L_q/\zeta_\eta)}{3\Theta_\mu + \log(L_q/\zeta_\eta)} (< 1), \quad \Theta_\mu := \left(\frac{1+\mu}{1-\mu}\right)^8, \quad \mu := \frac{1}{20}, \quad \zeta_\eta := \frac{1+\eta}{\sqrt{2}(1-\eta)} \quad (16)$$

*Then we can establish norm inflation for all  $\alpha$  such that*

$$\frac{1}{q} < \alpha < \frac{\log(L_q/\zeta_\eta)}{3\Theta_\mu + \log(L_q/\zeta_\eta)} (< 1). \quad (17)$$

*See Proposition 3.6 and Remark 3.1 for more details.*

*In fact, for a fixed cone-slope parameter  $L$ , if one can extend our norm inflation range (17) to the full range  $1/q < \alpha < 1$ , then one does not need to adjust  $L$  to prove norm inflation for any  $q > 1$ . However, such extension of our norm inflation range is impossible. Our proof also shows that for a fixed  $L$ , one can rule out norm inflation when  $\alpha$  is close to 1. See Appendix B.2 for a*

proof. Therefore, tuning the geometry of  $\text{supp } \phi$ , or more precisely the cone-slope parameter  $L$ , is necessary in order to prove norm inflation for any  $q > 1$ .

Regarding the cone slope, it is worth comparing the initial cone slope with the slope of the  $m$ -th ring center at the norm inflation time. From Figure 1, one can find the cone slope of the  $m$ -th ring center:

$$L_q \frac{H_m(t)}{R_m(t)} = L_q \frac{1}{\tilde{x}_m(t)^3}.$$

At the norm-inflation time,  $\tilde{x}_m(t) \sim Am^\alpha/\varepsilon$ , and hence the cone slope at the norm-inflation time is of the following order

$$L_q \left( \frac{\varepsilon}{Am^\alpha} \right)^3 \ll 1$$

for large  $m$ . Thus, although the initial profile is placed on a large cone  $z_0/r_0 \sim L_q$ , the  $m$ -th ring is strongly flattened by the time it produces norm inflation.

Now to state our instantaneous blow-up result, let us first define a distributional solution and a Yudovich-type weak solution of the initial value problem:

$$\begin{cases} \partial_t \left( \frac{\omega}{r} \right) + u^r \partial_r \left( \frac{\omega}{r} \right) + u^z \partial_z \left( \frac{\omega}{r} \right) = 0, \\ \omega(x, 0) = \omega_0(x). \end{cases} \quad (18)$$

**Definition 1.1.** Let  $T \in (0, \infty]$  and let  $\omega_0 = \omega_0(r, z)$  be axisymmetric such that  $\omega_0/r \in L^1_{\text{loc}}(\mathbb{R}^3)$ .

- We say that a pair  $(u, \omega)$  is a distributional solution of the initial value problem (18) on  $(0, T)$  if

$$\begin{aligned} u \in L^1_{\text{loc}}((0, T) \times \mathbb{R}^3), \quad \frac{\omega}{r} \in L^1_{\text{loc}}([0, T) \times \mathbb{R}^3), \quad u \frac{\omega}{r} \in L^1_{\text{loc}}([0, T) \times \mathbb{R}^3), \\ u = u^r(r, z, t)e_r + u^z(r, z, t)e_z \text{ is divergence-free and axisymmetric without swirl,} \\ \text{curl } u = \omega e_\theta \quad \text{in } \mathcal{D}'((0, T) \times \mathbb{R}^3), \end{aligned}$$

and

$$\int_0^T \int_{\mathbb{R}^3} \frac{\omega(x, t)}{r} (\partial_t \psi(x, t) + u(x, t) \cdot \nabla_x \psi(x, t)) dx dt + \int_{\mathbb{R}^3} \frac{\omega_0(x)}{r} \psi(x, 0) dx = 0 \quad (19)$$

for every  $\psi \in C_c^\infty(\mathbb{R}^3 \times [0, T])$ .

- And we say that a distributional solution  $(u, \omega)$  is a Yudovich-type weak solution if  $\omega$  additionally satisfies  $\omega \in L^\infty(0, T; L^\infty \cap L^1(\mathbb{R}^3))$ , and the velocity field  $u$  is associated with  $\omega$  via the Biot–Savart law (5).

For the definition of a distributional solution, we only impose a minimal regularity requirement to make sense of the weak formulation (19). On the other hand, we include boundedness and decay in the definition of a Yudovich-type weak solution, which aligns with a convention as in [MB01, Definition 8.1].

In what follows, we refer to these as distributional and Yudovich-type weak solutions of (18). We do not explicitly include axisymmetry or the no-swirl condition in the terminology, since these properties are already encoded in the formulation of (18). In particular, any solution in the above sense is necessarily axisymmetric without swirl.

Using our data (14) with  $m = \infty$  (infinitely many rings), we prove instantaneous blow-up, which consists of two types of results: non-existence of a Yudovich-type weak solution, and existence of a distributional solution that blows up instantaneously.

**Theorem 1.2** (Instantaneous blow-up). *For any  $\tilde{\varepsilon} > 0$  and  $q > 1$ , there exists an axisymmetric initial datum  $\omega_0 \in C^\infty(\mathbb{R}^3 \setminus \{0\})$  with compact support such that*

$$\|\omega_0\|_{L^\infty \cap L^1(\mathbb{R}^3)} + \left\| \frac{\omega_0}{r} \right\|_{L^{3,q}(\mathbb{R}^3)} \leq \tilde{\varepsilon},$$

and the following properties hold:

- (1) For any  $T > 0$ , there does not exist a Yudovich-type weak solution  $(u, \omega)$  on  $(0, T)$  of (18) with the initial data  $\omega_0$  in the sense of Definition 1.1;
- (2) There exists a distributional solution  $(u, \omega)$  in  $(0, \infty)$  of (18) with the same initial data  $\omega_0$  in the sense of Definition 1.1 such that

$$\operatorname{ess\,sup}_{0 < t < T} \|\omega(t)\|_{L^\infty(\mathbb{R}^3)} = +\infty \quad \text{for any } T \in (0, \infty). \quad (20)$$

We call (20) *instantaneous blow-up*.

**Remark 1.2.** Although Theorem 1.2-(2) is stated only in terms of the existence of a distributional solution and instantaneous blow-up of  $\|\omega(t)\|_{L^\infty(\mathbb{R}^3)}$ , the solution constructed in the proof has additional local energy-type bounds. We record these bounds only as properties obtained by our construction; no optimality of the regularity is asserted.

More precisely, the proof constructs a single global-in-time axisymmetric no-swirl distributional solution  $(u, \omega)$  as a diagonal subsequential limit of the smooth finite-ring solutions; see Proposition 4.6 and Corollary 4.7. Writing

$$\xi := \frac{\omega}{r},$$

the constructed solution satisfies

$$u \in L_{\text{loc}}^\infty([0, \infty); L^2(\mathbb{R}^3)) \cap L_{\text{loc}}^\infty([0, \infty); H_{\text{loc}}^1(\mathbb{R}^3)), \quad \xi \in L_{\text{loc}}^\infty([0, \infty); L_{\text{loc}}^2(\mathbb{R}^3)).$$

Moreover, for every  $T > 0$  and  $R > 0$ , along a suitable subsequence of the finite-ring approximations  $(u^{(m)}, \omega^{(m)})$ , one has

$$u^{(m)} \xrightarrow{*} u \quad \text{in } L^\infty(0, T; L^2(\mathbb{R}^3)), \quad u^{(m)} \rightarrow u \quad \text{strongly in } L^2((0, T) \times B_R),$$

and

$$\frac{\omega^{(m)}}{r} \xrightarrow{*} \frac{\omega}{r} \quad \text{in } L^\infty(0, T; L^2(B_R)).$$

Thus, the singular behavior in Theorem 1.2-(2) is specific to the  $L_x^\infty$ -norm of the vorticity: despite instantaneous blow-up of  $\|\omega(t)\|_{L^\infty}$ , the constructed solution still retains the above local energy-type regularity and local  $L^2$ -control of the relative vorticity.

**Remark 1.3.** For each finite-ring approximation, the vorticity is compactly supported at every time. Moreover, on the bootstrap time intervals used in the norm-inflation argument, the individual rings remain quantitatively localized and scale-separated. It is therefore natural to expect that the limiting distributional solution also has compactly supported vorticity, at least for a suitable representative and for a.e. time. However, this compact-support property does not follow from the present compactness argument.

The obstruction is that the uniform estimates available for the finite-ring approximations are the transported bound

$$\left\| \xi^{(m)} \right\|_{L^\infty(0, \infty; L^{3,q}(\mathbb{R}^3))} \leq C, \quad \xi^{(m)} = \omega^{(m)}/r,$$

and the conserved energy

$$\left\| u^{(m)} \right\|_{L^\infty(0, \infty; L^2(\mathbb{R}^3))} \leq C,$$

both of which are independent of  $m$ . Together with local elliptic estimates, these bounds give the local compactness used to construct the distributional limit, but they do not give a uniform-in- $m$  finite-propagation estimate for the supports. In particular, for  $q > 1$ , they do not yield a uniform  $L_x^\infty$ -bound on the velocities  $u^{(m)}$ , nor on the limiting velocity. Consequently, we do not claim compact support of the limiting distributional solution.

**Remark 1.4.** We prove Theorem 1.2-(2) by using the finite-ring approximations from Theorem 1.1 and taking its subsequential limit. This part in fact shows this limiting solution blows up instantaneously. In contrast, Theorem 1.2-(1) shows there is no Yudovich-type weak solution, that is, there is no distributional solution  $\omega$  in  $L^\infty(0, T; L^\infty \cap L^1(\mathbb{R}^3))$  with the Biot–Savart law (5). Admittedly, Theorem 1.2-(1) does not rule out the existence of other distributional solutions  $\omega$  that remain bounded in  $L_x^\infty$  but fail the  $L_x^1$  condition, that is, the non-existence of a distributional solution  $\omega \in L^\infty(0, T; L^\infty(\mathbb{R}^3))$  but  $\omega \notin L^\infty(0, T; L^1(\mathbb{R}^3))$ . We leave it open. See Remark 4.2 for detailed discussion on difficulties of this problem.

**Remark 1.5.** In a forthcoming paper, we prove an analogous result (norm inflation) for the De Gregorio model, a one-dimensional model of the three-dimensional Euler equation. More precisely, the corresponding Lorentz quantity we consider is  $\|\omega_0/|x|\|_{L^{1,q}(\mathbb{R})}$ . The one-dimensional geometry eliminates the geometric self-slowdown mechanism, which leads to what we call strong ODEs. See § 1.8.1 for more discussions. The absence of the slowdown mechanism makes the analysis significantly simpler.

**1.7. Framework: Dominant Outer-Rings and ODE Reduction.** Inspired by [KJ22] and [CMZ25], we will perform our analysis in a regime where outer-ring contributions to vortex stretching dominate over inner-ring and self-induced contribution, which motivates an ansatz and ODE reduction. The authors of [CMZ25] introduced this ansatz to construct finite-time blow-up solutions starting from Hölder continuous initial data. See § 1.11 for further discussion of their results.

Using the data (14), we consider the solution prior to collision, and decompose the vorticity into individual vortex rings:

$$\omega^{(m)}(r, z, t) = \sum_{k=1}^m \omega_k(r, z, t).$$

For a fixed index  $k$ , we define the *outer* and *inner* rings by

$$\omega_- := \sum_{j=1}^{k-1} \omega_j, \quad \omega_+ := \sum_{j=k+1}^m \omega_j,$$

so that  $\omega^{(m)} = \omega_- + \omega_k + \omega_+$ . Correspondingly, we decompose the velocity field as

$$u^{(m)} = u_- + u_k + u_+,$$

where each component is generated by the corresponding vorticity through the Biot–Savart law.

The evolution of a fixed vortex ring  $\omega_k$  is governed by

$$\partial_t \omega_k + u^{(m),r} \partial_r \omega_k + u^{(m),z} \partial_z \omega_k = \omega_k \frac{u^{(m),r}}{r}. \quad (21)$$

The contribution of the inner rings  $u_+$  does not enhance vortex stretching. For very short times  $t > 0$ , the odd symmetry in  $z$  ensures that this contribution remains negligible. Moreover, the self-induced velocity  $u_k$  turns out to be subleading. Therefore, outer rings dominate, and thus one can approximate the contribution of the outer rings  $u_-$  near the origin  $(r, z) = (0, 0)$ :

$$u_-^r(r, z, t) \approx r \partial_r u_-^r(0, 0, t) = r a(t), \quad \text{where } a(t) := \partial_r u_-^r(0, 0, t).$$

In fact, we justified the outer-region dominance in a more general setting without relying on the multi-ring structure of a solution. See Section 2 and Proposition 2.1 for its statement, history, and our motivation behind it.

By axisymmetry and odd symmetry in  $z$ , we have

$$u_-^r(0, 0, t) = 0, \quad \partial_z u_-^r(0, 0, t) = 0.$$

Furthermore, using the divergence-free condition,

$$u_-^z(r, z, t) \approx z \partial_z u_-^z(0, 0, t) = -2z a(t).$$

Under these approximations, (21) reduces to

$$\partial_t \omega_k + r a(t) \partial_r \omega_k - 2z a(t) \partial_z \omega_k = \omega_k a(t).$$

Solving this equation by the method of characteristics yields

$$\begin{aligned} \omega_k(r, z, t) &= \exp\left(\int_0^t a(s) ds\right) \omega_{0,k}\left(r \exp\left(-\int_0^t a(s) ds\right), z \exp\left(2 \int_0^t a(s) ds\right)\right) \\ &= x_k^0 \exp\left(\int_0^t a(s) ds\right) \phi\left(\frac{r}{d^k \exp\left(\int_0^t a(s) ds\right)}, \frac{z \exp\left(2 \int_0^t a(s) ds\right)}{d^k}\right). \end{aligned}$$

Here,

$$x_k^0 = \frac{\varepsilon}{k^\alpha}, \quad \frac{1}{q} < \alpha < 1.$$

Defining

$$x_k(t) := x_k^0 \exp\left(\int_0^t a(s) ds\right), \quad \tilde{x}_k(t) := \frac{x_k(t)}{x_k^0}, \quad R_k(t) := d^k \tilde{x}_k(t), \quad H_k(t) := \frac{d^k}{(\tilde{x}_k(t))^2}, \quad (22)$$

we obtain the representation

$$\omega_k(r, z, t) = x_k(t) \phi\left(\frac{r}{R_k(t)}, \frac{z}{H_k(t)}\right).$$

Motivated by this formal computation, we adopt the ansatz

$$\omega_k(r, z, t) = x_k(t) W_k\left(\frac{r}{R_k(t)}, \frac{z}{H_k(t)}, t\right), \quad (23)$$

where the weak dependence of  $W_k$  on  $k$  and  $t$  is introduced to account for errors between the approximate dynamics and the true solution, although  $W_k$  is expected to remain close to the reference profile  $\phi$ .

In addition, regarding the data (14), a direct computation then shows that

$$\left\| \frac{\omega_0^{(m)}}{r} \right\|_{L^{3,q}(\mathbb{R}^3)}^q \sim \sum_{k=1}^m \frac{\varepsilon^q}{k^{\alpha q}} \leq \sum_{k=1}^{\infty} \frac{\varepsilon^q}{k^{\alpha q}} < \infty$$

as expected. In particular, by choosing  $\varepsilon$  sufficiently small, this norm can be made arbitrarily small uniformly in  $m$ .

**1.8. Main Idea: Evolution of the Stretching Rate  $S_k$  and Front-Migration.** A central point of this paper is that the stretching–slowdown competition can be captured, to leading order, by a coupled ODE cascade for the amplitudes and aspect ratios of the vortex rings. The advantage of this viewpoint is that it lets us track the evolution of the stretching rate itself and quantify how stretching combined with geometric flattening can either deplete or enhance the influence of outer rings.

We use superscript/subscript, such as *orig*, *loc*, *froz*, to distinguish various types of simplifications. In addition, we will denote  $x_k^{\text{orig}}(t) := x_k(t)$  throughout this Section 1.8, but after this section, we will come back to the original notation  $x_k(t)$ .

1.8.1. *The Weak ODEs, and Overview.* Under the ansatz and the outer-ring linearization described above, the  $L^\infty$ -amplitude  $x_k^{\text{orig}}(t)$  of the  $k$ -th ring satisfies

$$\frac{d}{dt} \log x_k^{\text{orig}}(t) = \partial_r u_-^r(0, 0, t),$$

where  $u_- = \sum_{j < k} u_j$  is generated by the outer rings  $\omega_- = \sum_{j < k} \omega_j$ .

From the axisymmetric Biot–Savart law, one can obtain

$$\partial_r u_-^r(0, 0, t) = C \int_{-\infty}^{\infty} \int_0^{\infty} \frac{r^2 z}{(r^2 + z^2)^{5/2}} (-\omega_-(r, z, t)) \, dr dz.$$

Rescaling the Biot–Savart contribution of the  $j$ -th ring by its length scales  $(R_j(t), H_j(t))$  yields a factor  $\Gamma_j(t)^2$  together with a profile-dependent correction:

$$\begin{aligned} \frac{d}{dt} \log x_k^{\text{orig}}(t) &= \sum_{j=1}^{k-1} x_j^{\text{orig}}(t) \Gamma_j^{\text{orig}}(t)^2 \iint \frac{r^2 z}{(r^2 + \Gamma_j^{\text{orig}}(t)^2 z^2)^{5/2}} (-W_j(r, z, t)) \, dr dz, \\ &= \sum_{j=1}^{k-1} x_j^{\text{orig}}(t) \Gamma_j^{\text{orig}}(t)^2 \Lambda_j(t, \Gamma_j^{\text{orig}}(t)), \quad \Gamma_j^{\text{orig}}(t) := \frac{H_j(t)}{R_j(t)} = \left( \frac{x_j^{\text{orig}}(0)}{x_j^{\text{orig}}(t)} \right)^3 \end{aligned} \quad (24)$$

where

$$\Lambda_j(t, \Gamma) := \int_{-\infty}^{\infty} \int_0^{\infty} K_\Gamma(r, z) (-W_j(r, z, t)) \, dr dz, \quad K_\Gamma(r, z) := \frac{r^2 z}{(r^2 + \Gamma^2 z^2)^{5/2}}.$$

As the profiles  $W_j(r, z, t) \approx \phi(r, z)$  are supposed to vary little in  $j, t$ , let us consider the following model with a “frozen” profile  $\phi$ :

$$\frac{d}{dt} \log x_k^{\text{froz}}(t) = \sum_{j < k} x_j^{\text{froz}}(t) \Gamma_j^{\text{froz}}(t)^2 \Lambda_{\text{froz}}(\Gamma_j^{\text{froz}}(t)), \quad \Gamma_j^{\text{froz}}(t) := \left( \frac{x_j^{\text{froz}}(0)}{x_j^{\text{froz}}(t)} \right)^3, \quad (25)$$

where

$$\Lambda_{\text{froz}}(\Gamma) := \int_{-\infty}^{\infty} \int_0^{\infty} \frac{r^2 z}{(r^2 + \Gamma^2 z^2)^{5/2}} (-\phi(r, z)) \, dr dz.$$

Let us call  $\Lambda_j(t, \Gamma), \Lambda_{\text{froz}}(\Gamma)$  an *unfrozen and frozen Biot–Savart coefficient* respectively. (The dependence on the reference profile  $\phi$  is suppressed in the notation.)

The geometric self-slowdown mechanism is already encoded in the ODE structure: incompressibility forces  $\Gamma_j^{\text{froz}}(t)$  to decrease as  $x_j^{\text{froz}}(t)$  grows, which can weaken the subsequent contribution of the  $j$ -th ring to vortex stretching.

*Strong ODEs without Geometric Self-Slowdown.* If one ignores the geometric self-slowdown mechanism by treating the factor  $\Gamma^2 \Lambda(\Gamma) \sim 1$ , then vortex stretching enhances itself without any depletion because the ODEs become

$$\frac{d}{dt} \log x_k^{\text{str}}(t) = \sum_{j < k} x_j^{\text{str}}(t).$$

Let us call this equation *strong* ODEs whereas we call the original ODE (24) *weak* ODEs.

For this model, as it is expected from our discussion in § 1.3, one can simply use the strong initial vortex stretching by estimating  $\sum_{j < k} x_j^{\text{str}}(t) \geq \sum_{j < k} x_j^0 \sim k^{1-\alpha}$  on the right-hand side in order to establish norm inflation for any  $\alpha < 1$ . This is how vortex stretching is governed for the De Gregorio model, which is a one-dimensional model of the three-dimensional Euler equation (1). See Remark 1.5. And regarding the Euler equation (1), if one considers a backward problem instead of our forward problem, then it yields strong ODEs. However, we cannot use a backward problem in our case. See § 1.11.2 for discussion on this issue.

As discussed in § 1.4, in our case, the geometric self-slowdown depletes the vortex stretching rate  $u_-^r/r$ , which corresponds to  $\frac{d}{dt} \log x_k^{\text{orig}}(t)$  at the ODE level, as vorticity stretches. This entire section 1.8 is devoted to investigate how to quantify the stretching-slowdown competition and overcome the difficulty caused by the slowdown.

Proving norm inflation for (4) reduces to proving norm inflation at the ODE level, i.e. that for a fixed short time  $t > 0$  one has  $x_k^{\text{orig}}(t) \rightarrow \infty$  as  $k \rightarrow \infty$ . Let us call this type of result a *norm inflation result* (at the ODE level). In contrast, when one proves the other type of result, that is, for a fixed short time  $t > 0$ ,  $x_k^{\text{orig}}(t) \rightarrow 0$  as  $k \rightarrow \infty$ , let us call it a *decay result* (at the ODE level).

*Overview of Section 1.8.* We now outline the structure of this section. Our primary goal is to motivate the proof of norm inflation at the ODE level for the original, unsimplified *weak* ODEs (24) for any  $\alpha < 1$  after tuning  $L$  appropriately. To achieve this, we introduce several simplifications of the ODE system and analyze them using various techniques, demonstrating how the insights gained from these simplified models enable us to prove norm inflation for the full system. A diagram that shows the hierarchy of these ODE simplifications is drawn in Figure 2.

- (1) We first freeze the profile  $W_k(r, z, t) \approx \phi(r, z)$  and obtain the *frozen-profile* model (25) (or a *frozen model* in short):

$$\frac{d}{dt} (\log x_k^{\text{froz}}(t)) = \sum_{j=1}^{k-1} x_j^{\text{froz}}(t) \Gamma_j^{\text{froz}}(t)^2 \Lambda_{\text{froz}}(\Gamma_j^{\text{froz}}(t)),$$

- (2) (Section 1.8.2) As vortex stretching makes  $\Gamma_j(t)$  small in general, we simplify it further by approximating the Biot–Savart coefficient  $\Lambda_{\text{froz}}(\Gamma) \approx \Lambda_{\text{froz}}(0)$  and obtain a *model with a flattened Biot–Savart coefficient* (or a *flattened model* in short):

$$\frac{d}{dt} (\log x_k^{\text{flat}}(t)) = \sum_{j=1}^{k-1} x_j^{\text{flat}}(t) \Gamma_j^{\text{flat}}(t)^2.$$

We prove sharp norm inflation for  $\alpha < 2/7$  for this model by investigating evolution of vortex stretching rate  $S_k^{\text{flat}}(t) = \sum_{j \leq k} x_j^{\text{flat}}(t) \Gamma_j^{\text{flat}}(t)^2$  and obtaining a Riccati-type inequality. (A rigorous proof for this model can be found in Appendix B.1.)

- (3) (Section 1.8.3) Going back to the *frozen-profile* model (25), we apply similar ideas and obtain a similar Riccati-type inequality but with a profile-dependent correction. We can prove the same 2/7-norm inflation, which is now sharp only for the profile-independent approach. It suggests to utilize both the geometry of  $\text{supp } \phi$  and the profile-dependent correction to prove norm inflation beyond 2/7. (A rigorous proof for this part can be found in Appendix B.2.)
- (4) (Section 1.8.4) Therefore, we localize the profile  $\phi$ , which in turn “localizes” the frozen Biot–Savart coefficient  $\Lambda_{\text{froz}}(\Gamma) \approx \Lambda_{\text{loc}}(\Gamma)$ . Here,  $\Lambda_{\text{loc}}(\Gamma)$  has an explicit expression. Through change of variables, this localization leads to a *model with a localized Biot–Savart coefficient* (or a *localized model* in short):

$$\begin{aligned} \frac{d}{dt}(\log x_k^{\text{loc}}(t)) &\approx \sum_{j=1}^{k-1} x_j^{\text{loc}}(t) \Gamma_j^{\text{loc}}(t)^2 \Lambda_{\text{loc}}(\Gamma_j^{\text{loc}}(t)) \\ &= \sum_{j=1}^{k-1} x_j^{\text{loc}}(0) L^{-2/3} \Psi(\zeta_j^{\text{loc}}(t)), \quad \Psi(\zeta) = \zeta^{5/3} (1 + \zeta^2)^{-5/2}, \quad \zeta_j^{\text{loc}}(t) = L \Gamma_j^{\text{loc}}(t) \end{aligned} \quad (26)$$

where  $L$  is a cone slope parameter related to the geometry of  $\text{supp } \phi$ . Through the monotonicity of  $\Psi$ , which is related to what we call a front-migration mechanism, and an exact cascade identity for  $\Gamma_j$ , we can prove norm inflation in a certain range of  $\alpha$  that depends on the geometry of  $\text{supp } \phi$ , and this range reaches the full range  $\alpha < 1$  as  $L \rightarrow \infty$ .

- (5) (Section 1.8.5) We generalize this idea to the original weak ODEs (un-frozen profile) as the monotonicity of  $\Psi$  and the exact cascade identity are stable under multiplicative comparability bounds.

1.8.2. *A Model with a Flattened Biot–Savart Coefficient and Evolution of the Stretching Rate  $S_k$ .* To isolate the main ODE mechanism, it is convenient to simplify further the frozen-profile model (25) by “flattening” the frozen Biot–Savart coefficients, that is, setting  $\Lambda_{\text{froz}}(\Gamma) \approx \Lambda_{\text{froz}}(0)$  in the flattened regime  $\Gamma \ll 1$ . This simplification is based on the fact that norm inflation makes  $\Gamma$  small in general. Hence in this simplification, we suppress the  $\Gamma$ -dependence of  $\Lambda_{\text{froz}}$  and keep only the  $\Gamma^2$  slowdown, isolating the core depletion mechanism.

Absorbing harmless constants by rescaling the time variable, the system (25) becomes

$$\frac{d}{dt}(\log x_k^{\text{flat}}(t)) = \sum_{j < k} x_j^{\text{flat}}(t) \Gamma_j^{\text{flat}}(t)^2, \quad \Gamma_j^{\text{flat}}(t) := \left( \frac{x_j^{\text{flat}}(0)}{x_j^{\text{flat}}(t)} \right)^3. \quad (27)$$

Define

$$b_j^{\text{flat}}(t) := x_j^{\text{flat}}(t) \Gamma_j^{\text{flat}}(t)^2, \quad S_k^{\text{flat}}(t) := \sum_{j \leq k} b_j^{\text{flat}}(t).$$

Then (27) reads  $\frac{d}{dt} \log x_k^{\text{flat}}(t) = S_{k-1}^{\text{flat}}(t)$ . Differentiating  $b_j^{\text{flat}}$  using

$$\frac{d}{dt} \Gamma_j^{\text{flat}}(t) = -3 \Gamma_j^{\text{flat}}(t) S_{j-1}^{\text{flat}}(t)$$

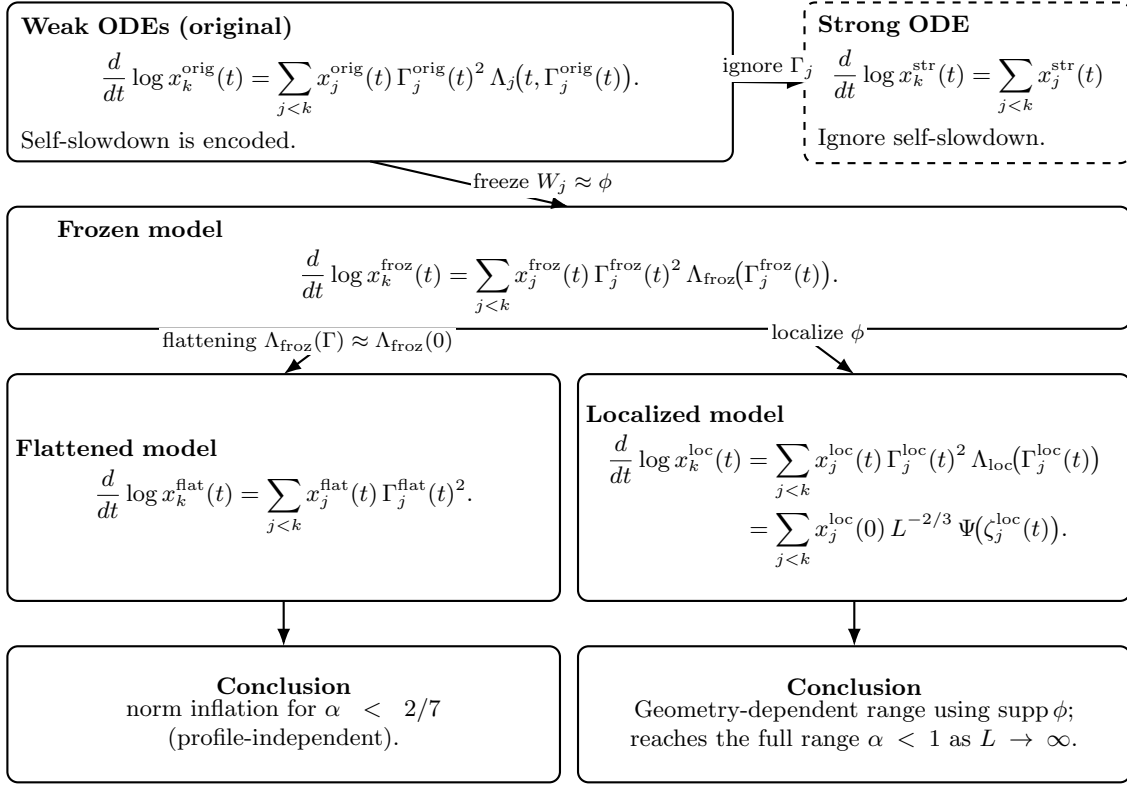


FIGURE 2. Hierarchy of the ODE simplifications used in Section 1.8

yields the depletion law

$$\frac{d}{dt} b_j^{\text{flat}}(t) = -5 b_j^{\text{flat}}(t) S_{j-1}^{\text{flat}}(t), \quad \text{and hence} \quad \frac{d}{dt} S_k^{\text{flat}}(t) = -5 \sum_{j \leq k} b_j^{\text{flat}}(t) S_{j-1}^{\text{flat}}(t). \quad (28)$$

Equivalently, using  $(S_j^{\text{flat}})^2 - (S_{j-1}^{\text{flat}})^2 = 2b_j^{\text{flat}} S_{j-1}^{\text{flat}} + (b_j^{\text{flat}})^2$ , one obtains

$$\frac{d}{dt} S_k^{\text{flat}}(t) = -\frac{5}{2} \left( S_k^{\text{flat}}(t)^2 - \sum_{j \leq k} b_j^{\text{flat}}(t)^2 \right). \quad (29)$$

As  $\frac{d}{dt} b_j^{\text{flat}}(t) \leq 0$ , it holds that  $b_j^{\text{flat}}(t) \leq b_j^{\text{flat}}(0) = \frac{\varepsilon}{j^\alpha} \leq \varepsilon$ . Hence  $\sum_{j \leq k} b_j^{\text{flat}}(t)^2$  is lower order. Ignoring this lower order term,  $\sum b_j^{\text{flat}}(t)^2 \geq 0$ , one is led to a Riccati-type differential inequality of  $S_k^{\text{flat}}(t)$  with a  $1/t$  bound of  $S_k^{\text{flat}}(t)$  with the Riccati constant  $5/2$ :

$$S_k^{\text{flat}}(t) \geq \frac{1}{\frac{5}{2}t + \frac{1}{S_k^{\text{flat}}(0)}}, \quad \text{and thus,} \quad \int_0^t S_k^{\text{flat}}(s) ds \geq \log(k^{\frac{2}{5}(1-\alpha)}) + C(\varepsilon, t, \alpha). \quad (30)$$

Therefore, the ODEs  $\frac{d}{dt} \log x_k^{\text{flat}}(t) = S_{k-1}^{\text{flat}}(t)$  yields

$$x_k^{\text{flat}}(t) \geq \frac{C(\varepsilon, t, \alpha)}{k^\alpha} k^{\frac{2}{5}(1-\alpha)}.$$

This in turn yields the norm inflation range for the ODEs:

$$\frac{2}{5}(1 - \alpha) > \alpha, \quad \text{that is,} \quad \alpha < \frac{2/5}{1 + 2/5} = \frac{2}{7}. \quad (31)$$

This threshold  $2/7$  is in fact sharp for the flattened model (27). More precisely, for  $\alpha > 2/7$ , one can show a decay result, that is, for any fixed small time  $t > 0$ ,  $x_k^{\text{flat}}(t) \rightarrow 0$  as  $k \rightarrow \infty$ . See Appendix B.1 for more details. This computation highlights the basic obstruction coming from self-slowdown when the Biot–Savart coefficient  $\Lambda$  is treated as essentially constant.

1.8.3. *A Model with a Non-Flattened Coefficient and Geometry of the Profile  $\phi$ .* For the original frozen-profile ODEs (25), one must retain the factor  $\Lambda_{\text{froz}}(\Gamma_j(t))$  in (25). Define

$$b_j^{\text{froz}}(t) := x_j^{\text{froz}}(t) \Gamma_j^{\text{froz}}(t)^2 \Lambda_{\text{froz}}(\Gamma_j^{\text{froz}}(t)), \quad S_k^{\text{froz}}(t) := \sum_{j \leq k} b_j^{\text{froz}}(t), \quad (32)$$

so that (25) again reads  $\frac{d}{dt} \log x_k^{\text{froz}}(t) = S_{k-1}^{\text{froz}}(t)$ . The difference is that the evolution of  $b_j^{\text{froz}}$  now includes a  $\Gamma$ -dependent correction. Using  $\frac{d}{dt} \Gamma_j^{\text{froz}}(t) = -3\Gamma_j^{\text{froz}}(t) S_{j-1}^{\text{froz}}(t)$ , one finds

$$\frac{d}{dt} b_j^{\text{froz}}(t) = b_j^{\text{froz}}(t) S_{j-1}^{\text{froz}}(t) \left( -5 + Q_{\text{froz}}(\Gamma_j^{\text{froz}}(t)) \right), \quad Q_{\text{froz}}(\Gamma) = 3\Gamma \frac{|\Lambda'_{\text{froz}}(\Gamma)|}{\Lambda_{\text{froz}}(\Gamma)}, \quad (33)$$

where we used  $\Lambda'_{\text{froz}}(\Gamma) \leq 0$ .

Hence the coefficient  $-5$  responsible for the  $2/7$ -threshold in the flattened model heuristic (§ 1.8.2) is shifted upward by the correction  $Q_{\text{froz}}(\Gamma)$ .

First of all, simply treating  $Q_{\text{froz}}(\Gamma) \geq 0$  as an “error” recovers the same  $2/7$ -norm inflation result as before. On the other hand, using the simple upper bound  $\max_{0 \leq \Gamma \leq 1} Q_{\text{froz}}(\Gamma)$  of  $Q_{\text{froz}}(\Gamma)$ , one can establish a decay result for a certain range of  $\alpha$ . In addition, one can make this upper bound  $\max_{0 \leq \Gamma \leq 1} Q_{\text{froz}}(\Gamma)$  arbitrary small by modifying the geometry of  $\text{supp } \phi$ , which leads to the full decay range  $\alpha > 2/7$ . See Appendix B.2 for a proof. Therefore, the  $2/7$ -norm inflation threshold is in fact sharp for the profile-independent approach.

This observation has several consequences. First, given the fact that the  $2/7$ -norm inflation threshold is in fact independent of a choice of a profile  $\phi$  whereas our decay range depends on it, it is reasonable to speculate that the upward shifting of the coefficient  $-5$  by  $Q_{\text{froz}}(\Gamma)$  might in fact lead to norm inflation beyond  $2/7$ , and the real norm inflation range might depend on the profile  $\phi$ . In addition, as one can make the upper bound  $\max_{0 \leq \Gamma \leq 1} Q_{\text{froz}}(\Gamma)$  small by adjusting the profile  $\phi$ , one can also make it large, which will make our decay range a small interval near  $\alpha = 1$ . Hence, one might be able to prove norm inflation in the full range, any  $\alpha < 1$ , by changing the profile  $\phi$ .

To this end, heuristically, if one can somehow increase the coefficient  $-5$  in (28) to an arbitrary small negative number  $-\delta'$ , then it will lead to the full inflation range:

$$\alpha < \frac{2/\delta'}{1 + 2/\delta'} \sim 1, \quad (34)$$

It can be seen by replacing the coefficient  $-5$  by  $-\delta'$  in (28)–(31).

However, it is delicate to extract a net gain from  $Q_{\text{froz}}(\Gamma)$  because early-time, large-scale enhancement of stretching can feed back into a stronger later-time, small-scale slowdown. More precisely, when time  $t > 0$  is small and the scale index  $k$  is small, the aspect ratio  $\Gamma_k(t)$  does not become small, which leads to strong stretching. However, at the same time, it leads to stronger slowdown for larger time  $t > 0$  and large scale index  $k$ .

Therefore, it is natural to try to effectively utilize the geometry of  $\text{supp } \phi$  in order to prove a norm inflation result beyond  $\alpha = 2/7$ . To this end, we localize  $\phi$  around the center  $(r_0, \pm z_0)$  of its support and make explicit the dependence of the Biot–Savart coefficient  $\Lambda_{\text{froz}}(\Gamma)$  on the geometry of  $\text{supp } \phi$ .

The front-migration mechanism that we present in the next section 1.8.4, produces an effective small Riccati constant (depending on geometry of  $\text{supp } \phi$ ).

1.8.4. *A Model with a Localized Biot–Savart Coefficient, and Front-Migration.* The idea of localization suggests to introduce ODEs with a “localized” Biot–Savart coefficient in which the Biot–Savart kernel  $K_\Gamma$  is frozen at a representative point  $(r_0, z_0)$  of the support:

$$\Lambda_{\text{froz}}(\Gamma) \rightsquigarrow \Lambda_{\text{loc}}(\Gamma) := \frac{r_0^2 z_0}{(r_0^2 + \Gamma^2 z_0^2)^{5/2}} = \frac{z_0}{r_0^3} \left(1 + L^2 \Gamma^2\right)^{-5/2}, \quad L := \frac{z_0}{r_0}. \quad (35)$$

In this subsection § 1.8.4, we do not fix  $L, \alpha$  by (16), (17). At the moment, let us regard them as unfixed parameters  $L > 0, \alpha \in (0, 1)$ . We will identify conditions of  $L, \alpha$  later on. (As usual, harmless positive constants depending on the localized profile are suppressed in the discussion below.) Then the original frozen model (25) becomes the localized one (26).

Recall the frozen model

$$b_j^{\text{froz}}(t) = x_j^{\text{froz}}(t) \Gamma_j^{\text{froz}}(t)^2 \Lambda_{\text{froz}}(\Gamma_j^{\text{froz}}(t)), \quad S_k^{\text{froz}}(t) = \sum_{i \leq k} b_i^{\text{froz}}(t), \quad \Gamma_j^{\text{froz}}(t) = \left( \frac{x_j^{\text{froz}}(0)}{x_j^{\text{froz}}(t)} \right)^3.$$

In the localized model, using  $x_j^{\text{loc}}(t) = x_j^{\text{loc}}(0) \Gamma_j^{\text{loc}}(t)^{-1/3}$ , we can rewrite the outer-ring contribution purely in terms of the single parameter  $\Gamma_j^{\text{loc}}(t)$ :

$$b_j^{\text{loc}}(t) = x_j^{\text{loc}}(t) \Gamma_j^{\text{loc}}(t)^2 \Lambda_{\text{loc}}(\Gamma_j^{\text{loc}}(t)) = x_j^{\text{loc}}(0) \Gamma_j^{\text{loc}}(t)^{5/3} \Lambda_{\text{loc}}(\Gamma_j^{\text{loc}}(t)), \quad \Gamma_j^{\text{loc}}(t) := \left( \frac{x_j^{\text{loc}}(0)}{x_j^{\text{loc}}(t)} \right)^3.$$

Introducing the cone variable

$$\zeta_j^{\text{loc}}(t) := L \Gamma_j^{\text{loc}}(t),$$

and substituting (35), we obtain the structural form

$$b_j^{\text{loc}}(t) = x_j^{\text{loc}}(0) L^{-2/3} \Psi(\zeta_j^{\text{loc}}(t)), \quad \Psi(\zeta) := \zeta^{5/3} (1 + \zeta^2)^{-5/2}. \quad (36)$$

We call  $\Psi$  the *Biot–Savart profile*. The key point is that  $\Psi$  is monotone on a fixed “productive” range: indeed,  $\Psi$  is strictly decreasing on  $[\zeta_*, \infty)$ , where  $\zeta_* := 1/\sqrt{2}$ . Since  $x_j^{\text{loc}}(t)$  is increasing,  $\Gamma_j^{\text{loc}}(t)$  (and hence  $\zeta_j^{\text{loc}}(t)$ ) is decreasing in time. Hence the composition  $t \mapsto \Psi(\zeta_j^{\text{loc}}(t))$  is increasing in time as long as  $\zeta_j^{\text{loc}}(t) \geq \zeta_*$ , which captures the exact window where stretching has not yet been overtaken by geometric self-slowdown. See Figure 3 for an illustration of this monotonicity.

Since  $\frac{d}{dt} x_1^{\text{loc}}(t) = 0$ , one has  $\Gamma_1^{\text{loc}} \equiv 1$  and therefore  $\zeta_1^{\text{loc}} \equiv L$ , which is chosen to be large. In addition,  $\Gamma_j^{\text{loc}}(0) = 1$  for all  $j$ , hence  $\zeta_j^{\text{loc}}(0) = L$  for all  $j$ . Hence, starting in the productive regime,  $\zeta_j^{\text{loc}}(t)$ 's decreases from  $L$  and then eventually passes the threshold  $\zeta_*$ .

*Front index and the  $t^{-1}$  lower bound for  $S_{m-1}^{\text{loc}}(t)$ .* Define the time-integrated contributions

$$B_j^{\text{loc}}(t) := \int_0^t b_j^{\text{loc}}(s) ds,$$

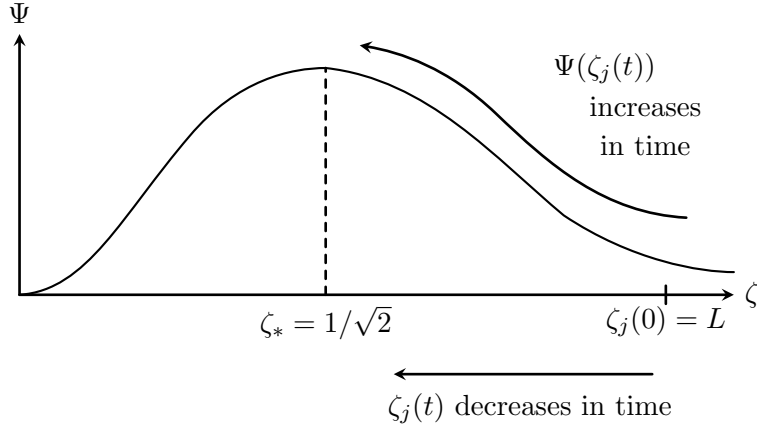


FIGURE 3. An illustration of the monotonicity of the Biot–Savart profile  $\Psi$ .

and recall the exact identity

$$\frac{d}{dt}\Gamma_{j+1}^{\text{loc}}(t) = -3\Gamma_{j+1}^{\text{loc}}(t)S_j^{\text{loc}}(t), \quad \frac{d}{dt}\Gamma_j^{\text{loc}}(t) = -3\Gamma_j^{\text{loc}}(t)S_{j-1}^{\text{loc}}(t).$$

Subtracting the logarithmic derivatives gives

$$\frac{d}{dt}\left(\log \Gamma_{j+1}^{\text{loc}}(t) - \log \Gamma_j^{\text{loc}}(t)\right) = -3(S_j^{\text{loc}}(t) - S_{j-1}^{\text{loc}}(t)) = -3b_j^{\text{loc}}(t),$$

and integrating yields the *exact  $\Gamma$ -cascade identity*

$$\Gamma_{j+1}^{\text{loc}}(t) = \Gamma_j^{\text{loc}}(t) e^{-3B_j^{\text{loc}}(t)}, \quad \text{and thus,} \quad \zeta_{j+1}^{\text{loc}}(t) = \zeta_j^{\text{loc}}(t) e^{-3B_j^{\text{loc}}(t)}. \quad (37)$$

As  $\zeta_j^{\text{loc}}(t)$  decreases in  $t$ , the front index  $J_{\zeta_0}^{\text{loc}}(t)$  is non-increasing in time, too. We call this behavior of the front index *front-migration*.

Fix a threshold  $\zeta_0 \in [\zeta_*, L]$  and define the *front index*

$$J_{\zeta_0}^{\text{loc}}(t) := \max \left\{ 1 \leq j \leq m-1 : \zeta_j^{\text{loc}}(t) \geq \zeta_0 \right\}.$$

A schematic profile of the cone variable  $\zeta_j^{\text{loc}}(t)$ , which shows the behavior of the front index  $J_{\zeta_0}^{\text{loc}}(t)$  is drawn in Figure 4.

Assume that the front has passed the smallest scale by time  $t$ , i.e.  $\zeta_m^{\text{loc}}(t) < \zeta_0$ . Then, defining  $J := J_{\zeta_0}^{\text{loc}}(t)$  temporarily, we have  $\zeta_{J+1}^{\text{loc}}(t) < \zeta_0$ . Iterating (37) from 1 to  $J$  and using  $\zeta_1^{\text{loc}} = L$  gives

$$\zeta_{J+1}^{\text{loc}}(t) = L \exp\left(-3 \sum_{k=1}^J B_k^{\text{loc}}(t)\right),$$

hence

$$\sum_{k=1}^J B_k^{\text{loc}}(t) = \frac{1}{3} \log\left(\frac{L}{\zeta_{J+1}^{\text{loc}}(t)}\right) \geq \frac{1}{3} \log\left(\frac{L}{\zeta_0}\right). \quad (38)$$

This is the first input: *to drive the cone variables from their initial value  $L$  across the threshold  $\zeta_0$ , the system must accumulate at least  $\frac{1}{3} \log(L/\zeta_0)$  units of integrated outer influence up to the front.*

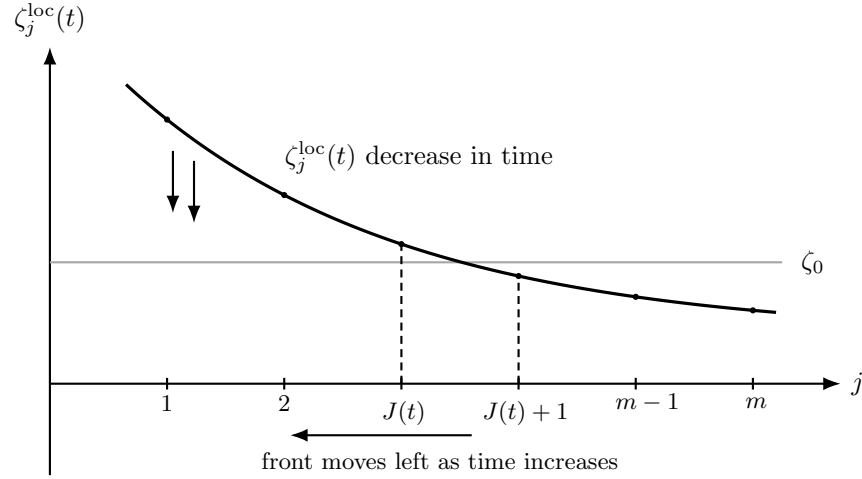


FIGURE 4. Schematic profile of the cone variable at a fixed time. Here  $J(t) := J_{\zeta_0}^{\text{loc}}(t)$  is the largest index such that  $\zeta_j^{\text{loc}}(t) \geq \zeta_0$ , so that  $\zeta_{J(t)}^{\text{loc}}(t) \geq \zeta_0 > \zeta_{J(t)+1}^{\text{loc}}(t)$ . Since each  $t \mapsto \zeta_j^{\text{loc}}(t)$  is nonincreasing, the values  $\zeta_j^{\text{loc}}(t)$  move downward in time and the front index moves to smaller values of  $j$ . Strictly speaking, the profile consists of the discrete values  $\{\zeta_j^{\text{loc}}(t)\}_{j=1}^m$  at integer indices  $j$ ; the continuous curve is drawn only as a visual guide connecting these discrete points.

The second input is monotonicity on the productive regime. For every  $k \leq J$  and every  $s \in [0, t]$ , we have  $\zeta_k^{\text{loc}}(s) \geq \zeta_k^{\text{loc}}(t) \geq \zeta_0 \geq \zeta_*$  because each  $\zeta_k^{\text{loc}}$  is nonincreasing in time. Since  $\Psi$  is decreasing on  $[\zeta_*, \infty)$ , the representation (36) implies that  $s \mapsto b_k(s)$  is nondecreasing on  $[0, t]$ . Consequently,

$$B_k^{\text{loc}}(t) = \int_0^t b_k^{\text{loc}}(s) ds \leq t b_k^{\text{loc}}(t) \quad (k \leq J),$$

and summing over  $k \leq J$  gives

$$\sum_{k=1}^J B_k^{\text{loc}}(t) \leq t \sum_{k=1}^J b_k^{\text{loc}}(t) \leq t S_{m-1}^{\text{loc}}(t). \quad (39)$$

Combining (38) and (39) yields the desired *front-induced*  $t^{-1}$  lower bound:

$$S_{m-1}^{\text{loc}}(t) \geq \frac{1}{3t} \log\left(\frac{L}{\zeta_0}\right) \quad \text{whenever} \quad \zeta_m^{\text{loc}}(t) < \zeta_0.$$

This estimate is the crux of the front-migration mechanism: given our discussion around (34), heuristically, the large coefficient  $\log(L/\zeta_0)$  here effectively replaces the Riccati constant  $5/2$  in (30) by an arbitrary small number and yields the full norm inflation range for large  $L$ :

$$\alpha < \frac{\log(L/\zeta_0)}{3 + \log(L/\zeta_0)} \rightarrow 1 \quad \text{as } L \rightarrow \infty.$$

1.8.5. *The Original Weak ODEs and Localization of  $\phi$ .* The localized model is only an intermediate simplification. The actual weak ODEs involve the unfrozen coefficients  $\Lambda_j(t, \Gamma)$  coming from the

transported profiles  $W_j(\cdot, \cdot, t)$ . Accordingly, define

$$b_j^{\text{orig}}(t) := x_j^{\text{orig}}(t)(\Gamma_j^{\text{orig}}(t))^2 \Lambda_j(t, \Gamma_j^{\text{orig}}(t)), \quad S_k^{\text{orig}}(t) := \sum_{j=1}^k b_j^{\text{orig}}(t),$$

and

$$B_j^{\text{orig}}(t) := \int_0^t b_j^{\text{orig}}(s) ds.$$

Then the original weak system still has the exact cascade form

$$\frac{d}{dt} \log x_k^{\text{orig}}(t) = S_{k-1}^{\text{orig}}(t), \quad \Gamma_{j+1}^{\text{orig}}(t) = \Gamma_j^{\text{orig}}(t) e^{-3B_j^{\text{orig}}(t)}.$$

To connect this system to the localized model, we use two comparisons. First, on the bootstrap interval, the flow-map bounds imply that the transported profiles stay close to the fixed profile  $\phi$  after rescaling, so

$$\Lambda_j(t, \Gamma) \approx \Lambda_{\text{froz}}(\Gamma).$$

Equivalently, if

$$b_{\text{froz},j}^{\text{orig}}(t) := x_j^{\text{orig}}(t)(\Gamma_j^{\text{orig}}(t))^2 \Lambda_{\text{froz}}(\Gamma_j^{\text{orig}}(t)), \quad S_{\text{froz},k}^{\text{orig}}(t) := \sum_{j=1}^k b_{\text{froz},j}^{\text{orig}}(t),$$

then

$$b_j^{\text{orig}}(t) \approx b_{\text{froz},j}^{\text{orig}}(t), \quad S_k^{\text{orig}}(t) \approx S_{\text{froz},k}^{\text{orig}}(t).$$

Second, localization acts on the frozen coefficient, not directly on  $\Lambda_j(t, \Gamma)$ . Since  $\phi$  is supported near  $(r_0, \pm z_0)$ , one has

$$\Lambda_{\text{froz}}(\Gamma) \approx \Lambda_{\text{loc}}(\Gamma).$$

Hence the correct chain is

$$\Lambda_j(t, \Gamma) \approx \Lambda_{\text{froz}}(\Gamma) \approx \Lambda_{\text{loc}}(\Gamma).$$

Therefore the monotonicity and front-migration estimates proved through the localized Biot–Savart profile  $\Psi$  apply first to the frozen quantities and then transfer, up to harmless constants, to the original weak system. Since the exact  $\Gamma$ -cascade already holds for  $\Gamma_j^{\text{orig}}$ , the same ODE norm-inflation mechanism remains valid for the original weak ODEs.

**1.9. Scale Separation and Stability of the Profiles.** In our construction, it is essential that the vortex rings remain well separated and the profiles  $W_k(r, z, t)$  do not depend much on the scale index  $k$  and time  $t$  throughout the entire time interval relevant for the analysis, even as norm inflation actually deforms the configuration.

More precisely, for scale separation, we must verify that the separation of spatial scales is preserved for all time across scales, namely that

$$R_k(t) \gg R_{k+1}(t), \quad \text{equivalently} \quad d \frac{\tilde{x}_{k+1}(t)}{\tilde{x}_k(t)} \ll 1 \quad (40)$$

uniformly for all  $k$  and for all  $t$  in the time interval of interest.

In addition, for the stability of the profile  $W_k(r, z, t)$ , we justify it through a bootstrap argument: Using the fact that  $W_k(r, z, t)$  does not change much in  $k, t$  for a short time interval, that is,  $W_k(r, z, t)$  satisfy “bootstrap bounds” for a short time interval, we improve the bootstrap bounds with a margin by using the norm inflation at the ODE level and choosing large  $m$ . It will justify the bootstrap bounds until the ODE norm inflation time.

Indeed, for scale separation, using the ODEs (25), one finds

$$\frac{\tilde{x}_{k+1}(t)}{\tilde{x}_k(t)} \sim \exp\left(\int_0^t b_k(s) ds\right), \quad b_k(s) = x_k(s)\Gamma_k(s)^2\Lambda(\Gamma_k(s)).$$

Thus, controlling the ratio  $\tilde{x}_{k+1}(t)/\tilde{x}_k(t)$  reduces to estimating the time integral of  $b_k$ .

Fix an arbitrary target amplitude  $A > 0$  and define the *norm inflation time*  $T_N(A, m)$  by

$$\sup_{1 \leq k \leq m} x_k(T_N(A, m)) = A.$$

Norm inflation at the ODE level implies that  $T_N(A, m) \rightarrow 0$  as  $m \rightarrow \infty$  for any fixed  $A$ . One can in fact obtain an algebraic decay rate.

Using the bound  $x_k(t) \leq A$  on the time interval  $[0, T_N(A, m)]$ , one can at once estimate the time-integral of  $b_k$ :

$$\int_0^t b_k(s) ds \leq CAT_N(A, m) \rightarrow 0 \quad \text{as } m \rightarrow \infty. \quad (41)$$

Therefore, by choosing a sufficiently small distance factor  $d$  and large  $m$ , we ensure that (40) holds for all  $k$  and all  $t \in [0, T_N(A, m)]$ . (In our actual estimate, we will use a bootstrap time interval  $[0, T_B]$  instead of the norm inflation time interval  $[0, T_N]$ . In addition, we will use a rescaled amplitude  $\bar{A}$  instead of  $A$ . See § 3.2 for an explanation.)

Regarding stability of profiles  $W_k$ , bootstrap improvement is also controlled by the same quantity  $AT_N(A, m)$ . Indeed, the profile stability is governed by the time integral of discrepancy between the real solution and our approximate ansatz solution. Following the heuristic argument behind the ansatz (§ 1.7), one can estimate the discrepancy by  $AT_N(A, m)$ . Hence choosing large  $m$  as like (41) will improve the bootstrap bounds.

Therefore, using scale-separation and stable profiles, we can transfer ODE-level norm inflation to the PDEs, using the smallness of  $AT_N(A, m)$  for large  $m$ . It finishes the main ideas of our proof for Theorem 1.1.

Before turning to the infinite-ring argument, we record why the bootstrap estimate used below contains an extra logarithmic factor. See (94). For smooth finite-ring solutions one could, in principle, exploit Calderón–Zygmund cancellations to obtain sharper self-interaction estimates. Since the same type of estimate must later be used in the contradiction framework for merely bounded Yudovich-type solutions, we instead use a robust  $L^\infty$ -based estimate already in the finite-ring bootstrap. This produces the factor  $\log m$ , which remains harmless because the ODE analysis gives an algebraically small time scale  $T_B(A, m) \lesssim m^{-\beta q}$ .

**1.10. Instantaneous Blow-Up.** To pass from norm inflation to instantaneous blow-up, we take  $m = \infty$  in (14), that is, we superpose infinitely many dyadic rings with  $\alpha > 1/q$ . Since this construction is tailored to model the worst-case profile (10), the resulting data satisfy

$$\omega_0^{(\infty)} \in L^\infty \cap L^1(\mathbb{R}^3), \quad \omega_0^{(\infty)}/r \in L^{3,q}(\mathbb{R}^3),$$

but  $\omega_0^{(\infty)}$  necessarily loses Hölder regularity. This loss of regularity is exactly what makes the instantaneous blow-up problem qualitatively different from the finite-time framework of [CMZ25].

**Lack of Calderón–Zygmund cancellation.** In the Hölder-based setting of [CMZ25], one exploits Calderón–Zygmund cancellations in the Biot–Savart law to estimate  $\nabla u^{(\infty)}$ . Making use of that

mechanism requires more than bounded vorticity: one must propagate a Hölder norm of  $\omega^{(\infty)}$  and, in turn, control the deformation gradient of the flow map through

$$\frac{d}{dt}DY(t) = \nabla u^{(\infty)}(Y(t), t) DY(t).$$

By contrast, in the contradiction argument for instantaneous blow-up (more precisely, non-existence of Yudovich-type weak solutions), we may assume only that a solution

$$\omega^{(\infty)} \in L^\infty(0, T; L^\infty \cap L^1(\mathbb{R}^3))$$

exists on some short interval. At this level, the associated velocity field is merely log-Lipschitz (see [AB15, Lemma 1]), so the Lagrangian flow map  $Y$  is still well-defined, but there is no available bootstrap bound on  $DY$  or on any Hölder norm of  $\omega^{(\infty)}(t)$ . In particular, the cancellation mechanism available in the Hölder regime is no longer accessible.

**Logarithmic penalty.** Accordingly, in the instantaneous blow-up argument we estimate the self-induced velocity using only the  $L^\infty$  bound on the vorticity together with the geometry of its support, without exploiting any cancellation.

More precisely, using the crude bound

$$|u(x)| \lesssim \int_{\mathbb{R}^3} \frac{|\omega(y)|}{|x-y|^2} dy,$$

and the fact that  $\omega_k(\cdot, t)$  is supported in a region of radial scale  $R_k$  and vertical thickness  $H_k$ , one obtains

$$|u_k(x)| \lesssim \|\omega_k\|_{L^\infty} \int_{\text{supp } \omega_k(\cdot, t)} \frac{1}{|x-y|^2} dy \lesssim \|\omega_k\|_{L^\infty} H_k \log\left(\frac{R_k}{H_k}\right).$$

Therefore, for  $(r, z) \in \text{supp } \omega_k(\cdot, t)$ , where  $|z| \sim H_k$ , we obtain

$$\frac{|u_k^z(r, z, t)|}{|z|} \lesssim \|\omega_k\|_{L^\infty} \log\left(\frac{R_k}{H_k}\right) = \|\omega_k\|_{L^\infty} \log\left(\frac{1}{\Gamma_k}\right),$$

where  $\Gamma_k = H_k/R_k \ll 1$  is the aspect ratio.

Thus, in the absence of Calderón–Zygmund cancellation, a geometric logarithmic loss of order  $\log(1/\Gamma_k)$  naturally appears in the self-interaction estimate.

**How to overcome the logarithmic loss.** The key point is that our construction is designed so that this logarithmic loss is dominated by the shrinking time scale.

Along characteristics, one needs to control

$$\int_0^{T_N(A, k)} \left\| \frac{u_k^z}{z} \right\|_{L^\infty(\text{supp } \omega_k(\cdot, t))} dt \lesssim A \log\left(\frac{1}{\Gamma_k(T_N(A, k))}\right) T_N(A, k).$$

To reach amplitude  $A$ , the  $k$ -th ring must satisfy

$$\Gamma_k(T_N(A, k)) \sim k^{-3\alpha}, \quad \log\left(\frac{1}{\Gamma_k}\right) \sim \log k.$$

On the other hand, the ODE analysis shows that the norm-inflation time decays *algebraically*. Hence,  $\log k \cdot T_N(A, k) \rightarrow 0$ , so the logarithmic geometric loss remains perturbative.

**Further remarks.** For finite-ring solutions, one can bootstrap the deformation gradient and recover Calderón–Zygmund cancellation, eliminating the logarithmic loss. The appearance of the logarithmic factor is therefore a genuinely infinite-ring phenomenon tied to the lack of Hölder regularity.

It is worth noting that the extra log factor also appears in a heuristic estimate of  $u_k^z/z$  based on the local induction approximation. To see this, we approximate one vortex ring  $\text{supp } \omega_k(\cdot, \cdot, t) \cap \{z > 0\}$  by a vortex filament given by the centerline circle and compute the self-induced vertical velocity through local induction approximation. For the notion of local induction approximation, see [MB01, Chapter 7].

In addition, the infinite-ring configuration leads to a vanishing time scale. To handle this, we decompose the configuration into head and tail rings, applying the bootstrap argument only to the head and controlling the tail via outer-ring dominance (see Proposition 2.1).

**1.11. Comparison with the Córdoba–Martinez–Zoroa–Zheng Construction.** The recent work of Córdoba–Martinez–Zoroa–Zheng [CMZ25] constructs finite-time singularities for the 3D axisymmetric Euler equations without swirl from initial data in a Hölder-based local well-posedness regime. At a very high level, both [CMZ25] and the present paper (and [KJ22]) exploit the same multiscale “vortex-ring cascade” principle: one superposes rings indexed by  $k$  and uses that, at suitable points, the dominant contribution to the stretching of an inner ring comes from outer rings. (Multi-scale constructions also appear in [CM23], [CLM25].)

However, the comparison is subtle because there are *two different criticalities* at play:

- **Hölder criticality** (pointwise regularity of  $\omega$  or  $u$  near the axis), which is the natural scale for classical local well-posedness;
- **Lorentz criticality** (integrability of the transported quantity  $\omega/r$  in (6)), which is the natural scale for Danchin-type global estimates such as (7).

In particular, even though  $\omega/r$  is transported by (6), its Lorentz criticality is sensitive to the *geometry of the support near  $r = 0$* , since the weight  $r^{-1}$  amplifies concentration near the axis. This is precisely where the CMZ configuration differs from ours.

In this section 1.11.2, we will see that: a) CMZ’s data are supercritical in the Lorentz scale because their rings concentrate near the axis, yet this same anisotropy weakens the stretching kernel; b) Our construction instead targets the worst-case conical geometry relevant to Danchin’s threshold. c) Additionally, we will also study why our problem must be organized forward in time instead of backward as opposed to CMZ’s problem.

**1.11.1. The CMZ Construction: Data Given at the Singular Time, and Backward Evolution.** CMZ prove that there exist axisymmetric no-swirl solutions on a time interval  $[0, T)$  whose velocity remains in a Hölder class for every fixed time  $0 \leq t < T$  but whose vorticity blows up as  $t \uparrow T$ . More precisely, they construct solutions  $u(x, t)$  to the Euler equation (1) on  $t \in [0, T)$  such that for every  $t < T$ ,

$$u(\cdot, t) \in C^\infty(\mathbb{R}^3 \setminus \{0\}) \cap C^{1, \alpha_{\text{CMZ}}}(\mathbb{R}^3) \cap L^2(\mathbb{R}^3), \quad \omega(\cdot, t) = \nabla \times u(\cdot, t) \in C^{\alpha_{\text{CMZ}}}(\mathbb{R}^3),$$

while  $\max_{x \in \mathbb{R}^3} |\omega(x, t)| \approx 1/|T - t|$  as  $t \uparrow T$ . In fact, they worked on a time interval  $[-T, 0)$  where  $t = 0$  corresponds to the final time and  $t = -T$  the initial time, but for the sake of comparison, let us shift their time interval to  $[0, T)$ .

A key structural feature is that CMZ organize the cascade *backward in time*. They start by prescribing a singular “final state” at the blow-up time  $t = T$  via a dyadic superposition of vortex rings, and then solve the Euler dynamics backward to obtain regular initial data at  $t = 0$ .

To avoid confusion, no matter whether we consider a backward problem or a forward problem, we will always consider the time interval  $(0, T)$ , and the initial time always means  $t = 0$ , at which the evolution starts, whereas the final time means  $t = T$  where the evolution ends.

Concretely, for each truncation level  $m$  they prescribe at  $t = T$  the (truncated) vorticity

$$\omega_{(m)}^{\text{CMZ}}(r, z, T) = \sum_{k=0}^m \omega_k^{\text{CMZ}}(r, z, T), \quad \omega_k^{\text{CMZ}}(r, z, T) = A_{\text{CMZ}}^k \varphi \left( \frac{r}{d_{\text{CMZ}}^k}, \frac{z}{d_{\text{CMZ}}^k} \right), \quad (42)$$

where  $0 < A_{\text{CMZ}} - 1 \ll 1$ ,  $0 < d_{\text{CMZ}} \ll 1$ , and  $\varphi$  is a smooth profile supported near  $r = 1$  horizontally and in  $[-2Z, 2Z]$  for large parameter  $Z > 0$  vertically. The profile  $\varphi$  is odd in  $z$ . (see [CMZ25] for details). We have simplified some structure of the profile  $\varphi$  that is not essential for our discussion.

This terminal configuration makes the infinite sum (as  $m \rightarrow \infty$ ) singular at  $t = T$ , but for each finite  $m$ , the data are smooth and hence generate a global-in-time classical solution in the axisymmetric no-swirl class. CMZ then pass to a limit  $m \rightarrow \infty$  to obtain the singular solution on  $[0, T)$ .

We will call  $\omega_{(m)}^{\text{CMZ}}$  given in (42) *CMZ's terminal data* whereas we call  $\omega_{(m)}^{\text{CMZ}}(r, z, 0)$  *CMZ's backward-evolved initial data*.

Their multiscale ansatz for each  $\omega_k^{\text{CMZ}}$  may be written in the same form as ours but with  $x_k(0)$  replaced by  $x_k(T)$ . Indeed, [CMZ25, Eq. (15)] has the form

$$\omega_k^{\text{CMZ}}(r, z, t) = x_k^{\text{CMZ}}(t) W_k^{\text{CMZ}} \left( \frac{r}{R_k^{\text{CMZ}}(t)}, \frac{z}{H_k^{\text{CMZ}}(t)}, t \right),$$

where

$$R_k^{\text{CMZ}}(t) = d_{\text{CMZ}}^k \frac{x_k^{\text{CMZ}}(t)}{x_k^{\text{CMZ}}(T)}, \quad H_k^{\text{CMZ}}(t) = d_{\text{CMZ}}^k \frac{(x_k^{\text{CMZ}}(T))^2}{(x_k^{\text{CMZ}}(t))^2}, \quad x_k^{\text{CMZ}}(T) = A_{\text{CMZ}}^k.$$

Here  $d_{\text{CMZ}}$  is chosen to be small, and  $A_{\text{CMZ}} > 1$  is chosen to be close to 1. At the singular time  $t = T$ , one has  $x_k^{\text{CMZ}}(T) = A_{\text{CMZ}}^k$ , so  $R_k^{\text{CMZ}}(T) = H_k^{\text{CMZ}}(T) = d_{\text{CMZ}}^k$  and the rings are essentially “conical” at  $t = T$ . In the backward direction  $t < T$ ,  $x_k^{\text{CMZ}}(t)$  decreases and therefore the aspect ratio grows:

$$\Gamma_k^{\text{CMZ}}(t) := \frac{H_k^{\text{CMZ}}(t)}{R_k^{\text{CMZ}}(t)} = \left( \frac{A_{\text{CMZ}}^k}{x_k^{\text{CMZ}}(t)} \right)^3, \quad t < T. \quad (43)$$

Thus the backward evolution produces initial data at  $t = 0$  supported in increasingly *thin* regions (large  $\Gamma_k^{\text{CMZ}}$ .)

As CMZ utilized a backward problem, their backward-evolved initial data at  $t = 0$  is not given explicitly. Hence for later comparison, it is convenient to summarize the CMZ *initial* geometry and pointwise size by a *continuous envelope* model. To this end, the following schematic asymptotic behavior is useful: with a fixed  $t < T$ ,

$$x_k^{\text{CMZ}}(t) \sim A_{\text{CMZ}}^{-k}, \quad (44)$$

for large  $k$  when  $A_{\text{CMZ}} > 1$  is close to 1. See [CMZ25, § 1.3.2] for more detailed heuristic computations on this asymptotic behavior. We have simplified the asymptote,  $A_{\text{CMZ}}^{-k}$ , from the exact asymptote in [CMZ25, § 1.3.2], using the fact that  $A_{\text{CMZ}} > 1$  is close to 1.

A minimal envelope that captures both

- (1) the pointwise Hölder-type decay of  $\omega$  near the origin, and
- (2) the concentration of the support toward the axis,

is

$$\omega_{\text{env}}(r, z) := -|(r, z)|^\beta \mathbf{1}_{\{c|z|^\gamma \leq r \leq C|z|^\gamma\}} \mathbf{1}_{\{|z| \leq 1\}} \text{sgn}(z), \quad \beta > 0, \quad \gamma > 1, \quad (45)$$

where

$$\gamma \sim \frac{\log \frac{1}{d_{\text{CMZ}}} + 2 \log A_{\text{CMZ}}}{\log \frac{1}{d_{\text{CMZ}}} - 4 \log A_{\text{CMZ}}} > 1, \quad \beta \sim \frac{\log A_{\text{CMZ}}}{\log \frac{1}{d_{\text{CMZ}}} + 2 \log A_{\text{CMZ}}} \ll 1.$$

Here  $\gamma$  is close to 1. The expressions of  $\gamma, \beta$  are valid for an amplitude  $A_{\text{CMZ}} > 1$  close to 1. One can find the expression of  $\gamma, \beta$  by using (44) together with  $r \sim R_k^{\text{CMZ}}(t)$  and  $|z| \sim H_k^{\text{CMZ}}(t)$ . For the expression of  $\beta$ , it can be also found in [CMZ25, § 1.3.2]. We will use (45) below to make the Lorentz/Hölder comparison transparent.

1.11.2. *Comparison with Our data and Solution: Lorentz Spaces, Geometry, and the Impossibility of a Backward Problem.*

**(1) CMZ backward-evolved initial data are more singular than ours in the Lorentz scale.** The key quantity for Danchin-type criticality is the transported relative vorticity  $\omega/r$ , cf. (6), and Lorentz norms of  $\omega/r$  are propagated along the flow.

It is therefore enough to compute  $\omega/r$  from the explicit terminal configuration (42). On the support of the  $k$ -th CMZ ring at  $t = T$  one has  $r \sim d_{\text{CMZ}}^k$ , and hence

$$\left| \frac{\omega_k^{\text{CMZ}}(r, z, T)}{r} \right| \sim \frac{A_{\text{CMZ}}^k}{d_{\text{CMZ}}^k} = \left( \frac{A_{\text{CMZ}}}{d_{\text{CMZ}}} \right)^k.$$

Moreover, since each ring is localized at scale  $d_{\text{CMZ}}^k$  in all directions at  $t = T$ , its support has volume  $|\text{supp } \omega_k^{\text{CMZ}}(T)| \sim d_{\text{CMZ}}^{3k}$ . Consequently, for any  $1 \leq p < \infty$ ,

$$\left\| \frac{\omega_k^{\text{CMZ}}(T)}{r} \right\|_{L^p(\mathbb{R}^3)}^p \sim \left( \frac{A_{\text{CMZ}}^k}{d_{\text{CMZ}}^k} \right)^p d_{\text{CMZ}}^{3k} = A_{\text{CMZ}}^{kp} d_{\text{CMZ}}^{k(3-p)}. \quad (46)$$

Summing over  $k$  gives a sharp integrability threshold:

$$\frac{\omega_{(\infty)}^{\text{CMZ}}(t)}{r} \in L_{\text{loc}}^p \iff p < p_*, \quad p_* := \frac{3 \log(1/d_{\text{CMZ}})}{\log A_{\text{CMZ}} + \log(1/d_{\text{CMZ}})} < 3.$$

In particular,  $\omega_{(\infty)}^{\text{CMZ}}(t)/r \notin L_{\text{loc}}^{3,1}$  and hence it lies outside Danchin's endpoint class  $L^{3,1}$  (and outside  $L^{3,q}$  for any finite  $q$ ). More precisely, the ring counting implicit in (46) yields the distribution estimate  $|\{\omega_{(\infty)}^{\text{CMZ}}/r > \lambda\}| \sim \lambda^{-p_*}$ , so

$$\frac{\omega_{(\infty)}^{\text{CMZ}}(t)}{r} \in L_{\text{loc}}^{p_*, \infty} \quad \text{but} \quad \frac{\omega_{(\infty)}^{\text{CMZ}}(t)}{r} \notin L_{\text{loc}}^{p_*, q} \quad \text{for any } q < \infty. \quad (47)$$

By contrast, our construction starts from data  $\omega_0^{(\infty)}$  with  $\omega_0^{(\infty)}/r \in L^{3,q}(\mathbb{R}^3)$  for some  $q > 1$ , and we can make this  $L^{3,q}$  norm arbitrarily small. Thus, in terms of Lorentz criticality for  $\omega^{(\infty)}/r$ , the CMZ backward-evolved initial data are *strictly more singular* than ours: they sit only at a weaker exponent  $p_* < 3$ .

**(2) CMZ's backward-evolved data are more regular than ours in the Hölder scale.** Despite being more singular than our data in the Lorentz scale, CMZ's backward-evolved data (with infinite rings) is more regular than ours in the Hölder scale. Indeed, CMZ's backward-evolved data is Hölder continuous at the origin whereas ours  $\omega_0^{(\infty)}$  is not. Hence the evolution of their data is locally classical and well-posed in that topology (local well-posedness in Hölder spaces is explained in the next section 1.12) whereas our data are in an ill-posedness regime.

**(3) Why there is no contradiction: pointwise vs. integral scales, and the role of geometry.** The comparison between CMZ's backward-evolved data and ours is subtle because the two scales measure different aspects of singularity.

On the one hand, Hölder regularity is a *pointwise*,  $L^\infty$ -based notion. Near the origin it asks how fast  $\omega(r, z)$  itself vanishes at each point. On the other hand, the Lorentz scale relevant here is not attached to  $\omega$  itself, but to the transported quantity  $\omega/r$  in (6). This is an *integral*  $L^p$ -type measurement, so it depends not only on the pointwise size of  $\omega$ , but also on how much of the support lies in the region where  $r$  is very small. Thus the factor  $r^{-1}$  and the geometry of the support near the axis are largely invisible in the Hölder scale, but they are decisive in the Lorentz scale.

For CMZ, the backward-evolved initial data at  $t = 0$  are concentrated in increasingly thin regions near the axis; equivalently, their aspect ratios  $\Gamma_k^{\text{CMZ}}$  are large, see (43). In the envelope model (45), this is encoded by

$$r \sim |z|^\gamma, \quad \gamma > 1, \quad \omega_{\text{env}}(r, z) \sim -|(r, z)|^\beta \text{sgn}(z).$$

Hence CMZ have a genuine *pointwise power decay* of  $\omega$  near the origin, which is compatible with a Hölder-based local well-posedness regime. However, because  $r \ll |z|$  on the support, dividing by  $r$  creates a much larger quantity:

$$\frac{\omega_{\text{env}}(r, z)}{r} \sim -\frac{|z|^\beta}{|z|^\gamma} \text{sgn}(z) = -|z|^{\beta-\gamma} \text{sgn}(z).$$

Therefore  $\omega/r$  can be highly singular even though  $\omega$  itself is Hölder. Since Lorentz norms measure the distribution of large values of  $\omega/r$ , this thin concentration near the axis makes CMZ's backward-evolved data more singular in the Lorentz scale.

Our data have the opposite feature. Recall the continuous model of our data (10), that is,

$$\omega_0(r, z) \sim -\frac{1}{(\log(1/|(r, z)|))^\alpha} \text{sgn}(z) \quad \text{on } \{r \sim |z|\}$$

This is worse pointwise than any power  $|(r, z)|^\beta$ , so our data are not Hölder at the origin. But now there is no extra concentration toward the axis: on the support, the factor  $r^{-1}$  is comparable to  $|(r, z)|^{-1}$ . Hence,

$$\frac{\omega_0(r, z)}{r} \sim -\frac{1}{|(r, z)|(\log(1/|(r, z)|))^\alpha} \text{sgn}(z) \quad \text{on } \{r \sim |z|\}$$

which is the borderline behavior tailored to belong to  $L^{3,q}$  for  $q > 1$  as we already observed in Section 1.2.

So the difference is not merely that CMZ's backward-evolved data and our data have different norms. Rather, they optimize different features. CMZ are *pointwise milder* but *geometrically more concentrated* near the axis; we are *pointwise rougher* but *geometrically less concentrated* toward the axis. This is exactly why CMZ's backward-evolved data are more regular in the Hölder scale while being more singular in the Lorentz scale.

**(4) CMZ are not worst-case in their Lorentz class; a worst-case model.** Even though CMZ's backward-evolved initial data is more singular than ours in terms of Lorentz criticality, their solution does not exhibit more “singular” behavior than ours. To explain this discrepancy, the stretching rate  $u^r/r$  is controlled by an  $|x|^{-2}$ -type singular integral of  $\omega/r$ , as reflected in the heuristic behind (7). For a fixed Lorentz size of  $\omega/r$ , the strongest amplification is obtained by placing the vorticity where the kernel in the Biot–Savart law is largest. In particular, the kernel in

(9) carries a factor  $r^2 z / (r^2 + z^2)^{5/2}$ , so the dominant contribution comes from the conical region  $r \sim |z|$  (this is precisely why the worst-case scenario (10) is conical).

CMZ's configuration at the initial time  $t = 0$  is instead highly anisotropic (large  $\Gamma_k^{\text{CMZ}}$ ), meaning it is concentrated closer to the axis, where the kernel in (9) is suppressed by extra powers of  $r/|z|$ . This can be seen transparently on the envelope (45). Using (9) and  $r \sim |z|^\gamma$  (so  $r \ll |z|$ ), we have  $(r^2 + z^2)^{5/2} \sim |z|^5$ . Therefore, the stretching functional has the scaling

$$\iint \frac{r^2 z}{(r^2 + z^2)^{5/2}} \omega_{\text{env}}(r, z) dr dz \sim \int_0^1 |z|^\beta \int_{c|z|^\gamma}^{C|z|^\gamma} \frac{r^2}{|z|^4} dr dz \sim \int_0^1 z^{3\gamma + \beta - 4} dz,$$

which is finite whenever  $3\gamma + \beta > 3$ , in particular for any  $\gamma > 1$  and any  $\beta > 0$ . Thus CMZ can be Lorentz-supercritical while still having finite initial stretching in the sense of (9), because their support geometry avoids the worst-case region for the kernel.

By contrast, a natural "worst-case" model in the Lorentz class  $L^{p^*, \infty}$  suggested by (47) is to place  $\omega/r$  conically with the borderline power law

$$\frac{\omega_{\text{worst}}(r, z)}{r} \sim -\frac{1}{|(r, z)|^{3/p^*}} \mathbf{1}_{\{r \sim |z|, |(r, z)| \leq 1\}} \text{sgn}(z), \quad p^* < 3.$$

This saturates the weak- $L^{p^*}$  scaling and, when inserted into the heuristic  $u^r/r \sim |x|^{-2} * (\omega/r)$ , yields a divergent stretching rate at the origin. In this sense, the CMZ configuration is not the worst-case configuration inside its Lorentz class.

**(5) Why CMZ can run a backward problem, while we cannot (and the link to self-slowdown).** CMZ's backward organization is compatible with their goal: they prescribe a singular final state at  $t = T$  and evolve backward to obtain regular data at  $t = 0$  in a Hölder class. The required Hölder regularity does not have the same scaling as the blow-up quantity, the  $L^\infty$  norm of vorticity.

For our norm inflation, however, the required Lorentz regularity,  $\omega_0/r \in L^{3,q}(\mathbb{R}^3)$ , has the *same scaling* as the inflation quantity, the  $L^\infty$  norm of vorticity, and we must start from *small* data in the critical Lorentz class  $L^{3,q}$  for  $\omega/r$ .

Since  $\omega/r$  is transported by (6), its Lorentz norm is conserved in time. Moreover, for our dyadic vortex-ring architecture (finite superposition as in (14)), the  $L^{3,q}$  norm is essentially an  $\ell^q$  norm of the ring amplitudes. Indeed, assume at the final time  $t = T$  (more precisely, norm inflation time) the  $k$ -th ring has the canonical form

$$\omega_k(r, z, T) = x_k^T W\left(\frac{r}{d^k}, \frac{z}{d^k}\right),$$

a scaling computation gives

$$\left\| \frac{\omega^{(m)}|_{t=T}}{r} \right\|_{L^{3,q}(\mathbb{R}^3)}^q \sim \sum_{k=1}^m |x_k^T|^q. \quad (48)$$

Since (48) is invariant under the transport (6), any attempt to prescribe a *final* state at  $t = T$  and solve backward forces

$$\left\| \frac{\omega^{(m)}|_{t=0}}{r} \right\|_{L^{3,q}}^q = \left\| \frac{\omega^{(m)}|_{t=T}}{r} \right\|_{L^{3,q}}^q \sim \sum_{k=1}^m |x_k^T|^q \geq \left( \max_{1 \leq k \leq m} |x_k^T| \right)^q \sim \|\omega^{(m)}|_{t=T}\|_{L^\infty(\mathbb{R}^3)}^q.$$

Hence one cannot make  $\|\omega^{(m)}|_{t=T}\|_{L^\infty}$  large while keeping  $\|\omega^{(m)}|_{t=0}/r\|_{L^{3,q}}$  small: the backward problem is incompatible with the small-data norm inflation goal.

This obstruction is precisely why our analysis must be organized *forward in time*. But in forward time, as explained in Subsection 1.4 and encoded in the weak cascade model (24), vortex stretching drives the aspect ratios  $\Gamma_k(t) = H_k(t)/R_k(t)$  to become small, which suppresses the Biot–Savart coefficient and produces the *geometric self-slowdown* mechanism. Overcoming this self-slowdown in a Lorentz-critical regime is the main additional difficulty in our problem compared to the backward cascade strategy of CMZ.

**1.12. Hölder Spaces.** Lastly, as the study of well-posedness/ill-posedness in Lorentz spaces  $L^{3,q}(\mathbb{R}^3)$  is closely related to borderline Hölder regularity, we briefly review some relevant background.

First of all, without imposing axisymmetry (and allowing swirl), classical local well-posedness for  $u_0 \in C^{k,\alpha}(\mathbb{R}^3)$  ( $k \geq 1$ ,  $\alpha \in (0, 1)$ ) goes back to [Lic30, Gun27]. It was later extended to Sobolev data  $u_0 \in H^s(\mathbb{R}^3)$  with  $s > \frac{5}{2}$  (more generally,  $s > \frac{n}{2} + 1$  in  $\mathbb{R}^n$ ) in [EM70, Kat72].

On the other hand, ill-posedness in the critical Sobolev space  $H^{\frac{5}{2}}(\mathbb{R}^3)$  was proved in [BL15, BL21]. A simplified proof in a closely related spirit was later found by Kim–Jeong [KJ22].

**Axisymmetric no-swirl blow-up vs. global regularity.** Finite-time blow-up solutions in the axisymmetric no-swirl class have been constructed from low Hölder regularity in [Elg21, CMZ25]. Equivalently, these results may be viewed as singularity formation for  $C^{1,\alpha}$  velocities, or  $C^\alpha$  vorticities, with small  $\alpha > 0$ .

On the other hand, Danchin’s global well-posedness theory implies global regularity in the axisymmetric no-swirl setting for  $\alpha > \frac{1}{3}$ , assuming suitable decay at infinity. Indeed, if  $\omega_0 \in C^\alpha(\mathbb{R}^3)$  is axisymmetric without swirl, then  $\omega_0^\theta$  vanishes on the axis and satisfies  $|\omega_0(r, z)| \lesssim r^\alpha$  near  $r = 0$ , hence

$$\frac{|\omega_0(r, z)|}{r} \lesssim r^{\alpha-1} \in L_{\text{loc}}^{3,1}(\mathbb{R}^3) \quad \text{if and only if} \quad \alpha > \frac{1}{3}.$$

Combining this with local well-posedness in Hölder spaces and the Beale–Kato–Majda criterion yields global regularity for  $\omega_0 \in C^\alpha$  with  $\alpha > \frac{1}{3}$ .

During the final preparation of this paper, a recent preprint by Shkoller [Shk26] announced a construction of finite-time blow-up for every  $\alpha \in (0, \frac{1}{3})$  for axisymmetric no-swirl data in  $C^{1,\alpha}(\mathbb{R}^3) \cap L^2(\mathbb{R}^3)$ , which means the threshold  $\alpha = \frac{1}{3}$  is sharp up to the endpoint. Moreover, his blow-up mechanism is structurally stable, in the sense that it persists for an open set of admissible angular profiles.

Both our work and Shkoller’s reduce the axisymmetric Euler dynamics to an ODE mechanism capturing vortex stretching near the symmetry axis. The reductions, however, are fundamentally different: Shkoller works with a Lagrangian clock-and-driver system for the on-axis strain and pressure Hessian, while our argument uses a multiscale ansatz for dyadic vortex rings, leading to an outer-ring-driven ODE cascade for amplitudes and aspect ratios. Our key input is the geometric localization and front-migration mechanism for the Biot–Savart coefficient, whereas his key input is a nonperturbative strain-versus-pressure estimate.

### The critical Hölder space $C^{1/3}$ for vorticity.

Given Shkoller’s result [Shk26], it is worth noting that at the borderline Hölder exponent  $\alpha = 1/3$ , Danchin’s criterion still yields global regularity provided the vanishing of the angular vorticity on the symmetry axis is improved by an integrable logarithmic factor; if

$$|\omega_0(r, z)| \sim \frac{r^{1/3}}{(\log(e/r))^\beta}, \quad \beta \geq 0, \quad \text{near } r = 0,$$

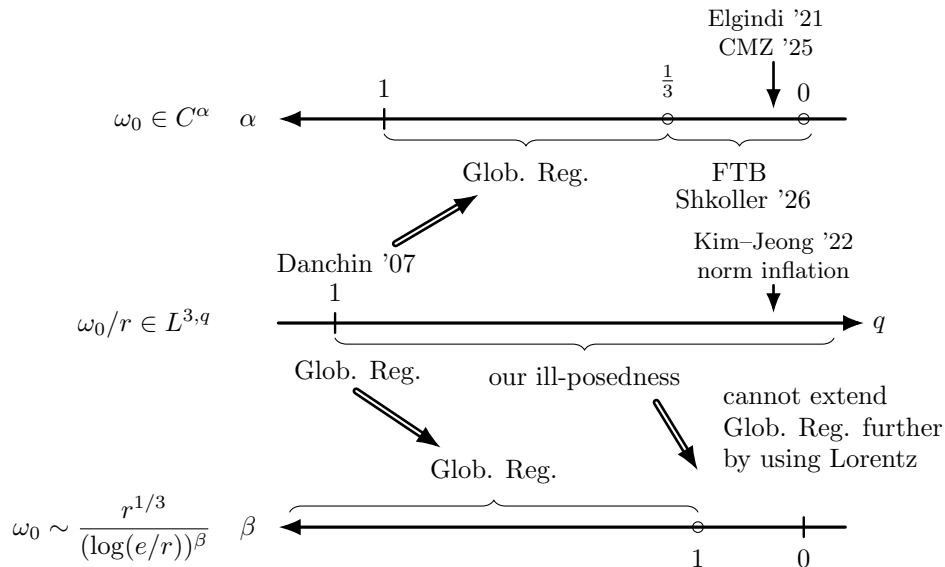


FIGURE 5. Schematic relation between the Hölder threshold and the Lorentz threshold for axisymmetric no-swirl Euler. Here, Glob. Reg. and FTB stand for global regularity and finite-time blow-up respectively. Top: Danchin plus local Hölder theory imply global regularity for  $\alpha > \frac{1}{3}$ , while Shkoller’s result gives finite-time blow-up for every  $\alpha \in (0, \frac{1}{3})$ ; earlier blow-up results of Elgindi and CMZ covered the case when  $\alpha > 0$  is small. Middle: Danchin gives global well-posedness at  $\omega_0/r \in L^{3,1}$ , Kim–Jeong proved ill-posedness for sufficiently large  $q$ , whereas our result is ill-posedness for every  $q > 1$ . Bottom: at the borderline  $\alpha = \frac{1}{3}$ , the logarithmically improved model  $\omega_0 \sim r^{1/3}/(\log(e/r))^\beta$  is still covered by Danchin when  $\beta > 1$ ; the right-hand arrow indicates that our Lorentz-space ill-posedness prevents one from extending this global regularity statement further by Lorentz methods alone.

and  $\omega_0$  is bounded with suitable decay at infinity, then

$$\frac{\omega_0}{r} \in L^{3,q}(\mathbb{R}^3), \quad \beta q > 1, \quad 1 \leq q < \infty.$$

Therefore, if  $\beta > 1$ , then  $\omega_0/r \in L^{3,1}(\mathbb{R}^3)$  so the corresponding axisymmetric no-swirl Euler solution is global.

On the other hand, when  $\beta \in (0, 1]$ , the relative vorticity  $\omega_0/r$  only belongs to  $L^{3,q}(\mathbb{R}^3)$  for  $q > 1/\beta \geq 1$ . As our ill-posedness results imply these Lorentz spaces are ill-posed for any  $q > 1$ , one cannot extend the global regularity in the Hölder scale beyond  $\beta > 1$  towards  $\beta \in (0, 1]$  by merely using well-posedness in the Lorentz scale for  $q > 1$ .

A schematic relation between the Hölder and the Lorentz criticality is drawn in Figure 5.

**1.13. Notation Conventions.** We record the notation conventions used throughout the paper. First, we distinguish three levels of variables. The physical solution is denoted by  $u$  and  $\omega$ , and physical points are written in cylindrical coordinates  $(r, \theta, z)$ . When the reference point matters, we write  $(r_x, \theta_x, z_x)$  for  $x \in \mathbb{R}^3$ . The  $k$ -th vortex ring is described in rescaled coordinates by the profile variables  $W_k, V_k$ , and the flow map  $X_k$ , together with the amplitude and geometry parameters  $x_k$ ,

$R_k$ , and  $H_k$ . Since the  $k$ -th ring is placed at spatial scale  $d^k$ , smaller indices correspond to larger, more outer rings; accordingly, sums over  $j < k$  represent the influence of outer rings on the  $k$ -th ring. Finally, the quantities  $\Gamma_k$ ,  $\Lambda$ ,  $\Lambda_j$ ,  $b_j$ ,  $S_k$ ,  $\zeta_k$ , and  $\Psi$  belong to the ODE/stretching cascade and should be read as reduced bookkeeping variables for the multiscale dynamics. A comprehensive lookup table for all these symbols is given in Appendix C.

In the main parts of the proofs of Theorems 1.1 and 1.2, we use the following convention for constants. The fundamental parameters are  $\tilde{\varepsilon} > 0$  and  $q > 1$ . After  $q$  is fixed, the associated quantities  $L_q$ ,  $\alpha_q$ , and  $\phi_q$  are also regarded as fixed. After  $\tilde{\varepsilon}$  is fixed and  $\varepsilon = \varepsilon(\tilde{\varepsilon}, q)$  is chosen in § 3.1, this  $\varepsilon$  is likewise treated as fixed. Unsubscripted constants  $C, c, \dots$  may depend on all of these fixed parameters including the globally fixed, geometric parameters introduced below, but unsubscripted constants are independent of the running parameters  $k, m, A, t, T_N, T_B$  unless explicitly indicated.

We also regard the geometric parameters  $r_0, \eta, \mu, d$  as fixed once and for all. In the present paper we take

$$r_0 = 1, \quad \eta = \frac{1}{4}, \quad \mu = \frac{1}{20}, \quad d = 10^{-2}.$$

We continue to write the letters  $r_0, \eta, \mu$ , and  $d$  in the estimates in order to keep the geometric meaning of the formulas visible. The particular numerical choice of these constants is not essential. Harmless constants may depend on these fixed parameters without further comment, but we suppress this dependence.

When we write  $C(q)$  or  $C_E(q)$ , the displayed  $q$  indicates only the dependence relevant to the discussion; such constants may still depend on the other fixed background parameters introduced above. Similarly, named constants such as  $C_E$  or  $C_{\text{sep}}$  are simply labels for constants and obey the same convention unless a different dependence is stated locally.

When the domain of integration or of a norm is the whole space and no confusion can arise, we omit it. Unsubscripted constants  $C, c, \dots$  are positive and may change from line to line. We likewise suppress nonessential dependence in symbols such as  $\omega^{(m)}$ ,  $W_k$ ,  $x_k$ ,  $R_k$ ,  $H_k$ ,  $X_k$ ,  $T_N$ , and  $T_B$ , unless that dependence is being used explicitly. This convention is used only in the main parts of the proofs of Theorems 1.1 and 1.2. In lemmas, propositions, and appendices that are stated independently of the main theorems, any special dependence and constant conventions are stated locally.

Lastly, meridional  $(r, z)$ -functions, such as  $W_k, \phi_q$  and  $\omega_k$ , are also identified with their axisymmetric lifts to  $\mathbb{R}^3$ . For example, all  $L^\infty$  norms are taken with respect to this identification. We will write  $\|\phi_q\|_{L^\infty(\mathbb{R}^3)}$  instead of  $\|\phi_q\|_{L^\infty(\mathbb{R}_+ \times \mathbb{R})}$ .

**1.14. Outline of the Paper.** Before we prove the main result, we will first establish a tool (cone-free outer-ring dominance, Proposition 2.1) in Section 2. Section 3 treats the finite-ring problem and proves the norm inflation statement, Theorem 1.1. Section 4 treats the infinite-ring problem and proves instantaneous blow-up, Theorem 1.2. The first part develops the PDE-to-ODE reduction and closes a bootstrap argument; the second part revisits the same multiscale mechanism in a contradiction framework, where the infinitely many rings are handled through a finite-head bootstrap together with a separate control of the tail.

More precisely, in Section 3 we first fix the initial data, the rescaled variables, and the ansatz in § 3.1, and we summarize the bootstrap strategy in § 3.2. In § 3.3, we derive the Cauchy formula for the rescaled profiles and use the bootstrap assumptions to freeze the transported profiles inside the Biot–Savart integrals. Section 3.4 is the ODE core of the paper: there we analyze the weak cascade for the ring amplitudes and aspect ratios, establish the front-migration lower bound, and obtain

quantitative control of the ODE norm-inflation time. In § 3.5, we return to the PDE and prove confinement of supports, scale separation, and bounds for the inner, outer, and self-induced velocity contributions; these estimates improve the bootstrap assumptions and identify the bootstrap time with the ODE norm-inflation time. The proof of Theorem 1.1 is then completed in § 3.6.

Section 4 proves Theorem 1.2. In § 4.1, we collect the preliminary ingredients needed for Theorem 1.2-(1). In § 4.2, we carry out the finite-head bootstrap for the infinite-ring configuration and combine it with the contradiction hypothesis to prove the nonexistence result, Theorem 1.2-(1). Section 4.3 shows that subsequential limits of the finite-ring approximations yields an (axisymmetric no-swirl) distributional solution that blows up instantaneously, which proves Theorem 1.2-(2).

The appendices collect auxiliary material. Appendix A contains the proofs of the Danskin-type lemma and the Cauchy formula. Appendix B records two auxiliary ODE analyses discussed heuristically in § 1.8 but not used in the proofs of the main theorems: § B.1 treats the flattened-coefficient model, while § B.2 treats the frozen-profile model with a non-flattened Biot–Savart coefficient. Finally, Appendix C is a list of notation for quick reference.

## 2. CONE-FREE OUTER-REGION DOMINANCE

In this section, before we prove our main results, we prove one of the tools we will use. We will prove that the outer region is dominant when estimating the velocity field  $u$  induced by vorticity  $\omega$  via the Biot–Savart law provided that  $\omega$  is *odd-symmetric in  $z$* .

See our sign convention related to the Biot–Savart law in Appendix C.

Let us first briefly review a lemma on this topic established by Kim–Jeong [KJ22, Lemma 2.1]. They proved the dominance of the outer-region, that is,

$$\begin{aligned} \left| \frac{u^r(x)}{r_x} - \frac{3}{8\pi} \int_{Q(r_x)} \frac{r_y z_y}{|y|^5} (-\omega(y)) dy \right| &\leq C \|\omega\|_{L^\infty}, \\ \left| \frac{u^z(x)}{z_x} + \frac{3}{4\pi} \int_{Q(r_x)} \frac{r_y z_y}{|y|^5} (-\omega(y)) dy \right| &\leq C \left( 1 + \left| \log \frac{r_x}{|z_x|} \right| \right) \|\omega\|_{L^\infty} \end{aligned} \quad (49)$$

where  $Q(r_x) := \{y \in \mathbb{R}^3 : r_y \geq 2r_x\}$ , under the odd-symmetry assumption together with  $\omega \in L^\infty \cap L^2(\mathbb{R}^3)$  and a cone restriction

$$r_x \geq |z_x|. \quad (50)$$

Due to the cone restriction (50), it is not applicable to our situation since a large cone-slope  $L_q = z_{0,q}/r_0$  plays a central role in our analysis. Hence, one needs to generalize their cone restriction to an arbitrary cone slope  $L \geq |z_x|/r_x$ . At the same time, it is reasonable to try to generalize it while keeping the outer-region  $Q(r_x)$ , that is independent of the cone slope  $L$ . Otherwise, a large cone slope  $L_q$  will impose a more restrictive scale separation between rings.

To this end, our strategy is to first completely remove the cone restriction from Kim–Jeong’s lemma in order to isolate the role of the cone restriction. Then we apply a generalized cone restriction to the cone-free lemma when we utilize it for our main results.

With the cone restriction, it holds  $|x| \sim r_x$ . Hence, it is natural to try to make estimates with  $Q(r_x)$  in (49) replaced by  $Q(|x|)$ . However, we still want to keep the outer-region  $Q(r_x)$ . Hence, we will first derive the  $Q(|x|)$ -estimates and extend it to  $Q(r_x)$ -estimates.

**Proposition 2.1** (Cone-free outer-region dominance). *Assume that a function  $\omega = \omega(r, z) \in L^\infty \cap L^2(\mathbb{R}^3)$  and an axisymmetric, no-swirl velocity field  $u$  are related via the axisymmetric Biot–Savart law (5). Assume further that  $\omega$  is odd with respect to  $z$ :  $\omega(r, z) = -\omega(r, -z)$ . For any*

$x \in \mathbb{R}^3$  and any positive number  $\rho > 0$ , define an outer-region domain  $Q(\rho)$  by

$$Q(\rho) := \{y \in \mathbb{R}^3 : r_y \geq 2\rho\}.$$

and denote the velocity-errors that we want to estimate by

$$\begin{aligned} E^r(x; \rho) &:= \frac{u^r(x)}{r_x} - \frac{3}{8\pi} \int_{Q(\rho)} \frac{r_y z_y}{|y|^5} (-\omega(y)) dy, & r_x > 0 \\ E^z(x; \rho) &:= \frac{u^z(x)}{z_x} + \frac{3}{4\pi} \int_{Q(\rho)} \frac{r_y z_y}{|y|^5} (-\omega(y)) dy, & z_x \neq 0. \end{aligned}$$

Then there exists an absolute constant  $C > 0$  such that for any  $x \in \mathbb{R}^3$ , the following estimates hold whenever the displayed denominators are nonzero:

- **The outer-region  $Q(|x|)$  with the largest cut-off scale  $|x|$ .**

$$|E^r(x; |x|)| \leq C \frac{|x|}{r_x} \|\omega\|_{L^\infty(\mathbb{R}^3)}, \quad (51)$$

$$|E^z(x; |x|)| \leq C \left(1 + \log \frac{|x|}{|z_x|}\right) \|\omega\|_{L^\infty(\mathbb{R}^3)};$$

- **An outer-region  $Q(\rho)$  with a smaller cut-off scale  $\rho \leq |x|$ . For any  $0 < \rho \leq |x|$ ,**

$$|E^r(x; \rho)| \leq C \left(\frac{|x|}{r_x} + \log \frac{|x|}{\rho}\right) \|\omega\|_{L^\infty(\mathbb{R}^3)},$$

$$|E^z(x; \rho)| \leq C \left(1 + \log \frac{|x|}{|z_x|} + \log \frac{|x|}{\rho}\right) \|\omega\|_{L^\infty(\mathbb{R}^3)};$$

- **A special outer-region  $Q(r_x)$  with  $\rho = r_x$ .**

$$|E^r(x; r_x)| \leq C \frac{|x|}{r_x} \|\omega\|_{L^\infty(\mathbb{R}^3)}, \quad (52)$$

$$|E^z(x; r_x)| \leq C \left(1 + \left| \log \frac{r_x}{|z_x|} \right| \right) \|\omega\|_{L^\infty(\mathbb{R}^3)}.$$

The estimates for  $Q(\rho)$ ,  $\rho \leq |x|$ , and  $Q(r_x)$  follow from the  $Q(|x|)$  estimates and the elementary annular enlargement bound

$$\left| \int_{Q(\rho) \setminus Q(|x|)} \frac{r_y z_y}{|y|^5} \omega(y) dy \right| \leq \frac{4\pi}{3} \log \frac{|x|}{\rho} \|\omega\|_{L^\infty}, \quad 0 < \rho \leq |x|.$$

Indeed, in cylindrical coordinates,

$$\int_{Q(\rho) \setminus Q(|x|)} \left| \frac{r_y z_y}{|y|^5} \right| dy = 2\pi \int_{2\rho}^{2|x|} \int_{\mathbb{R}} \frac{s^2 |z|}{(s^2 + z^2)^{5/2}} dz ds = \frac{4\pi}{3} \int_{2\rho}^{2|x|} \frac{ds}{s} = \frac{4\pi}{3} \log \frac{|x|}{\rho}. \quad (53)$$

As a result of removing the cone restriction, the right-hand side of our radial estimate (52) has a new factor  $|x|/r_x$  as opposed to Kim–Jeong’s Key Lemma. However, a generalized cone condition  $L r_x \geq |z_x|$  will allow us to bound the new factor  $\frac{|x|}{r_x}$  by  $\sqrt{1 + L^2}$ . Thus, the new radial error factor is harmless in our application.

The  $L^2$  condition of  $\omega$  is not optimal but suffices for our proof.

To prove our main result, we will only use the  $Q(r_x)$ -estimates, and we will do so with a generalized cone condition  $L r_x \geq |z_x|$ . But we still stated  $Q(|x|)$ -and  $Q(\rho)$ -estimates since this statement indicates the structure of our proof, and this general statement might be useful for other problems

as various versions of this lemma were derived and used in other literature. See [KJ22, Page 6] for a historical note of the “Key Lemma” in the topic of ill-posedness of the Euler equations for more references.

*Proof.* Throughout the proof,  $C > 0$  denotes an absolute constant which may change from line to line. By rotational invariance, we may assume without loss of generality that

$$x = (r_x, 0, z_x).$$

We write

$$y = (r_y \cos \theta_y, r_y \sin \theta_y, z_y),$$

so that

$$x \cdot y = r_x r_y \cos \theta_y + z_x z_y.$$

For every axisymmetric set  $E \subset \mathbb{R}^3$  and every integrable axisymmetric function  $F = F(r_y, z_y)$ , we shall use

$$\int_E \cos \theta_y F(r_y, z_y) dy = 0, \quad \int_E \cos^2 \theta_y F(r_y, z_y) dy = \frac{1}{2} \int_E F(r_y, z_y) dy. \quad (54)$$

These identities are first justified on truncated sets  $E \cap B_R(0)$  and then by letting  $R \rightarrow \infty$ . The required convergence follows from  $\omega \in L^\infty \cap L^2$  and the fact that the far-field kernels appearing below are square-integrable at infinity.

First note that the main integral is well-defined. Indeed, on  $Q(\rho)$  we have  $|y| \geq r_y \geq 2\rho > 0$ , so there is no singularity near the origin, and

$$\left| \frac{r_y z_y}{|y|^5} \right| \leq \frac{1}{|y|^3}.$$

The function  $|y|^{-3}$  is locally integrable away from the origin and belongs to  $L^2(\{|y| \geq 1\})$ , while  $\omega \in L^\infty \cap L^2$ .

We will mainly estimate the velocity-errors  $E^r(x; |x|), E^z(x; |x|)$  with the outer-region  $Q(|x|)$ . The other estimates follow from elementary computations, which we will carry out at the last step.

**Step 1: the radial estimate.** From the radial component of the axisymmetric Biot–Savart law,

$$u^r(x) = \frac{1}{4\pi} \int_{\mathbb{R}^3} \frac{(z_x - z_y) \cos \theta_y}{|x - y|^3} \omega(y) dy.$$

We write

$$u^r(x) = \frac{1}{4\pi} (I_Q + I_{Q^c}),$$

where

$$I_Q := \int_{Q(|x|)} \frac{(z_x - z_y) \cos \theta_y}{|x - y|^3} \omega(y) dy,$$

$$I_{Q^c} := \int_{Q(|x|)^c} \frac{(z_x - z_y) \cos \theta_y}{|x - y|^3} \omega(y) dy$$

where  $Q(|x|)^c$  denotes the complement of  $Q(|x|)$ .

On  $Q(|x|)$ , we have  $|y| \geq r_y \geq 2|x|$ , and therefore

$$\left| \frac{1}{|x - y|^3} - \frac{1}{|y|^3} - \frac{3x \cdot y}{|y|^5} \right| \leq C \frac{|x|^2}{|y|^5}.$$

Since  $|z_x - z_y| \leq |x| + |y| \leq C|y|$  on  $Q(|x|)$ , the error satisfies

$$|\mathcal{E}_Q| \leq C|x|^2 \|\omega\|_{L^\infty} \int_{|y| \geq 2|x|} \frac{1}{|y|^4} dy \leq C|x| \|\omega\|_{L^\infty}.$$

Thus

$$I_Q = \int_{Q(|x|)} (z_x - z_y) \cos \theta_y \left( \frac{1}{|y|^3} + \frac{3x \cdot y}{|y|^5} \right) \omega(y) dy + \mathcal{E}_Q.$$

The term containing  $|y|^{-3}$  vanishes by the first identity in (54). Since

$$x \cdot y = r_x r_y \cos \theta_y + z_x z_y,$$

the part containing  $z_x z_y \cos \theta_y$  also vanishes by angular integration. Hence

$$I_Q = 3r_x \int_{Q(|x|)} \frac{(z_x - z_y) r_y \cos^2 \theta_y}{|y|^5} \omega(y) dy + \mathcal{E}_Q.$$

The contribution of  $z_x$  vanishes because  $Q(|x|)$  is symmetric with respect to  $z_y \mapsto -z_y$ , while  $r_y |y|^{-5} \cos^2 \theta_y$  is even in  $z_y$  and  $\omega$  is odd in  $z_y$ . Therefore, using the second identity in (54),

$$I_Q = \frac{3r_x}{2} \int_{Q(|x|)} \frac{r_y z_y}{|y|^5} (-\omega(y)) dy + \mathcal{E}_Q, \quad |\mathcal{E}_Q| \leq C|x| \|\omega\|_{L^\infty}. \quad (55)$$

Next, we estimate the complementary region  $Q(|x|)^c = \{r_y < 2|x|\}$ . Since

$$|z_x - z_y| \leq |x - y|,$$

we have

$$|I_{Q^c}| \leq \|\omega\|_{L^\infty} \int_{\{r_y < 2|x|\}} \frac{1}{|x - y|^2} dy.$$

Denoting the projections of  $x, y$  onto the horizontal plane by  $x_h, y_h \in \mathbb{R}^2$ , let  $h = y_h - x_h$  and  $s = z_y - z_x$ . If  $r_y < 2|x|$ , then

$$|h| \leq r_y + r_x \leq 3|x|.$$

Consequently,

$$\int_{\{r_y < 2|x|\}} \frac{1}{|x - y|^2} dy \leq \int_{\{|h| \leq 3|x|\}} \int_{\mathbb{R}} \frac{1}{|h|^2 + s^2} ds dh = C \int_0^{3|x|} d\rho = C|x|.$$

Thus

$$|I_{Q^c}| \leq C|x| \|\omega\|_{L^\infty}.$$

Combining the estimates above gives

$$\left| I_Q + I_{Q^c} - \frac{3r_x}{2} \int_{Q(|x|)} \frac{r_y z_y}{|y|^5} (-\omega(y)) dy \right| \leq C|x| \|\omega\|_{L^\infty}.$$

Since  $u^r(x) = \frac{1}{4\pi}(I_Q + I_{Q^c})$ , dividing by  $r_x$  proves (51).

**Step 2: an elementary logarithmic integral.** We shall use the following estimate: for all  $R > 0$  and  $a > 0$ ,

$$\int_{\{|h| \leq R\}} \int_0^\infty \frac{z}{(|h|^2 + (z - a)^2)(|h|^2 + (z + a)^2)} dz dh \leq C \left( 1 + \log_+ \frac{R}{a} \right), \quad (56)$$

where  $\log_+ s := \max\{\log s, 0\}$ .

Indeed, writing  $\rho = |h|$ , we first observe that

$$\begin{aligned} \int_0^\infty \frac{z}{(\rho^2 + (z-a)^2)(\rho^2 + (z+a)^2)} dz &= \frac{1}{4a} \int_0^\infty \left[ \frac{1}{\rho^2 + (z-a)^2} - \frac{1}{\rho^2 + (z+a)^2} \right] dz \\ &= \frac{1}{4a} \int_{-a}^a \frac{1}{\rho^2 + s^2} ds = \frac{1}{2a\rho} \arctan\left(\frac{a}{\rho}\right). \end{aligned}$$

Therefore,

$$\int_{\{|h| \leq R\}} \int_0^\infty \frac{z}{(|h|^2 + (z-a)^2)(|h|^2 + (z+a)^2)} dz dh = \frac{\pi}{a} \int_0^R \arctan\left(\frac{a}{\rho}\right) d\rho.$$

The part  $0 < \rho \leq a$  is bounded by an absolute constant, and for  $\rho \geq a$  we use  $\arctan(a/\rho) \leq a/\rho$ . This proves (56).

**Step 3: the vertical estimate.** We will estimate for  $u^z$ . By the reflection symmetry in  $z$ , it is enough to consider  $z_x > 0$ . Indeed, if  $\tilde{x} = (r_x, 0, -z_x)$ , then

$$u^z(\tilde{x}) = -u^z(x), \quad \tilde{z}_x = -z_x, \quad Q(|\tilde{x}|) = Q(|x|).$$

Thus the estimate for  $\tilde{x}$  is equivalent to the estimate for  $x$ .

Assume now  $z_x > 0$ . Let

$$\bar{y} := (y_h, -z_y), \quad A := |x - y|, \quad B := |x - \bar{y}|.$$

Using the oddness of  $\omega$  in  $z_y$ , we rewrite the vertical Biot–Savart law as

$$u^z(x) = -\frac{1}{4\pi} \int_{\{z_y > 0\}} (r_x \cos \theta_y - r_y) \left( \frac{1}{A^3} - \frac{1}{B^3} \right) \omega(y) dy.$$

Since

$$B^2 - A^2 = 4z_x z_y,$$

we have the exact identity

$$\frac{1}{A^3} - \frac{1}{B^3} = \frac{4z_x z_y (A^2 + AB + B^2)}{A^3 B^3 (A + B)}. \quad (57)$$

Write

$$u^z(x) = \frac{1}{4\pi} (J_Q + J_{Q^c}),$$

where the two terms are the integrals over

$$Q(|x|) \cap \{z_y > 0\}, \quad Q(|x|)^c \cap \{z_y > 0\},$$

respectively.

We first estimate  $J_Q$ . On  $Q(|x|)$ , we have

$$\frac{1}{2}|y| \leq A, B \leq \frac{3}{2}|y|.$$

Define

$$G(a, b) := \frac{a^2 + ab + b^2}{a^3 b^3 (a + b)}.$$

Then  $G$  is smooth near  $(1, 1)$  and  $G(1, 1) = 3/2$ . Hence

$$\left| \frac{A^2 + AB + B^2}{A^3 B^3 (A + B)} - \frac{3}{2|y|^5} \right| \leq C \frac{|x|}{|y|^6} \quad \text{on } Q(|x|).$$

Using (57), we obtain

$$J_Q = -6z_x \int_{Q(|x|) \cap \{z_y > 0\}} (r_x \cos \theta_y - r_y) \frac{z_y}{|y|^5} \omega(y) dy + \mathcal{E}_Q^z.$$

The term containing  $r_x \cos \theta_y$  vanishes by angular integration, and therefore

$$J_Q = 6z_x \int_{Q(|x|) \cap \{z_y > 0\}} \frac{r_y z_y}{|y|^5} \omega(y) dy + \mathcal{E}_Q^z.$$

The error satisfies

$$\begin{aligned} |\mathcal{E}_Q^z| &\leq C z_x |x| \|\omega\|_{L^\infty} \int_{|y| \geq 2|x|} \frac{(r_x + r_y) z_y}{|y|^6} dy \\ &\leq C z_x |x| \|\omega\|_{L^\infty} \int_{|y| \geq 2|x|} \frac{1}{|y|^4} dy \leq C z_x \|\omega\|_{L^\infty}. \end{aligned}$$

It remains to estimate  $J_{Q^c}$ , the contribution of  $Q(|x|)^c \cap \{z_y > 0\}$ . As above,

$$\left| (r_x \cos \theta_y - r_y) \left( \frac{1}{A^3} - \frac{1}{B^3} \right) \right| \leq C z_x \frac{z_y}{A^2 B^2}.$$

On  $Q(|x|)^c = \{r_y < 2|x|\}$ , if  $h = y_h - x_h$ , then  $|h| \leq 3|x|$ . Thus, by (56) with  $R = 3|x|$  and  $a = z_x$ ,

$$\begin{aligned} |J_{Q^c}| &\leq C z_x \|\omega\|_{L^\infty} \int_{\{|h| \leq 3|x|\}} \int_0^\infty \frac{z_y}{(|h|^2 + (z_y - z_x)^2)(|h|^2 + (z_y + z_x)^2)} dz_y dh \\ &\leq C z_x \left( 1 + \log \frac{|x|}{z_x} \right) \|\omega\|_{L^\infty}. \end{aligned}$$

Combining the estimates for  $J_Q, J_{Q^c}$ , we obtain

$$\left| J_Q + J_{Q^c} + 6z_x \int_{Q(|x|) \cap \{z_y > 0\}} \frac{r_y z_y}{|y|^5} (-\omega(y)) dy \right| \leq C z_x \left( 1 + \log \frac{|x|}{z_x} \right) \|\omega\|_{L^\infty}.$$

Finally, since  $z_y \omega(y)$  is even in  $z_y$ ,

$$\int_{Q(|x|) \cap \{z_y > 0\}} \frac{r_y z_y}{|y|^5} \omega(y) dy = \frac{1}{2} \int_{Q(|x|)} \frac{r_y z_y}{|y|^5} \omega(y) dy.$$

Therefore,

$$\left| J_Q + J_{Q^c} + 3z_x \int_{Q(|x|)} \frac{r_y z_y}{|y|^5} (-\omega(y)) dy \right| \leq C z_x \left( 1 + \log \frac{|x|}{z_x} \right) \|\omega\|_{L^\infty}.$$

Since

$$u^z(x) = \frac{1}{4\pi} (J_Q + J_{Q^c})$$

dividing by  $z_x > 0$  gives

$$\left| \frac{u^z(x)}{z_x} + \frac{3}{4\pi} \int_{Q(|x|)} \frac{r_y z_y}{|y|^5} (-\omega(y)) dy \right| \leq C \left( 1 + \log \frac{|x|}{z_x} \right) \|\omega\|_{L^\infty}.$$

As explained at the beginning of Step 3, the case  $z_x < 0$  follows by reflection. Replacing  $z_x$  by  $|z_x|$  inside the logarithm finishes the proof for the  $Q(|x|)$ -estimate.

**Step 4: smaller cutoffs and the special choice  $\rho = r_x$ .** Let

$$A(\rho) := \int_{Q(\rho)} \frac{r_y z_y}{|y|^5} (-\omega(y)) dy.$$

For  $0 < \rho \leq |x|$ , the annular estimate (53) gives

$$|A(\rho) - A(|x|)| \leq \frac{4\pi}{3} \log \frac{|x|}{\rho} \|\omega\|_{L^\infty}.$$

Hence

$$|E^r(x; \rho)| \leq |E^r(x; |x|)| + \frac{3}{8\pi} |A(\rho) - A(|x|)| \leq C \left( \frac{|x|}{r_x} + \log \frac{|x|}{\rho} \right) \|\omega\|_{L^\infty},$$

and similarly

$$|E^z(x; \rho)| \leq C \left( 1 + \log \frac{|x|}{|z_x|} + \log \frac{|x|}{\rho} \right) \|\omega\|_{L^\infty}.$$

Taking  $\rho = r_x$ , the radial estimate follows from

$$\log \frac{|x|}{r_x} \leq C \frac{|x|}{r_x}.$$

For the vertical estimate,

$$\log \frac{|x|}{|z_x|} + \log \frac{|x|}{r_x} = \log \frac{|x|^2}{|z_x| r_x} = \log \left( \frac{r_x}{|z_x|} + \frac{|z_x|}{r_x} \right) \leq C \left( 1 + \left| \log \frac{r_x}{|z_x|} \right| \right).$$

Therefore

$$|E^z(x; r_x)| \leq C \left( 1 + \left| \log \frac{r_x}{|z_x|} \right| \right) \|\omega\|_{L^\infty}.$$

□

### 3. NORM INFLATION

We are now ready to establish norm inflation.

**3.1. Initial Data and Ansatz.** Given any Lorentz exponent  $q > 1$ , we fix a cone-slope parameter  $L_q$  by (16) and the logarithmic decay exponent  $\alpha_q$  by (17). Then we fix a profile  $\phi_q(r, z)$  by (15), which will determine our data (14).

As we fix  $r_0 = 1$ , the fixed cone-slope  $L_q = z_0/r_0$  determines  $z_0$  uniquely. Let us denote this by  $z_{0,q}$ .

These parameters  $L_q$ ,  $\alpha_q$ , and  $\phi_q$  are fixed once and for all throughout the paper. We will indicate explicitly where the assumptions on them are used.

For an integer  $m \geq 2$  and a parameter  $\varepsilon > 0$ , define initial data  $\omega_0^{(m)}$  by (14) with the fixed profile  $\phi_q$ .

As  $0 < \alpha_q < 1$ ,

$$\left\| \frac{\omega_0^{(m)}(x)}{r} \right\|_{L^{3,q}(\mathbb{R}^3)}^q \leq C(q) \varepsilon^q \left\| \frac{\phi_q}{r} \right\|_{L^{3,q}(\mathbb{R}^3)}^q \sum_{k=1}^m \frac{1}{k^{\alpha_q q}} \leq C(q) \varepsilon^q \left\| \frac{\phi_q}{r} \right\|_{L^{3,q}(\mathbb{R}^3)}^q \sum_{k=1}^{\infty} \frac{1}{k^{\alpha_q q}} < \infty. \quad (58)$$

In addition, as  $\omega_{0,k}$ 's have disjoint support,

$$\|\omega_0^{(m)}\|_{L^1(\mathbb{R}^3)} = \sum_{k=1}^m \|\omega_{0,k}\|_{L^1(\mathbb{R}^3)} = \|\phi_q\|_{L^1(\mathbb{R}^3)} \sum_{k=1}^m \frac{\varepsilon}{k^{\alpha_q}} d^{3k} \leq \|\phi_q\|_{L^1(\mathbb{R}^3)} \varepsilon \sum_{k=1}^{\infty} d^{3k}.$$

And  $\|\omega_0^{(m)}\|_{L^\infty(\mathbb{R}^3)} \leq \varepsilon \|\phi_q\|_{L^\infty(\mathbb{R}^3)}$ . Therefore, given any  $\tilde{\varepsilon} > 0$ , we can choose a small  $\varepsilon \in (0, \tilde{\varepsilon})$  depending only on  $\tilde{\varepsilon}, q$  so that  $\|\omega_0^{(m)}\|_{L^\infty \cap L^1(\mathbb{R}^3)} + \|\omega_0^{(m)}/r\|_{L^{3,q}(\mathbb{R}^3)} < \tilde{\varepsilon}$ .

Several quantities in the proof, such as  $T_N$  and  $T_B$ , depend on  $\varepsilon$ . However, once  $\varepsilon = \varepsilon(\tilde{\varepsilon}, q)$  is chosen, it is regarded as fixed, and this dependence will be suppressed unless it is used explicitly. One can refer to § 1.13 for notation conventions regarding all these quantities, such as  $L_q, \alpha_q, \phi_q$  and  $\varepsilon(\tilde{\varepsilon}, q)$ .

As our initial data (14) is smooth and has compact support, by Danchin's global existence and uniqueness [Dan07a] together with classical local existence theory and the Beale-Kato-Majda criterion, there exists a unique global-in-time smooth solution  $\omega^{(m)}$ .

Regarding the solution,  $\omega^{(m)}$ , odd symmetry of  $\omega^{(m)}$  in  $z$  and non-positivity of  $\omega^{(m)}$  in  $\{z > 0\}$  are preserved under the evolution. Indeed, the reflected vorticity  $\bar{\omega}^{(m)}(r, z, t) := -\omega^{(m)}(r, -z, t)$  solves the equation (4) with the same initial data. Hence from uniqueness, one can obtain  $\bar{\omega}^{(m)} \equiv \omega^{(m)}$ . Then one can find corresponding symmetry of the velocity field  $u$  via the Biot-Savart law, which implies that the flow map of  $u$  preserves the lower and upper half-spaces. Then the transport of  $\omega^{(m)}/r$  implies the non-positivity.

The relative vorticity  $\omega^{(m)}/r$  is transported by the flow map associated with the velocity field  $u^{(m)}$  induced by  $\omega^{(m)}$ . Hence, the vortex ring that evolved from  $\omega_{0,k}$  is well-defined for  $t \in [0, \infty)$ , and let us denote it by  $\omega_k(r, z, t)$ . It allows us to decompose our solution into multi vortex rings:

$$\omega^{(m)}(r, z, t) = \sum_{k=1}^m \omega_k(r, z, t), \quad 0 \leq t < \infty. \quad (59)$$

We first define amplitude factors  $\{x_k(t)\}_{k=1}^m$  by the ODE systems on  $t \in [0, \infty)$ :

$$\left. \begin{aligned} x'_k(t) &= x_k(t) \partial_r u_-^r(0, 0, t), & k \geq 2, \\ x'_1(t) &= 0, \\ x_k(0) &= \frac{\varepsilon}{k^{\alpha_q}}, & k \geq 1. \end{aligned} \right\} \quad (60)$$

Recall for a fixed scale index  $k$ , we denote, by  $u_-(r, z, t) = \sum_{j=1}^{k-1} u_j(r, z, t)$ , the velocity field induced by outer rings  $\omega_-(r, z, t) = \sum_{j=1}^{k-1} \omega_j(r, z, t)$ .

Then we define  $\tilde{x}_k(t), R_k(t), H_k(t)$  for  $k = 1, \dots, m$  by (22). We define time-dependent profiles  $W_k(r, z, t)$  by

$$W_k(r, z, t) := \frac{1}{x_k(t)} \omega_k(R_k(t)r, H_k(t)z, t), \quad k = 1, \dots, m \quad (61)$$

for  $(r, z)$  such that  $(R_k(t)r, H_k(t)z) \in \text{supp } \omega_k(\cdot, \cdot, t)$ . This implies the ansatz that we will use:

$$\omega_k(r, z, t) = x_k(t) W_k\left(\frac{r}{R_k(t)}, \frac{z}{H_k(t)}, t\right), \quad k = 1, \dots, m$$

together with

$$W_k(r, z, 0) = \phi_q(r, z), \quad k = 1, \dots, m.$$

Our bootstrap argument will show  $W_k$  remains close to  $\phi_q$  uniformly in  $k$ , on the relevant time interval. The quantity  $x_k(t)$  is the amplitude factor and, under the bootstrap bounds, is comparable to the  $L^\infty$ -size of  $\omega_k$ . The point  $(R_k(t)r_0, H_k(t)z_{0,q})$  encodes a representative location in the  $rz$  plane of the  $k$ -th vortex ring, and  $2\eta r_0 R_k(t)$  represents the radial width of  $\text{supp } \omega_k$  whereas  $2\eta z_{0,q} H_k(t)$  represents the width of the support in the  $z$  direction.

The profiles  $W_k$  satisfy the following equation: for all  $k = 1, \dots, m$

$$\partial_t W_k + V_k^r \partial_r W_k + V_k^z \partial_z W_k = W_k \frac{V_k^r}{r}, \quad (62)$$

where

$$\begin{cases} V_k^r(r, z, t) = \frac{u^{(m),r}(R_k(t)r, H_k(t)z, t)}{R_k(t)} - r \frac{x_k'(t)}{x_k(t)}, \\ V_k^z(r, z, t) = \frac{u^{(m),z}(R_k(t)r, H_k(t)z, t)}{H_k(t)} + 2z \frac{x_k'(t)}{x_k(t)}. \end{cases} \quad (63)$$

Note that for  $(r, z) \in \text{supp } W_k(\cdot, \cdot, t)$ , the quantity  $V_k^r(r, z, t)/r$  represents the difference between the real and approximate values of the vortex stretching rate  $u^r/r$  at the point  $(R_k(t)r, H_k(t)z)$  in the  $k$ -th vortex ring.

Note that all these quantities  $\omega_k, W_k, x_k, R_k, H_k$  in fact also depend on  $m$ . However, for simplicity, we do not indicate this dependence in the notation. See § 1.13 for more notation conventions.

As a reminder for a notation convention, meridional  $(r, z)$ -functions, such as  $W_k, \phi_q$  and  $\omega_k$ , are also identified with their axisymmetric lifts to  $\mathbb{R}^3$ . For example, all  $L^\infty$  norms are taken with respect to this identification. We will write  $\|\phi_q\|_{L^\infty(\mathbb{R}^3)}$  instead of  $\|\phi_q\|_{L^\infty(\mathbb{R}_+ \times \mathbb{R})}$ .

For  $0 \leq t$  and  $k = 1, \dots, m$ , let  $X_k(r, z, t) = (X_k^r(r, z, t), X_k^z(r, z, t))$  be the flow map for  $W_k$ 's given by

$$\begin{aligned} X_k(r, z, 0) &= (r, z) \in \text{supp } \phi_q, \\ \frac{\partial}{\partial t} X_k(r, z, t) &= V_k^r(X_k(r, z, t), t) e_r + V_k^z(X_k(r, z, t), t) e_z. \end{aligned}$$

**3.2. Roadmap of a Bootstrap Argument.** For an arbitrary target amplitude  $A > \varepsilon$ , define

$$\mu := \frac{1}{20}, \quad \bar{A} := \frac{A}{1-\mu}, \quad T_N(A, m) := \sup \left\{ t \geq 0 : \max_{1 \leq k \leq m} x_k(t) \leq \bar{A} \right\}. \quad (64)$$

We will call  $T_N(A, m)$  the *norm-inflation time* at the ODE level.

In addition, it holds  $T_N(A, m) > 0$  because  $\bar{A} > \varepsilon = \max_{1 \leq k \leq m} x_k(0)$ . If  $T_N(A, m) < \infty$ , then by continuity of the finite family  $(x_k)_{k=1}^m$ ,

$$\max_{1 \leq k \leq m} x_k(T_N(A, m)) = \bar{A}.$$

At this moment,  $T_N(A, m)$  could be infinite even though we will show later it is in fact finite.

If  $A \leq \varepsilon$ , then norm inflation is trivial.

**Bootstrap bounds.** We impose the following bootstrap bounds: for all  $t \in [0, T]$ ,

$$F_m(t) := \sup_{\substack{(r,z) \in \text{supp } \phi_q \\ k=1, \dots, m}} \max \left\{ \left| \frac{X_k^r(r, z, t)}{r} - 1 \right|, \left| \frac{X_k^z(r, z, t)}{z} - 1 \right| \right\} \leq \mu. \quad (65)$$

with the bootstrap parameter  $\mu = 1/20$ . It is satisfied at least at  $t = 0$ .

For each  $k$ , the function  $(r, z, t) \mapsto (X_k^r/r, X_k^z/z)$  is continuous on the compact set  $\text{supp } \phi_q \times [0, T]$ , which gives uniform continuity. Hence thanks to finiteness of  $k = 1, \dots, m$ , the bootstrap deviation functional  $F_m(t)$  is continuous.

We define the maximal bootstrap time  $T_B(A, m)$  by

$$T_B(A, m) := \sup \{ T \in [0, T_N(A, m)] : (65) \text{ holds for all } t \in [0, T] \}. \quad (66)$$

Since  $F_m(0) = 0$  and  $F_m(t)$  is continuous for  $t \geq 0$ , it holds that  $T_B(A, m) > 0$ . At this stage we do not know whether  $T_B(A, m) = T_N(A, m)$  or not; if not, then we cannot use the bootstrap bounds at the norm-inflation time  $T_N(A, m)$ .

In the roadmap below, comparison symbols such as  $\ll$ ,  $\gtrsim$ , and  $\lesssim$  are used only heuristically to indicate the mechanism. All rigorous constants and displayed dependences will be stated in the subsequent lemmas and propositions.

**Logical structure.** The proof of the norm inflation statement (Theorem 1.1) reduces to:

- (1) **ODE control of  $T_B(A, m)$ .** Using the bootstrap bound (65) on  $[0, T_B(A, m)]$ , we show in § 3.3 that the stretching rate  $\partial_r u_-^r(0, 0, t)$  felt by the  $k$ th ring can be expressed in terms of the profiles  $W_j$  and aspect ratios  $\Gamma_j(t)$ , yielding a weak ODE cascade for  $(x_k(t))_{k=1}^m$  up to a small multiplicative error. Section 3.4 then analyzes this ODE system; by using the conditions (15),(16),(17) of  $L_q, \phi_q, \alpha_q$ , we establish quantitative upper bounds on  $T_B(A, m)$  and in particular  $T_B(A, m) \lesssim m^{-\beta_q} \rightarrow 0$  as  $m \rightarrow \infty$ .
- (2) **Bootstrap improvement.** Using the flow-map estimates derived under (65), we prove in § 3.5 that on a short time interval the bootstrap inequalities improve with a strict margin, provided the short-time smallness mechanism

$$\bar{A} \log m T_B(A, m) \ll 1$$

for large  $m$ . By a standard continuity argument this forces  $T_B(A, m) = T_N(A, m)$ , so that (65) holds on  $[0, T_N(A, m)]$ , and  $T_N(A, m) \rightarrow 0$  as  $m \rightarrow \infty$ .

- (3) **Completion of Norm Inflation.** Once (65) holds on  $[0, T_N(A, m)]$ , the Cauchy formula for  $W_k$  implies a uniform lower bound  $\|W_k(\cdot, \cdot, t)\|_{L^\infty} \gtrsim \|\phi_q\|_{L^\infty}$  on this interval. Evaluating at  $t = T_N(A, m)$  then converts the amplitude bound defining  $T_N(A, m)$  into  $\|\omega^{(m)}(\cdot, T_N(A, m))\|_{L^\infty} \gtrsim A$ . Finally, since  $T_N(A, m)$  can be made arbitrarily small by choosing  $m$  large (via the ODE step and the choice of  $\phi_q$ ), this yields norm inflation on any prescribed time scale.

To summarize it, let us provide a dependency diagram:

$$\begin{aligned} \text{initial data} &\implies \text{weak ODEs on } [0, T_B(A, m)] \\ &\implies \text{quantitative control of } T_B(A, m) \text{ using the bootstrap bounds} \\ &\implies A \log m T_B(A, m) \ll 1 \text{ for large } m \\ &\implies \text{bootstrap improvement} \\ &\implies T_B = T_N \implies L^\infty\text{-norm inflation.} \end{aligned}$$

It is worth noting that we only use a bootstrap bound on  $X$  without introducing a bootstrap bound on  $DY$  for a flow map  $Y$  associated with the physical flow  $u$  as opposed to [CMZ25]. For norm inflation, in fact, such a bound on  $DY$  is available and we can even use it for self-interaction estimate later on, which will give us a stronger estimate without a logarithmic penalty as discussed in § 1.10. However, it does not carry over to prove instantaneous blow-up. Therefore, we do not use a bootstrap bound on  $DY$  even for norm inflation.

**3.3. Cauchy Formula and Freezing the Profiles.** In this first section, we record the Cauchy formula for the rescaled relative vorticity  $W_k/r$  and “freeze” the profiles  $W_k(r, z, t)$  by using the bootstrap bounds (65). Keep in mind that we freeze the profiles  $W_k(r, z, t)$  not just in terms of time  $t$  but also in terms of scale index  $k$ .

**Lemma 3.1** (Cauchy formula for  $W_k/r$ ). *Fix  $k \in \{1, \dots, m\}$ . For every  $t \in [0, \infty)$ , the flow map  $X_k(\cdot, \cdot, t)$  associated with  $V_k$  satisfies*

$$\frac{W_k(X_k(r, z, t), t)}{X_k^r(r, z, t)} = \frac{\phi_q(r, z)}{r}, \quad (r, z) \in \text{supp } \phi_q. \quad (67)$$

In particular, using the bootstrap bound (65) for  $t \in [0, T_B(A, m)]$ ,

$$\|W_k(\cdot, \cdot, t)\|_{L^\infty(\mathbb{R}^3)} \leq (1 + \mu)\|\phi_q\|_{L^\infty(\mathbb{R}^3)}, \quad \|\omega_k(\cdot, t)\|_{L^\infty(\mathbb{R}^3)} \leq (1 + \mu)x_k(t)\|\phi_q\|_{L^\infty(\mathbb{R}^3)}.$$

*Proof.* Starting from (62), divide by  $r$  and use  $\partial_r(1/r) = -1/r^2$  to obtain

$$\partial_t \left( \frac{W_k}{r} \right) + V_k^r \partial_r \left( \frac{W_k}{r} \right) + V_k^z \partial_z \left( \frac{W_k}{r} \right) = 0.$$

Therefore  $W_k/r$  is transported by the characteristics of  $V_k$ , i.e. by  $X_k$ . Since  $X_k(r, z, 0) = (r, z)$  and  $W_k(\cdot, \cdot, 0) = \phi_q$ , the transport identity gives (67). The  $L^\infty$  bounds follow immediately from (67) and the bootstrap control of  $X_k^r/r$ .  $\square$

The discussion below is heuristic until the next lemma; comparison symbols are used only to describe the expected mechanism.

Let us now freeze the profiles  $W_k(r, z, t)$  using the bootstrap bounds on  $[0, T_B(A, m)]$ . We need to estimate

$$- \iint \frac{r^2 z}{(r^2 + z^2)^{\frac{5}{2}}} W_k \left( \frac{r}{R_k(t)}, \frac{z}{H_k(t)}, t \right) dr dz \geq 0.$$

As explained in § 1.8, heuristically, as  $W_k(\cdot, \cdot, t)$  is concentrated near  $r = r_0$ , one can estimate

$$- \iint \frac{r^2 z}{(r^2 + z^2)^{\frac{5}{2}}} W_k \left( \frac{r}{R_k}, \frac{z}{H_k}, t \right) dr dz \sim \frac{H_k^2}{R_k^2} \int_{\{z \sim z_0\}} \frac{z}{\left(1 + \frac{H_k^2}{R_k^2} z^2\right)^{\frac{5}{2}}} dz.$$

Here,  $H_k(t)^2/R_k(t)^2$  decreases in time from  $H_k^2(0)/R_k^2(0) = 1$  to a small number, and it also decreases in  $k$ . When  $H_k^2/R_k^2 \ll 1$ , we can further simplify the estimate:

$$- \iint \frac{r^2 z}{(r^2 + z^2)^{\frac{5}{2}}} W_k \left( \frac{r}{R_k}, \frac{z}{H_k}, t \right) dr dz \sim \frac{H_k(t)^2}{R_k(t)^2}.$$

To be more clear, this estimate only makes sense for large  $k$ 's, and a fixed time  $t > 0$  that is not so small.

Now, let us make this estimate rigorous.

**Lemma 3.2.** *For any  $k = 1, \dots, m$  and  $t \in [0, T_B(A, m)]$ , it holds*

$$c_\mu \Gamma_k(t)^2 \Lambda_{\text{froz}}(\Gamma_k(t)) \leq - \iint \frac{r^2 z}{(r^2 + z^2)^{\frac{5}{2}}} W_k \left( \frac{r}{R_k(t)}, \frac{z}{H_k(t)}, t \right) dr dz \leq C_\mu \Gamma_k(t)^2 \Lambda_{\text{froz}}(\Gamma_k(t)). \quad (68)$$

where

$$\Gamma_k(t) := \frac{H_k(t)}{R_k(t)}, \quad \Lambda_{\text{froz}}(\Gamma) := \int_{-\infty}^{\infty} \int_0^{\infty} \frac{r^2 z}{(r^2 + \Gamma^2 z^2)^{5/2}} (-\phi_q(r, z)) dr dz, \quad \Gamma \in (0, 1]$$

and

$$c_\mu := \frac{(1-\mu)^3}{(1+\mu)^5}, \quad C_\mu := \frac{(1+\mu)^3}{(1-\mu)^5}.$$

*Proof.* Fix  $k = 1, \dots, m$  and  $t \in [0, T_B(A, m)]$ . We will omit the argument  $t$  in  $R_k(t), H_k(t)$  and  $\Gamma_k(t)$  for simplicity.

First, through change of variables, we rescale the variables:

$$\iint \frac{r^2 z}{(r^2 + z^2)^{\frac{5}{2}}} W_k \left( \frac{r}{R_k}, \frac{z}{H_k}, t \right) dr dz = \Gamma_k^2 \iint \frac{r^2 z}{(r^2 + \Gamma_k^2 z^2)^{\frac{5}{2}}} W_k(r, z, t) dr dz.$$

A direct computation shows that  $\operatorname{div}_{\mathbb{R}^3} V_k = 0$  viewing  $V_k$  as a vector fields in  $\mathbb{R}^3$  written in cylindrical coordinates. Then the corresponding 3D Jacobian determinant of the flow map  $X_k$  is 1.

Using it and re-writing the variables  $(r, z)$  as  $(r_x, z_x)$ , we apply change of variables via  $(r_x, z_x) = X_k(r_y, z_y, t)$  to obtain

$$\begin{aligned} \int_{-\infty}^{\infty} \int_0^{\infty} \frac{r_x^2 z_x}{(r_x^2 + \Gamma_k^2 z_x^2)^{\frac{5}{2}}} W_k(r_x, z_x, t) dr_x dz_x &= \frac{1}{2\pi} \int_{\mathbb{R}^3} \frac{r_x z_x}{(r_x^2 + \Gamma_k^2 z_x^2)^{\frac{5}{2}}} W_k(r_x, z_x, t) dx \\ &= \frac{1}{2\pi} \int_{\mathbb{R}^3} \frac{X_k^r X_k^z}{((X_k^r)^2 + \Gamma_k^2 (X_k^z)^2)^{\frac{5}{2}}} W_k(X_k(r_y, z_y, t), t) dy \\ &= \int_{-\infty}^{\infty} \int_0^{\infty} \frac{X_k^r X_k^z}{((X_k^r)^2 + \Gamma_k^2 (X_k^z)^2)^{\frac{5}{2}}} W_k(X_k(r_y, z_y, t), t) r_y dr_y dz_y \end{aligned}$$

where  $X_k^r := X_k^r(r_y, z_y, t)$ ,  $X_k^z := X_k^z(r_y, z_y, t)$ . Now using the bootstrap bound (65), one can obtain:

$$\begin{aligned} - \int_{-\infty}^{\infty} \int_0^{\infty} \frac{r_x^2 z_x}{(r_x^2 + \Gamma_k^2 z_x^2)^{\frac{5}{2}}} W_k(r_x, z_x, t) dr_x dz_x &= - \int_{-\infty}^{\infty} \int_0^{\infty} \frac{X_k^r X_k^z}{((X_k^r)^2 + \Gamma_k^2 (X_k^z)^2)^{\frac{5}{2}}} W_k(X_k(r_y, z_y, t), t) r_y dr_y dz_y \\ &= - \int_{-\infty}^{\infty} \int_0^{\infty} \frac{(X_k^r)^2 X_k^z}{((X_k^r)^2 + \Gamma_k^2 (X_k^z)^2)^{\frac{5}{2}}} \phi_q(r_y, z_y) dr_y dz_y \\ &\leq - \frac{(1+\mu)^3}{(1-\mu)^5} \int_{-\infty}^{\infty} \int_0^{\infty} \frac{r_y^2 z_y}{(r_y^2 + \Gamma_k^2 z_y^2)^{\frac{5}{2}}} \phi_q(r_y, z_y) dr_y dz_y \end{aligned}$$

where we used the Cauchy formula for  $W_k/r$  (67). From here, one can obtain the upper bound in (68) at once. Similarly, the lower bound in (68) follows by replacing the upper bootstrap inequalities by the lower ones in the same argument.  $\square$

**3.4. Study of ODEs.** As explained in § 3.2, throughout this section we study the weak ODE system (69) below on the bootstrap interval  $[0, T_B(A, m)]$ , using the bootstrap bounds (65). The constants introduced in this subsection may depend on the fixed background parameters from § 1.13, but they are independent of the running parameters  $k, m, A, t, T_N, T_B$  unless such dependence is displayed explicitly. In particular, the constants  $c_\mu, C_\mu$ , and  $\Theta_\mu$  are fixed once introduced. See § 1.13 for more notation conventions.

We use superscript/subscript, such as orig, loc, froz, to distinguish various types of simplifications. In addition, we will denote  $x_k^{\text{orig}}(t) := x_k(t)$  throughout this Section 3.4, but after this section, we will come back to the original notation  $x_k(t)$ .

**Roadmap of this subsection.** As already foreshadowed in the introduction, the purpose of this subsection is to isolate the ODE cascade that drives norm inflation.

- § 3.4.1: On the bootstrap interval, we first use the flow-map control to freeze the transported profiles  $W_j$  against the fixed profile  $\phi_q$ , thereby reducing the weak ODEs to outer-ring contributions depending essentially on the amplitudes  $x_j$  and aspect ratios  $\Gamma_j$ .
- § 3.4.2: We then rewrite the system in cascade form, which yields an exact identity for the evolution of the  $\Gamma_j$ 's, and then we compare the frozen and unfrozen quantities.
- § 3.4.3: After introducing the cone variables  $\zeta_j = L_q \Gamma_j$ , we exploit the monotonicity of the localized Biot–Savart kernel on a fixed productive range: while the front moves toward smaller scales, the cumulative outer stretching must build up at a quantitative rate.
- § 3.4.4, § 3.4.5: This front-migration mechanism gives a front-induced  $t^{-1}$  lower bound for the total stretching, and from there we derive an upper bound for the ODE norm-inflation time. These ODE estimates are the main output of the subsection and will be used in the next subsection to close the bootstrap.

3.4.1. *Weak ODEs and Freezing of Profiles.* Fix  $k \in \{2, \dots, m\}$ . As derived in § 1.8.1, one needs to study the weak ODEs

$$\frac{d}{dt} \log x_k^{\text{orig}}(t) = \sum_{j=1}^{k-1} x_j^{\text{orig}}(t) \Gamma_j^{\text{orig}}(t)^2 \Lambda_j(t, \Gamma_j^{\text{orig}}(t)), \quad 0 \leq t < T_B(A, m). \quad (69)$$

Introduce the true outer-ring contributions

$$b_j^{\text{orig}}(t) := x_j^{\text{orig}}(t) \Gamma_j^{\text{orig}}(t)^2 \Lambda_j(t, \Gamma_j^{\text{orig}}(t)), \quad S_k^{\text{orig}}(t) := \sum_{j=1}^k b_j^{\text{orig}}(t), \quad B_j^{\text{orig}}(t) := \int_0^t b_j^{\text{orig}}(s) ds.$$

Then the cascade form is

$$\frac{d}{dt} \log x_k^{\text{orig}}(t) = S_{k-1}^{\text{orig}}(t) \quad (2 \leq k \leq m), \quad (70)$$

On  $[0, T_B(A, m)]$ , Lemma 3.2 allows one to *freeze* each transported profile  $W_j(\cdot, \cdot, t)$  against the initial profile  $\phi_q$ . One has the uniform bounds

$$c_\mu \sum_{j=1}^{k-1} x_j^{\text{orig}}(t) \Gamma_j^{\text{orig}}(t)^2 \Lambda_{\text{froz}}(\Gamma_j^{\text{orig}}(t)) \leq \frac{d}{dt} \log x_k^{\text{orig}}(t) \leq C_\mu \sum_{j=1}^{k-1} x_j^{\text{orig}}(t) \Gamma_j^{\text{orig}}(t)^2 \Lambda_{\text{froz}}(\Gamma_j^{\text{orig}}(t)). \quad (71)$$

As in § 1.8.4, it is convenient to rewrite the outer-ring contribution in terms of  $\Gamma_j^{\text{orig}}(t)$  alone. One has the exact identities

$$\Gamma_j^{\text{orig}}(t) = \left( \frac{x_j^{\text{orig}}(0)}{x_j^{\text{orig}}(t)} \right)^3, \quad x_j^{\text{orig}}(t) \Gamma_j^{\text{orig}}(t)^2 = x_j^{\text{orig}}(0) \Gamma_j^{\text{orig}}(t)^{5/3}.$$

Define the frozen outer-ring contributions and partial sums

$$b_{\text{froz},j}^{\text{orig}}(t) := x_j^{\text{orig}}(t) \Gamma_j^{\text{orig}}(t)^2 \Lambda_{\text{froz}}(\Gamma_j^{\text{orig}}(t)) = x_j^{\text{orig}}(0) \Gamma_j^{\text{orig}}(t)^{5/3} \Lambda_{\text{froz}}(\Gamma_j^{\text{orig}}(t)),$$

$$S_{\text{froz},k}^{\text{orig}}(t) := \sum_{j=1}^k b_{\text{froz},j}^{\text{orig}}(t).$$

Note that the Biot–Savart coefficient  $\Lambda_{\text{froz}}$  is frozen. These definitions of  $b_{\text{froz},j}^{\text{orig}}$ ,  $S_{\text{froz},k}^{\text{orig}}$  are slightly different from (32) because we are considering both the frozen and original models to compare them in this rigorous proof whereas we only considered one model in heuristic arguments. Then (71) becomes

$$c_\mu S_{\text{froz},k-1}^{\text{orig}}(t) \leq \frac{d}{dt} \log x_k^{\text{orig}}(t) = S_{k-1}^{\text{orig}}(t) \leq C_\mu S_{\text{froz},k-1}^{\text{orig}}(t)$$

for  $2 \leq k \leq m$  and  $0 \leq t < T_B(A, m)$ .

**3.4.2. Cascade Form for the Original Weak ODEs and Bootstrap Comparison.** The cascade form (70) implies the exact cascade identity

$$\Gamma_{j+1}^{\text{orig}}(t) = \Gamma_j^{\text{orig}}(t) e^{-3B_j^{\text{orig}}(t)}. \quad (72)$$

On  $[0, T_B(A, m)]$ , Lemma 3.2 yields the pointwise comparison

$$c_\mu b_{\text{froz},j}^{\text{orig}}(t) \leq b_j^{\text{orig}}(t) \leq C_\mu b_{\text{froz},j}^{\text{orig}}(t), \quad (73)$$

and hence also

$$c_\mu S_{\text{froz},k}^{\text{orig}}(t) \leq S_k^{\text{orig}}(t) \leq C_\mu S_{\text{froz},k}^{\text{orig}}(t) \quad (1 \leq k \leq m-1). \quad (74)$$

We record the fixed ratio

$$\Theta_\mu := \frac{C_\mu}{c_\mu} = \left( \frac{1+\mu}{1-\mu} \right)^8. \quad (75)$$

Then differentiating  $b_{\text{froz},j}^{\text{orig}}$  and using the cascade form (70) gives a differential equation for  $b_{\text{froz},j}^{\text{orig}}$ .

**Lemma 3.3** (A differential equation for  $b_{\text{froz},j}^{\text{orig}}$ ). *For each  $j \geq 2$ , it holds*

$$\frac{d}{dt} b_{\text{froz},j}^{\text{orig}}(t) = -\kappa_{\text{froz}}(\Gamma_j^{\text{orig}}(t)) b_{\text{froz},j}^{\text{orig}}(t) S_{j-1}^{\text{orig}}(t), \quad \kappa_{\text{froz}}(\Gamma) := 5 + 3\Gamma \frac{\Lambda'_{\text{froz}}(\Gamma)}{\Lambda_{\text{froz}}(\Gamma)}. \quad (76)$$

This equation isolates the sign issue in the ODE analysis. Once  $\kappa_{\text{froz}}(\Gamma)$  is shown to be non-positive on the relevant cone range, the frozen quantities  $b_{\text{froz},j}^{\text{orig}}$  become monotone, and that monotonicity is exactly what later drives the front-migration argument.

*Proof.* Differentiate  $b_{\text{froz},j}^{\text{orig}}(t) = \Lambda_{\text{froz}}(\Gamma_j^{\text{orig}}(t)) x_j^{\text{orig}}(t) \Gamma_j^{\text{orig}}(t)^2$  and use

$$\frac{d}{dt} \log x_j^{\text{orig}}(t) = S_{j-1}^{\text{orig}}(t)$$

from (70). Together with  $\Gamma_j^{\text{orig}}(t) = (x_j^{\text{orig}}(0)/x_j^{\text{orig}}(t))^3$ , we have

$$\frac{d}{dt} \Gamma_j^{\text{orig}}(t) = -3\Gamma_j^{\text{orig}}(t) S_{j-1}^{\text{orig}}(t),$$

and a direct computation gives (76). □

3.4.3. *Localization of  $\phi_q$  and a Productive Regime.* Define the Biot–Savart profile

$$\Psi(\zeta) := \zeta^{5/3}(1 + \zeta^2)^{-5/2}.$$

Direct computation yields

$$\Psi'(\zeta) \leq 0 \quad \text{for all } \zeta \geq \zeta_* = 1/\sqrt{2}.$$

Recall that  $\phi_q$  is odd in  $z$  and nonpositive on  $\{z > 0\}$  (cf. (15)), and we impose the fixed geometric localization

$$\text{supp } \phi_q \cap \{z > 0\} \subset [(1 - \eta)r_0, (1 + \eta)r_0] \times [(1 - \eta)z_{0,q}, (1 + \eta)z_{0,q}], \quad (77)$$

Define the fixed cone slopes

$$L_{q,-} := \frac{1 - \eta}{1 + \eta} L_q, \quad L_{q,+} := \frac{1 + \eta}{1 - \eta} L_q. \quad (78)$$

Localization reduces the profile dependence of  $\Lambda_{\text{froz}}(\Gamma)\Gamma^{5/3}$  to a one-parameter shape function of  $\zeta = L_q\Gamma$ , which is the Biot–Savart profile  $\Psi$ . More precisely, we can estimate  $\kappa_{\text{froz}}(\Gamma)$  in terms of  $\Psi'$ , which yields a monotonicity range for  $t \mapsto b_{\text{froz},j}^{\text{orig}}(t)$ .

**Lemma 3.4** (Comparison to  $\Psi$ ). *For every  $\Gamma \in (0, 1]$ ,*

$$\kappa_{\text{froz}}(\Gamma) \leq 3\Gamma L_{q,-} \frac{\Psi'(\Gamma L_{q,-})}{\Psi(\Gamma L_{q,-})}, \quad (79)$$

hence, for  $j \geq 2$ ,

$$\frac{d}{dt} b_{\text{froz},j}^{\text{orig}}(t) \geq 0 \quad \text{whenever } \Gamma_j^{\text{orig}}(t)L_q \geq \frac{1 + \eta}{1 - \eta} \zeta_*. \quad (80)$$

Therefore, as long as the cone variable  $\Gamma_j^{\text{orig}}L_q$  is in the range (80), the frozen individual stretching rate  $b_{\text{froz},j}^{\text{orig}}(t)$  is non-decreasing despite the geometric slow-down mechanism. We call the range (80) a *productive* regime.

*Proof.* Differentiate under the integral sign:

$$\Lambda'_{\text{froz}}(\Gamma) = -5\Gamma \int_{-\infty}^{\infty} \int_0^{\infty} \frac{r^2 z^3}{(r^2 + \Gamma^2 z^2)^{7/2}} (-\phi_q(r, z)) \, dr \, dz \leq 0.$$

Moreover,

$$-\Gamma \frac{\Lambda'_{\text{froz}}(\Gamma)}{\Lambda_{\text{froz}}(\Gamma)} = 5 \frac{\iint K_{\Gamma}(r, z) \frac{\Gamma^2 z^2}{r^2 + \Gamma^2 z^2} (-\phi_q(r, z)) \, dr \, dz}{\iint K_{\Gamma}(r, z) (-\phi_q(r, z)) \, dr \, dz},$$

so  $-\Gamma\Lambda'_{\text{froz}}/\Lambda_{\text{froz}}$  is a weighted average of  $\frac{\Gamma^2 z^2}{r^2 + \Gamma^2 z^2}$ . Since  $(r, z) \in \text{supp } \phi_q$  implies  $z/r \in [L_{q,-}, L_{q,+}]$  and  $a \mapsto \frac{a^2}{1+a^2}$  is increasing for  $a \geq 0$ , we obtain

$$\frac{(\Gamma L_{q,-})^2}{1 + (\Gamma L_{q,-})^2} \leq \frac{\Gamma^2 z^2}{r^2 + \Gamma^2 z^2},$$

and multiplying by 15 yields

$$15 \frac{(\Gamma L_{q,-})^2}{1 + (\Gamma L_{q,-})^2} \leq -3\Gamma \frac{\Lambda'_{\text{froz}}(\Gamma)}{\Lambda_{\text{froz}}(\Gamma)}. \quad (81)$$

Direct computation yields

$$3\zeta \frac{\Psi'(\zeta)}{\Psi(\zeta)} = 5 - \frac{15\zeta^2}{1 + \zeta^2}. \quad (82)$$

Using (81) and (82), one can obtain (79) at once. And (80) follows from (76).  $\square$

**3.4.4. Front-Migration and a Front-Induced  $t^{-1}$  Lower Bound.** Based on (80), it is reasonable to introduce the cone variables

$$\zeta_j^{\text{orig}}(t) := L_q \Gamma_j^{\text{orig}}(t) \in (0, L_q],$$

and define a fixed threshold  $\zeta_\eta$  by

$$\zeta_\eta := \frac{1 + \eta}{1 - \eta} \zeta_*. \quad (83)$$

From the exact cascade identity (72),  $\Gamma_{j+1}^{\text{orig}}(t) = \Gamma_j^{\text{orig}}(t) e^{-3B_j^{\text{orig}}(t)}$ , it follows that

$$\zeta_{j+1}^{\text{orig}}(t) \leq \zeta_j^{\text{orig}}(t). \quad (84)$$

For each  $t > 0$  define the front index at the fixed threshold  $\zeta_\eta$  by

$$J_{\zeta_\eta}^{\text{orig}}(t) := \max \left\{ 1 \leq j \leq m - 1 : \zeta_j^{\text{orig}}(t) \geq \zeta_\eta \right\}. \quad (85)$$

Then  $\zeta_k^{\text{orig}}(t) \geq \zeta_\eta$  for every  $k \leq J_{\zeta_\eta}^{\text{orig}}(t)$ .

When the front has crossed the  $m$ -th scale, i.e. when  $\zeta_m^{\text{orig}}(t) < \zeta_\eta$ , one can estimate the cumulative outer stretching  $S_{m-1}^{\text{orig}}(t)$  using the monotonicity of  $b_{\text{froz},j}^{\text{orig}}$  in the productive regime.

**Lemma 3.5** (Front-migration and a front-induced  $t^{-1}$  lower bound). *For  $t \in (0, T_B(A, m))$ , if*

$$\zeta_m^{\text{orig}}(t) < \zeta_\eta,$$

then

$$S_{m-1}^{\text{orig}}(t) \geq \frac{1}{3\Theta_\mu t} \log \frac{L_q}{\zeta_\eta}, \quad \Theta_\mu \text{ as in (75)}. \quad (86)$$

*Proof.* Let  $t \in (0, T_B(A, m))$  and set  $J := J_{\zeta_\eta}^{\text{orig}}(t)$  as in (85). If  $\zeta_m^{\text{orig}}(t) < \zeta_\eta$ , then  $\zeta_{J+1}^{\text{orig}}(t) < \zeta_\eta$  by definition. Using (72) and  $\zeta_1^{\text{orig}}(t) \equiv L_q$ ,

$$\zeta_{J+1}^{\text{orig}}(t) = L_q \exp \left( -3 \sum_{k=1}^J B_k^{\text{orig}}(t) \right),$$

hence

$$\sum_{k=1}^J B_k^{\text{orig}}(t) = \frac{1}{3} \log \frac{L_q}{\zeta_{J+1}^{\text{orig}}(t)} \geq \frac{1}{3} \log \frac{L_q}{\zeta_\eta}. \quad (87)$$

Now fix  $1 \leq k \leq J$ . Since  $\zeta_k^{\text{orig}}(t) \geq \zeta_\eta$  and  $\Gamma_k^{\text{orig}}(\cdot)$  is nonincreasing in time, we have  $\Gamma_k^{\text{orig}}(s)L_q \geq \zeta_\eta$  for all  $s \in [0, t]$ , which implies  $\Gamma_k^{\text{orig}}(s)L_{q,-} \geq \zeta_*$ . By Lemma 3.4 the frozen  $b_{\text{froz},k}^{\text{orig}}(s)$  is non-decreasing on  $[0, t]$  when  $k \geq 2$ , while  $b_{\text{froz},1}^{\text{orig}}(s)$  is constant, hence non-decreasing. Therefore  $\int_0^t b_{\text{froz},k}^{\text{orig}}(s) ds \leq t b_{\text{froz},k}^{\text{orig}}(t)$ , and using the bootstrap comparison (73),

$$B_k^{\text{orig}}(t) = \int_0^t b_k^{\text{orig}}(s) ds \leq C_\mu \int_0^t b_{\text{froz},k}^{\text{orig}}(s) ds \leq C_\mu t b_{\text{froz},k}^{\text{orig}}(t) \leq \frac{C_\mu}{c_\mu} t b_k^{\text{orig}}(t) = \Theta_\mu t b_k^{\text{orig}}(t).$$

Summing over  $k \leq J$  and combining with (87) yields

$$S_{m-1}^{\text{orig}}(t) \geq \sum_{k=1}^J b_k^{\text{orig}}(t) \geq \frac{1}{\Theta_\mu t} \sum_{k=1}^J B_k^{\text{orig}}(t) \geq \frac{1}{3\Theta_\mu t} \log \frac{L_q}{\zeta_\eta},$$

which is (86).  $\square$

**3.4.5. ODE-Level Norm Inflation and Decay of  $T_B(A, m)$ .** Define a threshold-hitting time (at the fixed threshold  $\zeta_\eta$ )

$$t_{\zeta_\eta}^{\text{orig}} := \inf\{t > 0 : \zeta_m^{\text{orig}}(t) = \zeta_\eta\}.$$

If the set is empty,  $t_{\zeta_\eta}^{\text{orig}}$  is understood as  $+\infty$ .

In the next proposition, the target amplitude  $A$  is still a free parameter. Accordingly, any bound that depends on  $A$  will display that dependence explicitly.

Combining the pre-hitting monotonicity estimate with the front-induced  $1/t$  lower bound after  $t_{\zeta_\eta}^{\text{orig}}$ , we obtain an upper bound for  $T_B(A, m)$ . The argument splits at the threshold-hitting time  $t_{\zeta_\eta}^{\text{orig}}$ . For  $0 \leq t \leq t_{\zeta_\eta}^{\text{orig}}$ , one still has  $\zeta_m^{\text{orig}}(t) \geq \zeta_\eta$ , so the frozen coefficients remain monotone and  $S_{m-1}^{\text{orig}}(t)$  is bounded from below by its initial frozen value; this already shows that  $t_{\zeta_\eta}^{\text{orig}}$  is short. For  $t_{\zeta_\eta}^{\text{orig}} < t \leq T_B$ , the front-migration estimate yields a  $1/t$  lower bound for  $S_{m-1}^{\text{orig}}(t)$ . Integrating

$$\frac{d}{dt} \log x_m^{\text{orig}}(t) = S_{m-1}^{\text{orig}}(t)$$

from  $t_{\zeta_\eta}^{\text{orig}}$  to  $T_B$  gives algebraic growth of  $x_m^{\text{orig}}(t)$ , and comparing this with the bootstrap bound  $x_m^{\text{orig}}(T_B) \leq \bar{A}$  yields the desired estimate for  $T_B(A, m)$ .

**Proposition 3.6** (Norm inflation for the original weak ODEs). *Assume  $A > \varepsilon$ . It holds*

$$T_B(A, m) \leq C(q) \bar{A}^{\gamma_q} m^{\alpha_q - 1 + \gamma_q \alpha_q}, \quad \gamma_q := \frac{3\Theta_\mu}{\log(L_q/\zeta_\eta)}.$$

In particular, if

$$\beta_q := \frac{1}{1 + \gamma_q} - \alpha_q = \frac{\log(L_q/\zeta_\eta)}{3\Theta_\mu + \log(L_q/\zeta_\eta)} - \alpha_q > 0,$$

then

$$T_B(A, m) \leq C(q, A) m^{-\beta_q} \rightarrow 0 \quad \text{as } m \rightarrow \infty. \quad (88)$$

**Remark 3.1.** *Compared to a fixed cone-slope  $L$ , the entire role of a large cone-slope  $L_q$  is to make  $\beta_q > 0$ .*

*Proof of Proposition 3.6.* Write  $T_B := T_B(A, m)$ . Since  $T_B \leq T_N(A, m)$ , we have

$$\max_{k \leq m} x_k^{\text{orig}}(t) \leq \bar{A}$$

for all  $t \in [0, T_B]$ , and in particular  $x_m^{\text{orig}}(t) \leq \bar{A}$  on  $[0, T_B]$ .

**Step 1: a bound up to the threshold-hitting time.** Set  $t_* := \min\{T_B, t_{\zeta_\eta}^{\text{orig}}\}$ . For  $t \in [0, t_*)$  we have  $\zeta_m^{\text{orig}}(t) \geq \zeta_\eta$ , hence, by (84),  $\Gamma_j^{\text{orig}}(t)L_q \geq \zeta_\eta$  for all  $1 \leq j \leq m$ . By Lemma 3.4, each

frozen  $b_{\text{froz},j}^{\text{orig}}(t)$  is nondecreasing on  $[0, t_*)$  for  $j \geq 2$ , while  $b_{\text{froz},1}^{\text{orig}}(t)$  is constant; hence  $S_{\text{froz},m-1}^{\text{orig}}(t) \geq S_{\text{froz},m-1}^{\text{orig}}(0)$  on  $[0, t_*)$ . Using (74) we obtain

$$S_{m-1}^{\text{orig}}(t) \geq c_\mu S_{\text{froz},m-1}^{\text{orig}}(t) \geq c_\mu S_{\text{froz},m-1}^{\text{orig}}(0) \quad (0 \leq t < t_*). \quad (89)$$

Since  $\zeta_m^{\text{orig}}(t) = L_q \Gamma_m^{\text{orig}}(t) = L_q (x_m^{\text{orig}}(0)/x_m^{\text{orig}}(t))^3$  and  $\frac{d}{dt} \log x_m^{\text{orig}}(t) = S_{m-1}^{\text{orig}}(t)$ , we have the exact identity

$$\zeta_m^{\text{orig}}(t) = L_q \exp\left(-3 \int_0^t S_{m-1}^{\text{orig}}(s) ds\right).$$

Therefore, for every  $\tau \in [0, t_*)$ ,

$$\int_0^\tau S_{m-1}^{\text{orig}}(s) ds = \frac{1}{3} \log \frac{L_q}{\zeta_m^{\text{orig}}(\tau)} \leq \frac{1}{3} \log \frac{L_q}{\zeta_\eta},$$

because  $\zeta_m^{\text{orig}}(\tau) \geq \zeta_\eta$  for  $\tau < t_*$ . Combining this with (89) gives

$$\tau \leq \frac{1}{3c_\mu S_{\text{froz},m-1}^{\text{orig}}(0)} \log \frac{L_q}{\zeta_\eta} \quad \text{for all } \tau < t_*.$$

Hence

$$t_* \leq \frac{1}{3c_\mu S_{\text{froz},m-1}^{\text{orig}}(0)} \log \frac{L_q}{\zeta_\eta}.$$

In particular,  $t_* < \infty$ .

At  $t = 0$  one has  $\Gamma_j^{\text{orig}}(0) = 1$ , hence

$$b_{\text{froz},j}^{\text{orig}}(0) = x_j^{\text{orig}}(0) \Lambda_{\text{froz}}(1) = \varepsilon j^{-\alpha_q} \Lambda_{\text{froz}}(1),$$

and therefore

$$S_{\text{froz},m-1}^{\text{orig}}(0) = \varepsilon \Lambda_{\text{froz}}(1) \sum_{j=1}^{m-1} j^{-\alpha_q} \geq c(\alpha_q) \varepsilon \Lambda_{\text{froz}}(1) m^{1-\alpha_q},$$

for some constant  $c(\alpha_q) > 0$ .

The frozen coefficient  $\Lambda_{\text{froz}}(1)$  evaluated at  $\Gamma = 1$  only depends on  $\phi_q$ . Hence

$$t_* \leq \frac{1}{3c_\mu S_{\text{froz},m-1}^{\text{orig}}(0)} \log \frac{L_q}{\zeta_\eta} \leq C(q) m^{\alpha_q-1} \log \frac{L_q}{\zeta_\eta}, \quad (90)$$

where the constant  $C(q)$  absorbs the fixed dependence on  $\tilde{\varepsilon}$ ,  $\eta$ ,  $\phi_q$ , and the other fixed background parameters. We know that  $t_* \leq t_{\zeta_\eta}^{\text{orig}}$ . In particular, if  $t_{\zeta_\eta}^{\text{orig}} \leq T_B$ , then  $t_{\zeta_\eta}^{\text{orig}} = t_*$  and it satisfies the same bound.

**Step 2: algebraic growth after the threshold-hitting time.** If  $T_B \leq t_{\zeta_\eta}^{\text{orig}}$ , then  $T_B = t_*$ . Hence by (90),

$$T_B \leq C(q) m^{\alpha_q-1}.$$

Since  $A > \varepsilon$  and  $\varepsilon = \varepsilon(\tilde{\varepsilon}, q)$  is fixed, we have

$$\bar{A} = \frac{A}{1-\mu} \geq \frac{\varepsilon}{1-\mu},$$

so  $\bar{A}^{\gamma_q} \geq c(q) > 0$ . Absorbing this fixed lower bound into the constant and using  $m^{\gamma_q \alpha_q} \geq 1$ , we obtain

$$T_B \leq C(q) \bar{A}^{\gamma_q} m^{\alpha_q-1+\gamma_q \alpha_q}.$$

Assume now that  $T_B > t_{\zeta_\eta}^{\text{orig}}$ . Then for every  $t \in (t_{\zeta_\eta}^{\text{orig}}, T_B)$ , Lemma 3.5 gives

$$S_{m-1}^{\text{orig}}(t) \geq \frac{1}{3\Theta_\mu t} \log \frac{L_q}{\zeta_\eta} = \frac{1}{\gamma_q t}.$$

Integrating  $\frac{d}{dt} \log x_m^{\text{orig}}(t) = S_{m-1}^{\text{orig}}(t)$  from  $t_{\zeta_\eta}^{\text{orig}}$  to  $t$  yields

$$\log \frac{x_m^{\text{orig}}(t)}{x_m^{\text{orig}}(t_{\zeta_\eta}^{\text{orig}})} \geq \frac{1}{\gamma_q} \log \frac{t}{t_{\zeta_\eta}^{\text{orig}}},$$

hence

$$x_m^{\text{orig}}(t) \geq x_m^{\text{orig}}(t_{\zeta_\eta}^{\text{orig}}) \left( \frac{t}{t_{\zeta_\eta}^{\text{orig}}} \right)^{1/\gamma_q}.$$

Since  $t < T_B \leq T_N(A, m)$ , we have  $x_m^{\text{orig}}(t) \leq \bar{A}$ . Therefore

$$t \leq t_{\zeta_\eta}^{\text{orig}} \left( \frac{\bar{A}}{x_m^{\text{orig}}(t_{\zeta_\eta}^{\text{orig}})} \right)^{\gamma_q} \quad \text{for all } t \in (t_{\zeta_\eta}^{\text{orig}}, T_B).$$

Hence

$$T_B \leq t_{\zeta_\eta}^{\text{orig}} \left( \frac{\bar{A}}{x_m^{\text{orig}}(t_{\zeta_\eta}^{\text{orig}})} \right)^{\gamma_q}.$$

In particular,  $T_B < \infty$ .

By definition of  $t_{\zeta_\eta}^{\text{orig}}$ , we have  $\zeta_m^{\text{orig}}(t_{\zeta_\eta}^{\text{orig}}) = \zeta_\eta$ . Since

$$\zeta_m^{\text{orig}}(t) = L_q \left( \frac{x_m^{\text{orig}}(0)}{x_m^{\text{orig}}(t)} \right)^3,$$

it follows that

$$x_m^{\text{orig}}(t_{\zeta_\eta}^{\text{orig}}) = x_m^{\text{orig}}(0) \left( \frac{L_q}{\zeta_\eta} \right)^{1/3} = \varepsilon m^{-\alpha_q} \left( \frac{L_q}{\zeta_\eta} \right)^{1/3}.$$

Moreover, because  $T_B > t_{\zeta_\eta}^{\text{orig}}$ , we have  $t_{\zeta_\eta}^{\text{orig}} = t_*$ , and thus (90) gives

$$t_{\zeta_\eta}^{\text{orig}} \leq C(q) m^{\alpha_q - 1}.$$

Combining the last three inequalities and absorbing the fixed factors depending only on the background parameters into  $C(q)$ , we arrive at

$$T_B(A, m) \leq C(q) \bar{A}^{\gamma_q} m^{\alpha_q - 1 + \gamma_q \alpha_q}.$$

Finally, since

$$\alpha_q - 1 + \gamma_q \alpha_q = -(1 + \gamma_q) \left( \frac{\log(L_q/\zeta_\eta)}{3\Theta_\mu + \log(L_q/\zeta_\eta)} - \alpha_q \right) = -(1 + \gamma_q) \beta_q \leq -\beta_q,$$

the first bound implies

$$T_B(A, m) \leq C(q, A) m^{-\beta_q} \rightarrow 0 \quad \text{as } m \rightarrow \infty.$$

□

**3.5. A bootstrap Argument.** In this subsection, fix  $A > \varepsilon(\tilde{\varepsilon}, q)$ . For  $m \geq 2$ , we work on the time interval  $[0, T_B(A, m)]$  so that we can use the bootstrap bounds in (65). In addition, we use the norm inflation at the ODE level, Proposition 3.6, that is,  $T_B(A, m) \rightarrow 0$  as  $m \rightarrow \infty$ , in order to improve the bootstrap bounds in (65).

The argument has three steps:

- (1) Confinement for  $W_k$  and scale separation of  $\text{supp } \omega_k(\cdot, t)$  (Lemmas 3.7, 3.8).
- (2) Estimates on velocity-error  $V_k$  (Lemma 3.9).
- (3) Integration along characteristics and bootstrap improvement (Lemma 3.10).

From this point on, ODE simplifications such as localization and freezing are no longer essential, so we return to the original notation  $x_k(t)$  and  $\Gamma_k(t)$  instead of  $x_k^{\text{orig}}(t)$  and  $\Gamma_k^{\text{orig}}(t)$ .

### 3.5.1. Confinement and Scale Separation.

**Lemma 3.7** (Confinement from  $X_k$ ). *Fix  $k \in \{1, \dots, m\}$ . For every  $t \in [0, T_B(A, m)]$ ,*

$$\text{supp } W_k(\cdot, \cdot, t) \subset [r_-, r_+] \times ([z_-, z_+] \cup [-z_+, -z_-]),$$

where

$$\begin{aligned} r_- &:= (1 - \mu)(1 - \eta)r_0 & r_+ &:= (1 + \mu)(1 + \eta)r_0, \\ z_- &:= (1 - \mu)(1 - \eta)z_0, & z_+ &:= (1 + \mu)(1 + \eta)z_0. \end{aligned}$$

Hence

$$\text{supp } \omega_k(\cdot, t) \subset [R_k(t)r_-, R_k(t)r_+] \times \left( [H_k(t)z_-, H_k(t)z_+] \cup [-H_k(t)z_+, -H_k(t)z_-] \right).$$

*Proof.* For any  $(r, z) \in \text{supp } \phi_q$  and any  $t \in [0, T_B]$ , the bootstrap bounds in (65) imply

$$X_k^r(r, z, t) \in [r_-, r_+], \quad |X_k^z(r, z, t)| \in [z_-, z_+].$$

Since the support of  $W_k$  is transported by  $X_k$  by (67), this yields the confinement of  $\text{supp } W_k(\cdot, \cdot, t)$ . Finally, if  $(r, z) \in \text{supp } \omega_k(\cdot, t)$  then  $(r/R_k(t), z/H_k(t)) \in \text{supp } W_k(\cdot, \cdot, t)$  by the ansatz  $\omega_k(r, z, t) = x_k(t)W_k(r/R_k(t), z/H_k(t), t)$ , which gives the confinement of  $\text{supp } \omega_k(\cdot, t)$ .  $\square$

Using Lemma 3.7, the ODEs (60), and the bound  $x_k(t) \leq \bar{A}$  on  $[0, T_B(A, m)]$ , we prove scale separation and disjointness of  $\text{supp } \omega_k(\cdot, t)$ .

**Lemma 3.8** (Scale separation). *There exists an integer  $m_0(A, q)$  (depending on  $A, q$  and the fixed background parameters) such that for all  $m \geq m_0(A, q)$ ,  $k \in \{1, \dots, m-1\}$  and  $t \in [0, T_B(A, m)]$ ,*

$$R_{k+1}(t)r_+ \leq \frac{1}{2}R_k(t)r_-, \tag{91}$$

and for any  $j > k$ , any  $x \in \text{supp } \omega_k(\cdot, t)$  and any  $y \in \text{supp } \omega_j(\cdot, t)$ ,

$$|x - y| \geq \frac{1}{2}r_- R_k(t). \tag{92}$$

In particular, the supports  $\{\text{supp } \omega_k(\cdot, t)\}_{k=1}^m$  are pairwise disjoint on  $[0, T_B(A, m)]$ .

*Proof. Step 1: control of  $\tilde{x}_{k+1}/\tilde{x}_k$ .* Using the ODEs  $x'_k/x_k = \partial_r u_k^r(0, 0, t)$ , one can obtain

$$\frac{d}{dt} \log\left(\frac{\tilde{x}_{k+1}(t)}{\tilde{x}_k(t)}\right) = \frac{d}{dt} \log\left(\frac{x_{k+1}(t)}{x_k(t)}\right) = \frac{x'_{k+1}(t)}{x_{k+1}(t)} - \frac{x'_k(t)}{x_k(t)} = \partial_r u_k^r(0, 0, t).$$

By the axisymmetric Biot–Savart representation at the origin,

$$\partial_r u_k^r(0, 0, t) = -x_k(t) \int_{-\infty}^{\infty} \int_0^{\infty} \frac{r^2 z}{(r^2 + z^2)^{5/2}} W_k \left( \frac{r}{R_k(t)}, \frac{z}{H_k(t)}, t \right) dr dz \geq 0.$$

Define

$$\Lambda_{\max} := \sup_{0 < \Gamma \leq 1} \Gamma^2 \Lambda_{\text{froz}}(\Gamma) < \infty,$$

where  $\Lambda_{\text{froz}}$  is defined in (3.2). Using the comparison estimate (68) (together with the definition of  $\Lambda_{\max}$ ) yields

$$\partial_r u_k^r(0, 0, t) \leq \frac{(1 + \mu)^3}{(1 - \mu)^5} x_k(t) \Lambda_{\max} \leq C_{\text{sep}} x_k(t) \leq C_{\text{sep}} \bar{A}.$$

for the constant  $C_{\text{sep}} := \frac{(1 + \mu)^3}{(1 - \mu)^5} \Lambda_{\max}$ . Integrating in time gives that for every  $k \in \{1, \dots, m - 1\}$  and every  $t \in [0, T_B(A, m)]$ ,

$$\log \left( \frac{\tilde{x}_{k+1}(t)}{\tilde{x}_k(t)} \right) \leq C_{\text{sep}} \bar{A} t. \quad (93)$$

**Step 2: disjointness of supports and the distance bound.** From Proposition 3.6, it follows that  $C_{\text{sep}} \bar{A} T_B(A, m) \rightarrow 0$  as  $m \rightarrow \infty$ . Hence, there exists an integer  $m_0(A, q)$  (which depends on the fixed background parameters in addition to  $A, q$ ) such that for all  $m \geq m_0(A, q)$ , it holds

$$d e^{C_{\text{sep}} \bar{A} T_B(A, m)} \leq \frac{1}{2} \frac{r_-}{r_+},$$

Then by (93),

$$\frac{R_{k+1}(t)}{R_k(t)} = d \frac{\tilde{x}_{k+1}(t)}{\tilde{x}_k(t)} \leq d e^{C_{\text{sep}} \bar{A} t} \leq d e^{C_{\text{sep}} \bar{A} T_B} \leq \frac{1}{2} \frac{r_-}{r_+},$$

which implies (91). By Lemma 3.7,

$$\text{supp } \omega_k(\cdot, t) \subset \{r \in [R_k(t)r_-, R_k(t)r_+]\}.$$

If  $j > k$ , then iterating (91) yields  $R_j(t)r_+ \leq R_{k+1}(t)r_+ \leq \frac{1}{2} R_k(t)r_-$ . Hence for  $x \in \text{supp } \omega_k(\cdot, t)$  and  $y \in \text{supp } \omega_j(\cdot, t)$ ,

$$|x - y| \geq |r_x - r_y| \geq R_k(t)r_- - R_j(t)r_+ \geq \frac{1}{2} R_k(t)r_-,$$

which is (92). The annuli in  $r$  therefore do not overlap, so the supports are pairwise disjoint.  $\square$

**3.5.2. Velocity-Error Estimates.** The goal of this subsection is to estimate the rescaled velocity error appearing in the equation for  $W_k$ . We use Proposition 2.1 directly. The point is that the leading outer-region integral in the  $Q(r_x)$  estimates of Proposition 2.1 agrees with the stretching rate  $\partial_r u^r(0, 0, t)$  used in the definition of the ODE for  $x_k(t)$ , up to a harmless possible contribution from the  $k$ -th ring itself.

**Lemma 3.9** (Velocity-error estimate from Proposition 2.1). *Choose  $m_0(A, q)$  as in Lemma 3.8. Then there exists a constant  $C_E = C_E(q) > 0$ , depending only on  $q$  and the fixed background parameters, such that for every  $m \geq m_0(A, q)$ ,*

$$\sup_{(r, z), t, k} \left( \left| \frac{V_k^r(r, z, t)}{r} \right| + \left| \frac{V_k^z(r, z, t)}{z} \right| \right) \leq C_E \bar{A} \left( 1 + \log \left( \frac{\bar{A}}{\varepsilon} \right) + \log m \right), \quad (94)$$

where the supremum is taken over all

$$1 \leq k \leq m, \quad 0 \leq t \leq T_B(A, m), \quad (r, z) \in \text{supp } W_k(\cdot, \cdot, t).$$

*Proof.* Throughout the proof,  $C(q) > 0$  denotes a constant depending only on  $q$  and the fixed background parameters, and it may change from line to line. Fix

$$1 \leq k \leq m, \quad 0 \leq t \leq T_B(A, m), \quad (r, z) \in \text{supp } W_k(\cdot, \cdot, t),$$

and set

$$x = (r_x, z_x) := (R_k(t)r, H_k(t)z).$$

By Lemma 3.7,

$$r \in [r_-, r_+], \quad |z| \in [z_-, z_+].$$

We use the thin-annulus condition

$$r_+ < 2r_-.$$

This condition is ensured by our choice of  $\mu = 1/20, \eta = 1/4$ .

**Step 1: preliminary bounds and the outer-region integral.** By Lemma 3.1 and the bootstrap bound  $x_j(t) \leq \bar{A}$  on  $[0, T_B(A, m)]$ ,

$$\|\omega_j(\cdot, t)\|_{L^\infty} \leq C(q)x_j(t) \leq C(q)\bar{A}, \quad 1 \leq j \leq m.$$

Since the supports are pairwise disjoint by Lemma 3.8, we obtain

$$\|\omega^{(m)}(\cdot, t)\|_{L^\infty} \leq C(q)\bar{A}. \quad (95)$$

Moreover,  $\omega^{(m)}(\cdot, t) \in L^\infty \cap L^2(\mathbb{R}^3)$ , and it is odd with respect to  $z$ . Hence Proposition 2.1 applies to  $\omega^{(m)}(\cdot, t)$ .

Since  $\omega_-$  is supported away from the origin, differentiating the axisymmetric Biot–Savart law at the origin gives

$$\partial_r u_-^r(0, 0, t) = \frac{3}{8\pi} \int_{\mathbb{R}^3} \frac{r_y z_y}{|y|^5} (-\omega_-(y, t)) dy. \quad (96)$$

**Step 2: exact identification of the outer region.** Let

$$Q(r_x) := \{y \in \mathbb{R}^3 : r_y \geq 2r_x\}.$$

We claim that

$$Q(r_x) \cap \text{supp } \omega^{(m)}(\cdot, t) = \bigcup_{j=1}^{k-1} \text{supp } \omega_j(\cdot, t), \quad (97)$$

where the right-hand side is empty when  $k = 1$ .

Indeed, if  $j < k$ , then Lemma 3.8 gives

$$R_k(t)r_+ \leq \frac{1}{2}R_{k-1}(t)r_- \leq \frac{1}{2}R_j(t)r_-.$$

Since  $r_x \leq R_k(t)r_+$ , for every  $y \in \text{supp } \omega_j(\cdot, t)$  we have

$$r_y \geq R_j(t)r_- \geq 2R_k(t)r_+ \geq 2r_x.$$

Thus every outer ring  $j < k$  is contained in  $Q(r_x)$ .

If  $j > k$ , then Lemma 3.8 gives

$$R_j(t)r_+ \leq R_{k+1}(t)r_+ \leq \frac{1}{2}R_k(t)r_-.$$

Since  $r_x \geq R_k(t)r_-$ , for every  $y \in \text{supp } \omega_j(\cdot, t)$  we have

$$r_y \leq R_j(t)r_+ \leq \frac{1}{2}R_k(t)r_- \leq \frac{1}{2}r_x < 2r_x.$$

Thus no inner ring  $j > k$  intersects  $Q(r_x)$ .

Finally, if  $y \in \text{supp } \omega_k(\cdot, t)$ , then the thin-annulus condition gives

$$r_y \leq R_k(t)r_+ < 2R_k(t)r_- \leq 2r_x.$$

Hence the  $k$ -th ring itself is disjoint from  $Q(r_x)$ . This proves (97).

Consequently, using (96),

$$\frac{3}{8\pi} \int_{Q(r_x)} \frac{r_y z_y}{|y|^5} (-\omega^{(m)}(y, t)) dy = \partial_r u_-^r(0, 0, t). \quad (98)$$

**Step 3: radial component.** By the definition of  $V_k$  in (63) and by the ODEs (60) with the convention  $x_1'(t) = 0$  and  $u_- = 0$  for  $k = 1$ , we have

$$\frac{V_k^r(r, z, t)}{r} = \frac{u^{(m),r}(x, t)}{R_k(t)r} - \partial_r u_-^r(0, 0, t) = \frac{u^{(m),r}(x, t)}{r_x} - \partial_r u_-^r(0, 0, t).$$

Applying Proposition 2.1 to  $\omega^{(m)}(\cdot, t)$ , and then using (98), gives

$$\left| \frac{V_k^r(r, z, t)}{r} \right| \leq C \frac{|x|}{r_x} \|\omega^{(m)}(\cdot, t)\|_{L^\infty}.$$

On the support under consideration,

$$\frac{|x|}{r_x} \leq 1 + \frac{|z_x|}{r_x} = 1 + \Gamma_k(t) \frac{|z|}{r} \leq C(q),$$

where we used  $\Gamma_k \leq 1$ ,  $r \geq r_-$ , and  $|z| \leq z_+$ . Combining with (95), we obtain

$$\left| \frac{V_k^r(r, z, t)}{r} \right| \leq C(q)\bar{A}. \quad (99)$$

**Step 4: vertical component.** Similarly, by the definition of  $V_k$ ,

$$\frac{V_k^z(r, z, t)}{z} = \frac{u^{(m),z}(x, t)}{H_k(t)z} + 2\partial_r u_-^r(0, 0, t) = \frac{u^{(m),z}(x, t)}{z_x} + 2\partial_r u_-^r(0, 0, t).$$

The vertical one in the  $Q(r_x)$ -estimates of Proposition 2.1, together with (98), gives

$$\left| \frac{V_k^z(r, z, t)}{z} \right| \leq C \left( 1 + \left| \log \frac{r_x}{|z_x|} \right| \right) \|\omega^{(m)}(\cdot, t)\|_{L^\infty}.$$

Therefore, by (95),

$$\left| \frac{V_k^z(r, z, t)}{z} \right| \leq C(q)\bar{A} \left( 1 + \left| \log \frac{r_x}{|z_x|} \right| \right). \quad (100)$$

It remains to bound the logarithm. Since

$$\frac{r_x}{|z_x|} = \frac{R_k(t)r}{H_k(t)|z|} = \frac{r}{|z|} \frac{1}{\Gamma_k(t)},$$

and  $r/|z|$  is bounded above and below on  $\text{supp } W_k$  by constants depending only on the fixed geometry,

$$1 + \left| \log \frac{r_x}{|z_x|} \right| \leq C(q) \log \left( \frac{e}{\Gamma_k(t)} \right).$$

Since  $x_k(t) \leq \bar{A}$  on  $[0, T_B(A, m)]$  and  $x_k(0) = \varepsilon k^{-\alpha_q}$ , we get

$$\frac{1}{\Gamma_k(t)} = \left( \frac{x_k(t)}{x_k(0)} \right)^3 \leq \left( \frac{\bar{A} k^{\alpha_q}}{\varepsilon} \right)^3 \leq \left( \frac{\bar{A} m^{\alpha_q}}{\varepsilon} \right)^3.$$

Hence

$$\log \left( \frac{e}{\Gamma_k(t)} \right) \leq C(q) \left( 1 + \log \left( \frac{\bar{A}}{\varepsilon} \right) + \log m \right).$$

Substituting this into (100) yields

$$\left| \frac{V_k^z(r, z, t)}{z} \right| \leq C(q) \bar{A} \left( 1 + \log \left( \frac{\bar{A}}{\varepsilon} \right) + \log m \right). \quad (101)$$

Combining (99) and (101), and enlarging the constant, proves (94).  $\square$

**3.5.3. Bootstrap Improvement.** For any  $A > \varepsilon(\tilde{\varepsilon}, q)$ , thanks to Proposition 3.6,

$$T_B(A, m) \leq C(q, A) m^{-\beta_q} \rightarrow 0 \quad \text{as } m \rightarrow \infty.$$

As the algebraic decay  $m^{-\beta_q}$  wins over the logarithmic growth  $\log m$ , there exists a large integer  $m_1(A, q) \geq m_0(A, q)$  such that any  $m \geq m_1(A, q)$  satisfies

$$C_E \bar{A} \left( 1 + \log \left( \frac{\bar{A}}{\varepsilon} \right) + \log m \right) T_B(A, m) \leq \min \left\{ \log \left( 1 + \frac{\mu}{2} \right), \log \left( \frac{1}{1 - \mu/2} \right) \right\} \quad (102)$$

where  $C_E$  is the constant defined in Lemma 3.9.

**Proposition 3.10** (Improved bounds for  $X_k$  and bootstrap improvement). *Fix  $m_1(A, q) \geq m_0(A, q)$  so that (102) holds for all  $m \geq m_1(A, q)$ , and fix such an  $m$ . Then for every  $t \in [0, T_B(A, m)]$  the following hold:*

(i) **Logarithmic control of  $X_k^r/r$  and  $X_k^z/z$ .**

$$\sup_{\substack{(r,z) \in \text{supp } \phi_q \\ k=1, \dots, m}} \left( \left| \log \frac{X_k^r(r, z, t)}{r} \right| + \left| \log \frac{X_k^z(r, z, t)}{z} \right| \right) \leq C_E \bar{A} \left( 1 + \log \left( \frac{\bar{A}}{\varepsilon} \right) + \log m \right) t, \quad (103)$$

where  $C_E$  is the constant defined in Lemma 3.9.

(ii) **Bootstrap improvement.**

$$\sup_{\substack{(r,z) \in \text{supp } \phi_q \\ k=1, \dots, m}} \max \left\{ \left| \frac{X_k^r(r, z, t)}{r} - 1 \right|, \left| \frac{X_k^z(r, z, t)}{z} - 1 \right| \right\} \leq \frac{\mu}{2}$$

In particular, the bootstrap bounds (65) improve with margin on  $[0, T_B]$ , and therefore  $T_B(A, m) = T_N(A, m)$ .

*Proof.* Fix  $k \in \{1, \dots, m\}$  and  $t \in [0, T_B]$ .

**Part (i).** Fix  $(r, z) \in \text{supp } \phi_q$  and consider the characteristic  $s \mapsto X_k(r, z, s)$  solving

$$\partial_s X_k(r, z, s) = V_k(X_k(r, z, s), s), \quad X_k(r, z, 0) = (r, z).$$

Since the bootstrap bounds (65) imply  $X_k^r(r, z, s)/r > 0$  and  $X_k^z(r, z, s)/z > 0$  for  $s \in [0, T_B]$ , the logarithms below are well-defined. Differentiating and using  $\partial_s X_k^r = V_k^r(X_k, s)$  and  $\partial_s X_k^z = V_k^z(X_k, s)$ ,

$$\frac{d}{ds} \log \frac{X_k^r(r, z, s)}{r} = \frac{V_k^r(X_k(r, z, s), s)}{X_k^r(r, z, s)}, \quad \frac{d}{ds} \log \frac{X_k^z(r, z, s)}{z} = \frac{V_k^z(X_k(r, z, s), s)}{X_k^z(r, z, s)}.$$

Since  $(r, z) \in \text{supp } \phi_q = \text{supp } W_k(\cdot, \cdot, 0)$  and  $W_k/r$  is transported by  $X_k$  via the Cauchy formula, the trajectory remains in the transported support, that is,  $X_k(r, z, s) \in \text{supp } W_k(\cdot, \cdot, s)$ . Hence (94) yields

$$\left| \frac{V_k^r(X_k(r, z, s), s)}{X_k^r(r, z, s)} \right| + \left| \frac{V_k^z(X_k(r, z, s), s)}{X_k^z(r, z, s)} \right| \leq C_E \bar{A} \left( 1 + \log \left( \frac{\bar{A}}{\varepsilon} \right) + \log m \right)$$

Integrating from 0 to  $t$  gives (103).

**Part (ii)** Using (103), as  $m \geq m_1(A, q)$  satisfies (102), it holds that  $1 - \mu/2 \leq X_k^r(r, z, t)/r \leq 1 + \mu/2$  and the same for  $X_k^z/z$ . Hence  $F_m(t) \leq \mu/2 < \mu$  on  $[0, T_B]$ . If  $T_B < T_N$ , continuity of  $F_m$  yields that there exists  $\tilde{\delta} > 0$  such that  $F_m(t) < \mu$  on  $[0, T_B + \tilde{\delta}]$ , contradicting maximality of  $T_B$ . Therefore,  $T_B = T_N$ .  $\square$

### 3.6. Norm inflation and Proof of Theorem 1.1.

*Proof of Theorem 1.1.* Fix  $q > 1$  and let  $\tilde{\varepsilon} > 0$ ,  $\delta > 0$ , and  $A > 0$  be given.

**Step 1: Choice of parameters and initial data.** Fix  $r_0 = 1, \eta = 1/4, \mu = 20^{-1}$ . (Recall  $\eta$  denotes the localization parameter that first appears in (78) whereas  $\mu$  the bootstrap parameter from (65)). Define  $\Theta_\mu$  by (75) and  $\zeta_\eta$  by (83) where  $\zeta_* = 1/\sqrt{2}$ . Fix a cone slope parameter  $L_q$  by

$$\frac{1}{q} < \frac{\log(L_q/\zeta_\eta)}{3\Theta_\mu + \log(L_q/\zeta_\eta)},$$

Fix  $\alpha_q$  by

$$\frac{1}{q} < \alpha_q < \frac{\log(L_q/\zeta_\eta)}{3\Theta_\mu + \log(L_q/\zeta_\eta)} (< 1). \quad (104)$$

Fix a profile  $\phi = \phi_q(r, z)$  satisfying (15) with  $z_0 = z_{0,q} = L_q r_0$ .

For any  $\varepsilon > 0$ , any integer  $m \geq 2$  and  $d = 10^{-2}$ , we define our initial data  $\omega_0^{(m)}$  by (14) with  $\phi = \phi_q$ . From (58), it follows that there exists  $\varepsilon = \varepsilon(\tilde{\varepsilon}, q) \in (0, \tilde{\varepsilon})$ , independent of  $m$ , such that

$$\|\omega_0^{(m)}\|_{L^\infty \cap L^1(\mathbb{R}^3)} + \left\| \frac{\omega_0^{(m)}}{r} \right\|_{L^{3,q}(\mathbb{R}^3)} < \tilde{\varepsilon}$$

For an integer  $m \geq 2$ , there exists a unique global-in-time smooth axisymmetric, no-swirl solution  $\omega^{(m)}$  to the Euler equation (2) with our initial data  $\omega_0^{(m)}$ . We decompose  $\omega^{(m)}$  into multi vortex rings,  $\omega_k$ 's, as in (59).

**Step 2: Bootstrap Improvement.** Define the amplitude factors  $\{x_k(t)\}_{k=1}^m$  and their initial values  $x_k(0)$  by (60) and the profiles  $\{W_k(r, z, t)\}_{k=1}^m$  by (61). Define the renormalized target amplitude  $\bar{A}$  by (64). Define the (ODE) norm inflation time  $T_N(A, m)$  by (64) and the maximal bootstrap time  $T_B(A, m) \geq 0$  by (66).

If  $A \leq \varepsilon$ , then norm inflation already holds at  $t = 0$ . Hence we only need to consider the case  $A > \varepsilon$ . Then  $T_N(A, m) > 0$ .

By Proposition 3.6, thanks to the choice of  $\alpha_q$ , (104), it holds that  $T_B(A, m) \rightarrow 0$  as  $m \rightarrow \infty$ . Therefore, there exists  $m_1 = m_1(A, q) \geq m_0(A, q)$  such that all  $m \geq m_1(A, q)$  satisfy (102). Then by bootstrap improvement, Proposition 3.10, it holds  $T_B(A, m) = T_N(A, m)$ , hence the bootstrap bound holds on  $[0, T_N(A, m)]$ , and also  $T_N(A, m) \rightarrow 0$  as  $m \rightarrow \infty$ .

**Step 3: Norm inflation in  $L^\infty$ .** Fix any  $m \geq m_1(A, q)$  and  $k \in \{1, \dots, m\}$ . On  $[0, T_N(A, m)]$ , Lemma 3.1 gives the exact Cauchy formula for the profile: for every  $(r, z) \in \text{supp } \phi_q$  and every  $t \in [0, T_N(A, m)]$ ,

$$W_k(X_k(r, z, t), t) = \frac{X_k^r(r, z, t)}{r} \phi_q(r, z).$$

Using the bootstrap lower bound  $X_k^r(r, z, t)/r \geq 1 - \mu$  on  $\text{supp } \phi_q$ , we obtain

$$\|W_k(\cdot, \cdot, t)\|_{L^\infty(\mathbb{R}^3)} \geq (1 - \mu) \|\phi_q\|_{L^\infty(\mathbb{R}^3)} \quad \text{for all } t \in [0, T_N(A, m)].$$

Using scale separation Lemma 3.8, the supports  $\{\text{supp } \omega_k(\cdot, t)\}_{k=1}^m$  are pairwise disjoint on  $[0, T_B(A, m)]$ . Hence, we can estimate the  $L^\infty$  norm of the solution  $\omega^{(m)}$  by

$$\|\omega^{(m)}(\cdot, t)\|_{L^\infty(\mathbb{R}^3)} = \sup_{1 \leq k \leq m} \|\omega_k(\cdot, t)\|_{L^\infty(\mathbb{R}^3)} = \sup_{1 \leq k \leq m} x_k(t) \|W_k(\cdot, \cdot, t)\|_{L^\infty(\mathbb{R}^3)}.$$

Evaluating at  $t = T_N(A, m)$  yields

$$\|\omega^{(m)}(\cdot, T_N(A, m))\|_{L^\infty(\mathbb{R}^3)} \geq (1 - \mu) \|\phi_q\|_{L^\infty(\mathbb{R}^3)} \sup_{1 \leq k \leq m} x_k(T_N(A, m)) \geq (1 - \mu) \|\phi_q\|_{L^\infty} \bar{A}.$$

We conclude

$$\|\omega^{(m)}(\cdot, T_N(A, m))\|_{L^\infty(\mathbb{R}^3)} \geq A.$$

Finally, since  $T_N(A, m) \rightarrow 0$  as  $m \rightarrow \infty$ , there exists an index  $m_2(A, \delta) \geq m_1(A, q)$  such that  $T_N(A, m) \leq \delta$  for all  $m \geq m_2(A, \delta)$ . Therefore, for  $m \geq m_2(A, \delta)$ , it holds

$$\sup_{0 \leq t \leq \delta} \|\omega^{(m)}(\cdot, t)\|_{L^\infty(\mathbb{R}^3)} \geq A.$$

This completes the proof of Theorem 1.1.  $\square$

#### 4. INSTANTANEOUS BLOW-UP

This section is devoted to establishing Theorem 1.2. This section is organized as follows:

- We first prove preliminary lemmas for Yudovich-type weak solutions  $(u, \omega)$ . (§ 4.1).
- Using the preliminary lemmas, we will prove the non-existence result, Theorem 1.2-(1) (§ 4.2).
- Next, we will prove the instantaneous blow-up result, Theorem 1.2-(2) by taking the limit of the sequence of our finite-ring approximations (§ 4.3).

**4.1. Preliminary Lemmas for Instantaneous Blow-Up.** This subsection is devoted to preliminary lemmas: primitive-variable formulation (Lemma 4.1), uniqueness (Lemma 4.2), a flow map and the Cauchy formula (Lemma 4.3) and a Danskin-type lemma (Lemma 4.4).

We will use these lemmas in the proof of Theorem 1.2-(1) as follows: Fix  $T_0 > 0$  and assume for contradiction that there exists a Yudovich-type weak solution  $(u, \omega)$  on  $(0, T_0)$ . We first derive primitive-variable and uniqueness consequences of this assumption, then use them to propagate the symmetry and sign structure, and finally run a finite-head bootstrap on the first  $M$  rings while treating the tail by Proposition 2.1, the flow map lemma and the Danskin-type lemma.

We prove Lemmas 4.1, 4.2 in this subsection, but the proof of Lemma 4.4 is deferred to Appendix A, which appears after the proofs of Theorem 1.2 so that the main proofs are not interrupted.

For instantaneous blow-up, we argue by contradiction, which leads to the existence of a bounded solution in a time interval.

As opposed to the proof for norm inflation, continuity of the bootstrap deviation functional  $F_m(t)$  breaks down when  $m = \infty$ ; in this case, the supremum over *infinitely many* indices  $k$  in the

definition (65) of  $F_m(t)$  prevents the functional from being continuous. It is not obvious how to make a bootstrap argument for infinitely many rings all together.

Instead, for infinitely many rings  $k = 1, 2, \dots$ , we make a bootstrap argument only for finitely many rings  $k = 1, \dots, M$ . Hence in the proof below,  $M$  denotes the number of rings for which we make a bootstrap argument.

**Primitive-Variable Formulation.** The next lemma isolates the passage from the weak formulation of the relative vorticity equation to the primitive-variable Euler formulation. The Lorentz exponent  $q$  plays no role here; only the weak transport identity (19) and the uniform  $L^1 \cap L^\infty$  bound are used.

**Lemma 4.1** (Primitive-variable formulation and strong  $L^2$  trace). *Let  $\omega_0 = \omega_0(r, z) \in L^1 \cap L^\infty(\mathbb{R}^3)$ , and assume that  $\omega_0/r \in L^1_{\text{loc}}(\mathbb{R}^3)$ . For  $T_0 > 0$ , let  $(u, \omega)$  be a Yudovich-type weak solution of (18) on  $(0, T_0)$  with initial data  $\omega_0$  in the sense of Definition 1.1. Let  $u_0$  be the velocity induced by  $\omega_0$ . Then there exists a distribution  $p \in \mathcal{D}'((0, T_0) \times \mathbb{R}^3)$  such that*

$$\partial_t u + \operatorname{div}(u \otimes u) + \nabla p = 0, \quad \operatorname{div} u = 0$$

in  $\mathcal{D}'((0, T_0) \times \mathbb{R}^3)$ , and

$$u \in L^\infty(0, T_0; H^1 \cap L^\infty(\mathbb{R}^3)) \cap W^{1, \infty}(0, T_0; H^{-1}(\mathbb{R}^3)) \subset C([0, T_0]; L^2(\mathbb{R}^3)),$$

with

$$u|_{t=0} = u_0 \quad \text{in } L^2(\mathbb{R}^3).$$

*Proof.* Define

$$\omega := \omega e_\theta, \quad A_1 := 1 + \|\omega\|_{L^\infty((0, T_0); L^1 \cap L^\infty(\mathbb{R}^3))}.$$

By interpolation,

$$\|\omega(t)\|_{L^p(\mathbb{R}^3)} \leq A_1, \quad 1 \leq p \leq \infty.$$

Standard Biot–Savart and Calderón–Zygmund estimates yield

$$\|u(t)\|_{L^2 \cap L^\infty(\mathbb{R}^3)} \leq C A_1, \tag{105}$$

and, for every  $p \in [2, \infty)$ ,

$$\|\nabla u(t)\|_{L^p(\mathbb{R}^3)} \leq C p \|\omega(t)\|_{L^p(\mathbb{R}^3)} \leq C p A_1 \tag{106}$$

for some constant  $C$  that is independent of  $p$ . In particular,

$$u \in L^\infty(0, T_0; H^1 \cap L^\infty(\mathbb{R}^3)).$$

We now recover the scalar vorticity equation from (19). Let  $\chi \in C^\infty([0, \infty))$  satisfy

$$0 \leq \chi \leq 1, \quad \chi(\rho) = 0 \text{ for } \rho \leq 1, \quad \chi(\rho) = 1 \text{ for } \rho \geq 2,$$

and define  $\chi_\varepsilon(r) := \chi(r/\varepsilon)$ . For a smooth compactly supported axisymmetric scalar test function  $\psi = \psi(r, z, t)$ , set  $\varphi_\varepsilon(x, t) := \chi_\varepsilon(r) r \psi(r, z, t)$ . Since  $\varphi_\varepsilon \in C_c^\infty(\mathbb{R}^3 \times [0, T_0))$ , it is admissible in (19). Using

$$\frac{1}{r} \partial_t \varphi_\varepsilon = \chi_\varepsilon \partial_t \psi, \quad \frac{1}{r} u \cdot \nabla \varphi_\varepsilon = \chi_\varepsilon (u^r \partial_r \psi + u^z \partial_z \psi) + \frac{u^r}{r} \chi_\varepsilon \psi + u^r \chi'_\varepsilon(r) \psi,$$

we obtain

$$\int_0^{T_0} \int_{\mathbb{R}^3} \omega \left[ \chi_\varepsilon \left( \partial_t \psi + u^r \partial_r \psi + u^z \partial_z \psi + \frac{u^r}{r} \psi \right) + u^r \chi'_\varepsilon(r) \psi \right] dx dt + \int_{\mathbb{R}^3} \omega_0 \chi_\varepsilon \psi(\cdot, 0) dx = 0.$$

Since  $\chi_\varepsilon \rightarrow 1$  pointwise and  $0 \leq \chi_\varepsilon \leq 1$ , the terms involving  $\omega \chi_\varepsilon \partial_t \psi$ ,  $\omega \chi_\varepsilon u \cdot \nabla \psi$ , and the initial datum converge by dominated convergence using  $\omega \in L^\infty(0, T_0; L^1_{\text{loc}})$ ,  $u \in L^\infty((0, T_0) \times \mathbb{R}^3)$  and

$\omega_0 \in L^1(\mathbb{R}^3)$ . The stretching term  $\omega \frac{u^r}{r} \chi_\varepsilon \psi$  converges by dominated convergence using  $u \omega / r \in L^1_{\text{loc}}([0, T_0] \times \mathbb{R}^3)$ . For the error term, since  $\chi'_\varepsilon$  is supported in  $\{\varepsilon \leq r \leq 2\varepsilon\}$ ,

$$\left| \int_0^{T_0} \int_{\mathbb{R}^3} \omega u^r \chi'_\varepsilon(r) \psi \, dx \, dt \right| \leq C_\psi \|\omega\|_{L^\infty_{t,x}} \|u\|_{L^\infty_{t,x}} \int_{\{\varepsilon \leq r \leq 2\varepsilon\}} \frac{r}{\varepsilon} \, dr \, d\theta \, dz \, dt \leq C_\psi \varepsilon \rightarrow 0.$$

Therefore,

$$\int_0^{T_0} \int_{\mathbb{R}^3} \omega \left( \partial_t \psi + u^r \partial_r \psi + u^z \partial_z \psi + \frac{u^r}{r} \psi \right) \, dx \, dt + \int_{\mathbb{R}^3} \omega_0 \psi(\cdot, 0) \, dx = 0,$$

that is, the vorticity equation (4) holding in distributions on  $(0, T_0) \times \mathbb{R}^3$ .

Equivalently, the vector field  $\boldsymbol{\omega} = \omega e_\theta$  satisfies

$$\partial_t \boldsymbol{\omega} + \operatorname{div}(u \otimes \boldsymbol{\omega} - \boldsymbol{\omega} \otimes u) = 0 \quad \text{in } \mathcal{D}'((0, T_0) \times \mathbb{R}^3).$$

Indeed, the equivalence follows because one can average a general test field in the angular variable and reduce to smooth axisymmetric swirl test fields of the form  $r\psi e_\theta$ .

Since  $\boldsymbol{\omega} = \operatorname{curl} u$  and  $\operatorname{div} u = 0$  by construction of the Biot–Savart law,

$$\operatorname{curl}(\partial_t u + \operatorname{div}(u \otimes u)) = \partial_t(\operatorname{curl} u) + \operatorname{div}(u \otimes \operatorname{curl} u - (\operatorname{curl} u) \otimes u) = 0$$

in distributions. Hence there exists  $p \in \mathcal{D}'((0, T_0) \times \mathbb{R}^3)$  such that

$$\partial_t u + \operatorname{div}(u \otimes u) + \nabla p = 0, \quad \operatorname{div} u = 0$$

in  $\mathcal{D}'((0, T_0) \times \mathbb{R}^3)$ .

Next, by (105),

$$u \otimes u \in L^\infty(0, T_0; L^2(\mathbb{R}^3)), \quad \text{hence } \operatorname{div}(u \otimes u) \in L^\infty(0, T_0; H^{-1}(\mathbb{R}^3)).$$

Applying the Leray projector  $\mathbb{P}$  to the Euler equation, we obtain

$$\partial_t u = -\mathbb{P} \operatorname{div}(u \otimes u) \in L^\infty(0, T_0; H^{-1}(\mathbb{R}^3)), \quad \text{so } u \in W^{1,\infty}(0, T_0; H^{-1}(\mathbb{R}^3)).$$

Since  $W^{1,\infty}(0, T_0; H^{-1}) \hookrightarrow C([0, T_0]; H^{-1})$ , for any  $t, s \in [0, T_0]$ ,

$$\|u(t) - u(s)\|_{L^2}^2 \leq \|u(t) - u(s)\|_{H^{-1}} \|u(t) - u(s)\|_{H^1} \leq 2 \|u\|_{L^\infty_t H^1} \|u(t) - u(s)\|_{H^{-1}},$$

which tends to 0 as  $t \rightarrow s$ . Thus

$$u \in C([0, T_0]; L^2(\mathbb{R}^3)).$$

It remains to identify the initial trace. By the weak formulation for  $\xi = \omega / r$ , we have

$$\xi(t) \rightarrow \xi_0 \quad \text{in } \mathcal{D}'(\mathbb{R}^3) \quad \text{as } t \downarrow 0.$$

Since

$$\boldsymbol{\omega}(t) = \omega(t) e_\theta = (-x_2 \xi(t), x_1 \xi(t), 0),$$

it follows that

$$\boldsymbol{\omega}(t) \rightarrow \boldsymbol{\omega}_0 := \omega_0 e_\theta \quad \text{in } \mathcal{D}'(\mathbb{R}^3).$$

Since  $u \in C([0, T_0]; L^2)$ , we have  $u(t) \rightarrow u(0)$  in  $L^2$ , hence in  $\mathcal{D}'(\mathbb{R}^3)$ . Passing to the limit in

$$\operatorname{curl} u(t) = \boldsymbol{\omega}(t), \quad \operatorname{div} u(t) = 0,$$

we obtain

$$\operatorname{curl} u(0) = \omega_0 e_\theta, \quad \operatorname{div} u(0) = 0 \quad \text{in } \mathcal{D}'(\mathbb{R}^3).$$

By construction,  $u_0$  also satisfies

$$\operatorname{curl} u_0 = \omega_0 e_\theta, \quad \operatorname{div} u_0 = 0 \quad \text{in } \mathcal{D}'(\mathbb{R}^3).$$

Hence  $w := u(0) - u_0 \in L^2(\mathbb{R}^3)$  satisfies

$$\operatorname{curl} w = 0, \quad \operatorname{div} w = 0 \quad \text{in } \mathcal{D}'(\mathbb{R}^3).$$

Then by the Helmholtz decomposition, it follows that  $w = 0$ , i.e.

$$u|_{t=0} = u_0 \quad \text{in } L^2(\mathbb{R}^3).$$

□

**Uniqueness.** To prove preservation of odd-symmetry and non-positivity in the upper half space, we need uniqueness beyond Danchin's critical regime for Yudovich-type weak solutions  $(u, \omega)$ , which satisfy  $\omega \in L^\infty((0, T_0); L^1 \cap L^\infty(\mathbb{R}^3))$ . The proof adapts the classical strategy of Yudovich's uniqueness result for two-dimensional flows (see [Yud63, Section 3] and [MB01, Theorem 8.2]); see also [Dan07b, Theorem 1.2]. Although the argument is a straightforward generalization of the 2D case, we provide a precise statement and full proof for the sake of completeness. In the proof, we will use a primitive-variable formulation proved in Lemma 4.1.

**Lemma 4.2** (Uniqueness). *Let  $\omega_0 = \omega_0(r, z) \in L^1 \cap L^\infty(\mathbb{R}^3)$ , and assume  $\omega_0/r \in L^1_{\text{loc}}(\mathbb{R}^3)$ . For  $T_0 > 0$ , let  $(u_1, \omega_1), (u_2, \omega_2)$  be Yudovich-type weak solutions of (18) on  $(0, T_0)$  with the same initial data  $\omega_0$  in the sense of Definition 1.1. Then*

$$u_1 \equiv u_2, \quad \text{hence} \quad \omega_1 \equiv \omega_2 \quad \text{on } [0, T_0] \times \mathbb{R}^3.$$

*Proof.* Set

$$A_2 := 1 + \sum_{i=1}^2 \|\omega_i\|_{L^\infty((0, T_0); L^1 \cap L^\infty(\mathbb{R}^3))}.$$

By Lemma 4.1, for  $i = 1, 2$ ,

$$u_i \in L^\infty(0, T_0; H^1 \cap L^\infty(\mathbb{R}^3)) \cap W^{1, \infty}(0, T_0; H^{-1}(\mathbb{R}^3)) \subset C([0, T_0]; L^2(\mathbb{R}^3)),$$

with  $u_i|_{t=0} = u_0$ . Moreover, by (105) and (106),

$$\|u_i(t)\|_{L^2 \cap L^\infty(\mathbb{R}^3)} \leq C A_2, \quad \|\nabla u_i(t)\|_{L^p(\mathbb{R}^3)} \leq C p A_2, \quad p \in [2, \infty)$$

for some constant  $C > 0$  that is independent of  $p$ .

Let

$$v := u_1 - u_2.$$

Then

$$v \in L^\infty(0, T_0; H^1(\mathbb{R}^3)) \cap W^{1, \infty}(0, T_0; H^{-1}(\mathbb{R}^3)) \subset C([0, T_0]; L^2(\mathbb{R}^3)), \quad v(0) = 0,$$

and, subtracting the two Euler equations and applying the Leray projector,

$$\partial_t v = -\mathbb{P}((u_2 \cdot \nabla)v + (v \cdot \nabla)u_1) \quad \text{in } L^\infty(0, T_0; H^{-1}(\mathbb{R}^3)).$$

Set

$$E(t) := \|v(t)\|_{L^2(\mathbb{R}^3)}^2.$$

Since  $v \in L_t^\infty H_x^1 \cap W_t^{1, \infty} H_x^{-1}$ , the Lions–Magenes lemma yields that  $E$  is absolutely continuous on  $[0, T_0]$  and

$$\frac{1}{2} E'(t) = \langle \partial_t v(t), v(t) \rangle_{H^{-1}, H^1} \quad \text{for a.e. } t \in [0, T_0].$$

Because  $\operatorname{div} v = 0$ , we have  $\mathbb{P}v = v$ , and therefore

$$\langle \mathbb{P}f, v \rangle_{H^{-1}, H^1} = \langle f, \mathbb{P}v \rangle_{H^{-1}, H^1} = \langle f, v \rangle_{H^{-1}, H^1}.$$

Thus

$$\frac{1}{2}E'(t) = -\langle (u_2 \cdot \nabla)v(t), v(t) \rangle_{H^{-1}, H^1} - \langle (v \cdot \nabla)u_1(t), v(t) \rangle_{H^{-1}, H^1} \quad (107)$$

for a.e.  $t$ .

For a.e. fixed  $t$ , define

$$B_t(a, b) := \int_{\mathbb{R}^3} (u_2(t) \cdot \nabla a) \cdot b \, dx, \quad a, b \in H^1(\mathbb{R}^3).$$

Since  $u_2(t) \in L^\infty(\mathbb{R}^3)$ ,  $B_t$  is continuous on  $H^1(\mathbb{R}^3) \times H^1(\mathbb{R}^3)$ . If  $a \in C_c^\infty(\mathbb{R}^3)$ , then

$$B_t(a, a) = \frac{1}{2} \int_{\mathbb{R}^3} u_2(t) \cdot \nabla (|a|^2) \, dx = 0$$

because  $\operatorname{div} u_2(t) = 0$ . By density,  $B_t(a, a) = 0$  for every  $a \in H^1(\mathbb{R}^3)$ , hence

$$\langle (u_2 \cdot \nabla)v(t), v(t) \rangle_{H^{-1}, H^1} = 0 \quad \text{for a.e. } t.$$

Also,

$$(v \cdot \nabla)u_1 \in L^\infty(0, T_0; L^2(\mathbb{R}^3)),$$

since  $v \in L_{t,x}^\infty$  and  $\nabla u_1 \in L_t^\infty L_x^2$ . Therefore (107) becomes

$$\frac{1}{2}E'(t) = - \int_{\mathbb{R}^3} (v \cdot \nabla)u_1 \cdot v \, dx \quad \text{for a.e. } t \in [0, T_0].$$

Let  $p \in [2, \infty)$ . By Hölder's inequality, interpolation, and (106),

$$\left| \int_{\mathbb{R}^3} (v \cdot \nabla)u_1 \cdot v \, dx \right| \leq \|\nabla u_1\|_{L^p} \|v\|_{L^{\frac{2p}{p-1}}}^2 \leq Cp A_2 \|v\|_{L^2}^{2(1-\frac{1}{p})} \|v\|_{L^\infty}^{\frac{2}{p}}$$

for some constant  $C > 0$  that is independent of  $p$ . Using (105),

$$\|v(t)\|_{L^\infty} \leq \|u_1(t)\|_{L^\infty} + \|u_2(t)\|_{L^\infty} \leq CA_2,$$

and therefore

$$E'(t) \leq Cp A_2^2 E(t)^{1-\frac{1}{p}} \quad \text{for a.e. } t \in [0, T_0].$$

Fix  $\varepsilon > 0$ . Then, for a.e.  $t \in [0, T_0]$ ,

$$\frac{d}{dt}(E(t) + \varepsilon)^{1/p} = \frac{1}{p}(E(t) + \varepsilon)^{\frac{1}{p}-1} E'(t) \leq CA_2^2 \left( \frac{E(t)}{E(t) + \varepsilon} \right)^{1-\frac{1}{p}} \leq CA_2^2.$$

Since  $E(0) = 0$ , integration gives

$$(E(t) + \varepsilon)^{1/p} \leq \varepsilon^{1/p} + CA_2^2 t.$$

Letting  $\varepsilon \downarrow 0$ , we obtain

$$E(t) \leq (CA_2^2 t)^p \quad \text{for every } p \in [2, \infty).$$

Hence, if  $t < (CA_2^2)^{-1}$ , letting  $p \rightarrow \infty$  yields  $E(t) = 0$ . Therefore

$$v \equiv 0 \quad \text{on } [0, (CA_2^2)^{-1}].$$

Since  $v \in C([0, T_0]; L^2)$ , we still have  $v((CA_2^2)^{-1}) = 0$ . Restarting the same argument finitely many times, we conclude that

$$v \equiv 0 \quad \text{on } [0, T_0] \times \mathbb{R}^3.$$

Thus  $u_1 \equiv u_2$ . Taking curl, we obtain

$$\omega_1 e_\theta = \operatorname{curl} u_1 = \operatorname{curl} u_2 = \omega_2 e_\theta,$$

hence  $\omega_1 = \omega_2$  a.e. on  $(0, T_0) \times \mathbb{R}^3$ .  $\square$

**Flow map and Cauchy formula under bounded vorticity.** Next, we prove the existence of a flow map and the Cauchy formula under bounded vorticity with a velocity field of finite energy. This lemma implies that as we consider bounded vorticity, it yields  $\nabla u \in BMO$ , hence  $u$  is log-Lipschitz. Then the Lagrangian transport of  $\xi = \omega/r$  is available.

We will use this lemma for both (1) and (2) of Theorem 1.2.

**Lemma 4.3** (Flow map and Cauchy formula under bounded vorticity). *Let  $T_0 > 0$ . Let  $u$  be divergence-free and axisymmetric without swirl on  $(0, T_0) \times \mathbb{R}^3$ , and let  $\omega_0 = \omega_0(r, z)$ ,  $\omega = \omega(r, z, t)$  be axisymmetric. Set*

$$\xi := \frac{\omega}{r}, \quad \xi_0 := \frac{\omega_0}{r}.$$

Assume that

$$u \in L^\infty(0, T_0; L^2(\mathbb{R}^3)), \quad \omega \in L^\infty((0, T_0) \times \mathbb{R}^3),$$

that

$$\operatorname{curl} u = \omega e_\theta, \quad \operatorname{div} u = 0$$

in  $\mathcal{D}'((0, T_0) \times \mathbb{R}^3)$ , and that  $\xi$  satisfies the distributional transport identity (19) with initial data  $\xi_0$ , where  $\xi_0 \in L^1(\mathbb{R}^3)$ .

Then the following hold.

(i) There exists a constant  $C > 0$  such that

$$|u(x, t) - u(y, t)| \leq C|x - y| \log \left( 2 + \frac{1}{|x - y|} \right) \quad (108)$$

for all  $x, y \in \mathbb{R}^3$  and for a.e.  $t \in (0, T_0)$ . In addition,  $u \in L^\infty((0, T_0) \times \mathbb{R}^3)$ .

(ii) After modifying  $u$  on a null set in time, the ODE

$$\partial_t Y(a, t) = u(Y(a, t), t), \quad Y(a, 0) = a$$

admits a unique flow map

$$Y : \mathbb{R}^3 \times [0, T_0] \rightarrow \mathbb{R}^3.$$

For each  $a \in \mathbb{R}^3$ , the map  $t \mapsto Y(a, t)$  is absolutely continuous, whereas  $(a, t) \mapsto Y(a, t)$  is continuous. Moreover, for each  $t \in [0, T_0]$ , the map  $Y_t := Y(\cdot, t)$  is a homeomorphism of  $\mathbb{R}^3$  onto itself and is measure-preserving. Furthermore, there exists  $\gamma \in (0, 1]$  such that for every compact set  $K \subset \mathbb{R}^3$ , there exists a constant  $C_{K, T_0} > 0$  such that for all  $x_1, x_2 \in K$  and  $t \in [0, T_0]$ ,

$$|Y_t(x_1) - Y_t(x_2)| + |Y_t^{-1}(x_1) - Y_t^{-1}(x_2)| \leq C_{K, T_0} |x_1 - x_2|^\gamma. \quad (109)$$

(iii) The relative vorticity is transported by the flow:

$$\xi(Y(a, t), t) = \xi_0(a) \quad \text{for a.e. } (a, t) \in \mathbb{R}^3 \times (0, T_0). \quad (110)$$

Equivalently,

$$\frac{\omega(Y(a, t), t)}{Y^r(a, t)} = \frac{\omega_0(a)}{r_a} \quad \text{for a.e. } (a, t) \in \mathbb{R}^3 \times (0, T_0). \quad (111)$$

*Proof of Lemma 4.3.* For a.e. fixed  $t$ , set  $\Omega(t) := \omega(t)e_\theta$ . Since

$$\operatorname{curl} u(t) = \Omega(t), \quad \operatorname{div} u(t) = 0$$

in  $\mathcal{D}'(\mathbb{R}^3)$ , we have

$$-\Delta u(t) = \operatorname{curl} \Omega(t).$$

The finite-energy condition  $u(t) \in L^2(\mathbb{R}^3)$  removes the possible harmonic ambiguity in this div–curl inversion. Hence, for every  $i, j$ ,

$$\partial_j u_i(t) = \sum_{\ell, m=1}^3 \varepsilon_{i\ell m} R_j R_\ell \Omega_m(t) \quad \text{in } \mathcal{D}'(\mathbb{R}^3),$$

where  $R_j$  denotes the  $j$ -th Riesz transform. Since the double Riesz transforms are Calderón–Zygmund operators and are bounded from  $L^\infty(\mathbb{R}^3)$  to  $BMO(\mathbb{R}^3)$ , it follows that

$$[\nabla u(t)]_{BMO(\mathbb{R}^3)} \leq C \|\Omega(t)\|_{L^\infty(\mathbb{R}^3)} = C \|\omega(t)\|_{L^\infty(\mathbb{R}^3)}. \quad (112)$$

On the other hand, standard local div-curl estimates imply that for every  $p \in [1, \infty)$ ,

$$\sup_{x_0 \in \mathbb{R}^3} \|u(t)\|_{W^{1,p}(B_1(x_0))} \leq C(p) \left( \|u(t)\|_{L^2(\mathbb{R}^3)} + \|\omega(t)\|_{L^\infty(\mathbb{R}^3)} \right) \quad (113)$$

for a.e.  $t \in (0, T_0)$ . Choosing  $p > 3$  and using Sobolev embedding on unit balls, we obtain

$$\|u(t)\|_{L^\infty(\mathbb{R}^3)} \leq C(p) \left( \|u(t)\|_{L^2(\mathbb{R}^3)} + \|\omega(t)\|_{L^\infty(\mathbb{R}^3)} \right)$$

for a.e.  $t \in (0, T_0)$ , and therefore

$$u \in L^\infty((0, T_0) \times \mathbb{R}^3).$$

Also, (113) with  $p = 1$  gives

$$\sup_{x_0 \in \mathbb{R}^3} \int_{B_1(x_0)} |\nabla u(t, x)| dx \leq C \left( \|u(t)\|_{L^2(\mathbb{R}^3)} + \|\omega(t)\|_{L^\infty(\mathbb{R}^3)} \right).$$

Combining this bound with (112), Lemma 1 in [AB15] yields

$$|u(x, t) - u(y, t)| \leq C|x - y| |\log|x - y|| \quad \text{for } |x - y| \leq \frac{1}{2},$$

uniformly for a.e.  $t \in (0, T_0)$ . Enlarging the constant and using the  $L^\infty$  bound for  $u$ , we obtain (108) for all  $x, y \in \mathbb{R}^3$  and a.e.  $t \in (0, T_0)$ . In particular,

$$u \in L^1(0, T_0; LL(\mathbb{R}^3))$$

in the sense of [Che95, Définition 5.2.1].

Hence, after modifying  $u$  on a null set in time, [Che95, Théorème 5.2.1] implies that  $u$  admits a unique flow map  $Y$ . For each  $a \in \mathbb{R}^3$ , the map  $t \mapsto Y(a, t)$  is absolutely continuous, whereas  $(a, t) \mapsto Y(a, t)$  is continuous. Moreover, for each  $t \in [0, T_0]$ , the map  $Y_t := Y(\cdot, t)$  is a homeomorphism of  $\mathbb{R}^3$  onto itself. Since  $\operatorname{div} u = 0$ , the flow is measure-preserving. Finally, the local Hölder estimate (109) holds on compact sets for  $Y_t$ .

Then using the Hölder estimate for  $Y_t$ , one can also prove the Hölder estimate for the inverse  $Y_t^{-1}$  by considering the reversed vector field and applying Chemin’s theorem again. See also [MB01, Lemma 8.2] for another related reference for this matter.

Applying Proposition A.1 (which will be proved in Appendix A below) to the distributional solution  $\xi$  with the flow map  $Y$  from part (ii), we obtain

$$\xi(x, t) = \xi_0(Y_t^{-1}(x)) \quad \text{for a.e. } (x, t) \in \mathbb{R}^3 \times (0, T_0),$$

hence

$$\xi(Y(a, t), t) = \xi_0(a) \quad \text{for a.e. } (a, t) \in \mathbb{R}^3 \times (0, T_0).$$

Since  $\omega = r\xi$ , this gives

$$\frac{\omega(Y(a, t), t)}{Y^r(a, t)} = \frac{\omega_0(a)}{r_a} \quad \text{for a.e. } (a, t) \in \mathbb{R}^3 \times (0, T_0).$$

This completes the proof.  $\square$

**Danskin-Type Lemma.** Next, we record a Danskin-type lemma, which will be used to handle rings closer to the origin. This lemma is likely known in related forms, but as we could not find a statement that exactly fits our situation, we include it here for completeness. This is an absolutely-continuous-in-time envelope lemma tailored to our Lagrangian radial extrema, rather than a direct invocation of the classical smooth Danskin theorem (See [Dan67], [BR95]).

**Lemma 4.4** (Danskin-type lemma). *Fix  $T_0 > 0$ , and let  $K \subset \mathbb{R}^N$  be compact, and let*

$$Y^r : K \times [0, T_0] \rightarrow \mathbb{R}$$

*be continuous. Assume that there exists a bounded function*

$$g : K \times (0, T_0) \rightarrow \mathbb{R}$$

*measurable in  $t$  for each fixed  $x \in K$ , such that, for every  $x \in K$  and every  $t \in [0, T_0]$ ,*

$$Y^r(x, t) = Y^r(x, 0) + \int_0^t g(x, s) ds.$$

*Assume furthermore that there exists a full-measure set  $E_g \subset (0, T_0)$  and a modulus of continuity  $\rho : [0, \infty) \rightarrow [0, \infty)$  with  $\lim_{s \rightarrow 0^+} \rho(s) = 0$ , such that*

$$|g(x, t) - g(y, t)| \leq \rho(|x - y|) \quad \text{for all } x, y \in K, t \in E_g. \quad (114)$$

*Define*

$$R_K(t) := \max_{x \in K} Y^r(x, t), \quad r_K(t) := \min_{x \in K} Y^r(x, t),$$

*and*

$$\mathcal{M}_K(t) := \operatorname{argmax}_{x \in K} Y^r(x, t), \quad \mathcal{A}_K(t) := \operatorname{argmin}_{x \in K} Y^r(x, t).$$

*The definition of  $\operatorname{argmax}_{x \in K} Y^r(x, t)$  is as follows:*

$$\operatorname{argmax}_{x \in K} Y^r(x, t) = \{y \in K : Y^r(y, t) = \max_{x \in K} Y^r(x, t)\},$$

*and we similarly define  $\operatorname{argmin}_{x \in K} Y^r(x, t)$ . Then  $R_K$  and  $r_K$  are Lipschitz on  $[0, T_0]$ . Moreover, there exists a full-measure set  $E \subset E_g$  such that for every  $t \in E$*

$$R'_K(t) = \max_{x \in \mathcal{M}_K(t)} g(x, t), \quad r'_K(t) = \min_{x \in \mathcal{A}_K(t)} g(x, t).$$

*In particular, these identities hold for a.e.  $t \in (0, T_0)$ .*

A proof of this Lemma 4.4 is written in Appendix A.

**4.2. Proof of Theorem 1.2-(1).** We are now ready to prove Theorem 1.2-(1). Fix  $q > 1$  and let  $\tilde{\varepsilon} > 0$  be given. We fix once and for all the parameters  $L_q, \alpha_q, \phi_q$  and the geometric constants  $r_0, \mu, \eta, d$  exactly as in the proof of Theorem 1.1 (see Section 3.1). For a parameter  $\varepsilon > 0$ , let  $\omega_0^{(\infty)}$  be the initial data obtained from (14) with infinitely many vortex rings, i.e.  $m = \infty$ .

The smallness in Theorem 1.2-(1) follows from (58): since  $\alpha_q q > 1$ , the series  $\sum_{k \geq 1} k^{-\alpha_q q}$  converges, hence there exists  $\varepsilon = \varepsilon(\tilde{\varepsilon}, q)$  such that

$$\left\| \omega_0^{(\infty)} \right\|_{L^\infty \cap L^1(\mathbb{R}^3)} + \left\| \frac{\omega_0^{(\infty)}}{r} \right\|_{L^{3,q}(\mathbb{R}^3)} \leq \tilde{\varepsilon}.$$

Assume for contradiction there exist  $T_0 > 0$  and a Yudovich-type weak solution  $(u^{(\infty)}, \omega^{(\infty)})$  to (18) on  $[0, T_0]$  with initial data  $\omega_0^{(\infty)}$  in the sense of Definition 1.1. Recall a Yudovich-type weak solution satisfies, by definition,

$$\omega^{(\infty)} \in L^\infty([0, T_0]; L^\infty \cap L^1(\mathbb{R}^3)).$$

Set  $A_\infty := \|\omega^{(\infty)}\|_{L^\infty([0, T_0] \times \mathbb{R}^3)} < \infty$ . Let

$$A := 2 \max\{A_\infty, \varepsilon(\tilde{\varepsilon}, q)\}, \quad \bar{A} := \frac{A}{1 - \mu}.$$

Since  $\omega^{(\infty)} \in L^\infty(0, T_0; L^\infty \cap L^1(\mathbb{R}^3))$ , it holds  $u^{(\infty)} \in L^\infty(0, T_0; L^2(\mathbb{R}^3))$  by Lemma 4.1. Hence we can apply Lemma 4.3 to obtain a unique flow map  $Y$  and the Cauchy formula (111).

We claim that

$$\begin{cases} \omega^{(\infty)}(r, z, t) = -\omega^{(\infty)}(r, -z, t) \text{ almost everywhere, and} \\ \omega^{(\infty)}(r, z, t) \leq 0 \text{ almost everywhere in } \{z > 0\}. \end{cases} \quad (115)$$

*Proof of (115).* Let

$$\bar{\omega}^{(\infty)}(r, z, t) := -\omega^{(\infty)}(r, -z, t),$$

and let  $\bar{u}^{(\infty)}$  be the velocity induced by  $\bar{\omega}^{(\infty)}$  through the Biot–Savart law. By symmetry of (6) and (5) under  $z \mapsto -z$ , the pair  $(\bar{u}^{(\infty)}, \bar{\omega}^{(\infty)})$  is also an (axisymmetric no-swirl) Yudovich-type weak solution with the same initial data  $\omega_0^{(\infty)}$ . Hence Lemma 4.2 gives

$$\bar{\omega}^{(\infty)} \equiv \omega^{(\infty)}, \quad \bar{u}^{(\infty)} \equiv u^{(\infty)}.$$

Thus  $\omega^{(\infty)}(r, z, t) = -\omega^{(\infty)}(r, -z, t)$  almost everywhere, and

$$u^{(\infty),r}(r, z, t) = u^{(\infty),r}(r, -z, t), \quad u^{(\infty),z}(r, z, t) = -u^{(\infty),z}(r, -z, t).$$

Hence the flow map associated with  $u^{(\infty)}$  preserves the upper and lower half-spaces. Since  $\omega^{(\infty)}/r$  is transported by the flow and  $\omega_0^{(\infty)} \leq 0$  on  $\{z > 0\}$ , it follows that  $\omega^{(\infty)}(r, z, t) \leq 0$  almost everywhere in  $\{z > 0\}$ .  $\square$

We decompose  $\omega_0^{(\infty)} = \sum_{k=1}^{\infty} \omega_{0,k}$  as in (14). For each  $k \geq 1$ , define  $\omega_k(x, t)$  by

$$\omega_k(x, t) := r_x \left( \frac{\omega_{0,k}}{r} \right) (Y^{-1}(x, t)), \quad x = (r_x, z_x).$$

Hence the Cauchy formula for  $\omega_k/r$  holds *by definition*. Then  $\omega^{(\infty)}(r, z, t) = \sum_{k=1}^{\infty} \omega_k(r, z, t)$  for a.e.  $(r, z)$  and  $t$ . We define  $u_k(r, z, t)$  by using  $\omega_k$  through the Biot–Savart law, and for  $k \geq 2$ , we define  $u_- := \sum_{j=1}^{k-1} u_j$ ,  $u_+ := \sum_{j=k+1}^{\infty} u_j$ . Then  $u^{(\infty)} = u_- + u_k + u_+$  for every  $(r, z)$  and  $t$ .

Next, we will use the existence of the flow map  $Y$  to prove the following claim:

$$\left\{ \begin{array}{l} \exists \rho_k > 0 \text{ s.t. for all } t \in [0, T_0], \text{ the velocity } u_-(\cdot, t) \text{ is } C^1 \text{ on } B_{\rho_k}(0) \subset \mathbb{R}^3. \\ \text{the map: } t \mapsto \nabla u_-(0, 0, t) \text{ is continuous on } [0, T_0]. \\ \text{In particular, the map: } t \mapsto \partial_r u_-^r(0, 0, t) \text{ is continuous on } [0, T_0]. \end{array} \right. \quad (116)$$

*Proof of (116).* For each fixed  $t \in [0, T_0]$ , the flow map  $Y_t := Y(\cdot, t)$  is a homeomorphism of  $\mathbb{R}^3$  with inverse  $Y_t^{-1} = Y^{-1}(\cdot, t)$ . Since  $u^{(\infty)}(0, 0, t) = 0$ , the origin is a fixed trajectory, so  $Y_t(0) = 0$  and hence  $Y_t^{-1}(0) = 0$ . Therefore, for each  $1 \leq j \leq k-1$ , because  $\text{supp } \omega_{0,j}$  is compact and does not contain the origin, its image  $Y_t(\text{supp } \omega_{0,j})$  also does not contain the origin for any  $t \in [0, T_0]$ . Since  $(a, t) \mapsto Y(a, t)$  is continuous on the compact set  $\text{supp } \omega_{0,j} \times [0, T_0]$ , the set

$$K_j := \bigcup_{t \in [0, T_0]} Y(\text{supp } \omega_{0,j}, t)$$

is a compact subset of  $\mathbb{R}^3 \setminus \{0\}$ . Hence,

$$\rho_k := \frac{1}{2} \text{dist} \left( 0, \bigcup_{j=1}^{k-1} K_j \right) > 0.$$

Fix  $t \in [0, T_0]$ . For  $x \in B_{\rho_k}(0)$  and  $1 \leq j \leq k-1$ , the distance from  $x$  to  $\text{supp } \omega_j(\cdot, t)$  is at least  $\rho_k$ . Hence the Biot–Savart kernel and its first  $x$ -derivatives are smooth and bounded on

$$B_{\rho_k}(0) \times \left( \bigcup_{j=1}^{k-1} K_j \right).$$

Differentiating under the integral sign in the Biot–Savart formula therefore gives that each  $u_j(\cdot, t)$  is  $C^1$  on  $B_{\rho_k}(0)$ , and hence so is  $u_-(\cdot, t)$ .

To prove continuity in time at the origin, let  $\mathcal{K}(y)$  denote the matrix-valued kernel appearing in the formula for  $\nabla u(0, t)$  after differentiating the Biot–Savart law in the evaluation variable. Since  $\mathcal{K}$  is smooth on  $\mathbb{R}^3 \setminus \{0\}$ , for each  $1 \leq j \leq k-1$  we may write

$$\nabla u_j(0, t) = \int_{\mathbb{R}^3} \mathcal{K}(y) \omega_j(y, t) dy.$$

Using volume preservation of  $Y$  and the definition of  $\omega_j$ , this becomes

$$\nabla u_j(0, t) = \int_{\text{supp } \omega_{0,j}} \mathcal{K}(Y(a, t)) \frac{Y^r(a, t)}{r_a} \omega_{0,j}(a) da,$$

where  $r_a$  denotes the radial coordinate of  $a$ .

For  $a \in \text{supp } \omega_{0,j}$  and  $t \in [0, T_0]$ , the point  $Y(a, t)$  stays in the compact set  $K_j \subset \mathbb{R}^3 \setminus \{0\}$ . Thus the integrand is continuous in  $t$  and uniformly bounded on  $\text{supp } \omega_{0,j} \times [0, T_0]$ . By dominated convergence,  $t \mapsto \nabla u_j(0, t)$  is continuous. Summing over  $j = 1, \dots, k-1$  yields continuity of  $t \mapsto \nabla u_-(0, t)$ . By axisymmetry, this implies continuity of  $t \mapsto \partial_r u_-^r(0, 0, t)$ . It finishes the proof of (116).  $\square$

For every  $k \geq 2$ , define  $x_k(t)$  by

$$x_k'(t) = x_k(t) \partial_r u_-^r(0, 0, t), \quad x_k(0) = \frac{\varepsilon}{k^{\alpha_q}},$$

and set

$$x_1(t) \equiv \varepsilon.$$

Define  $\tilde{x}_k$ ,  $R_k$ , and  $H_k$  from  $x_k$  by (22), and define  $W_k$  by (61). Also define  $V_k$  by (63).

In the present contradiction setting, we define the rescaled flow map  $X_k$  directly from the global flow map  $Y$ . For  $(r, z) \in \text{supp } \phi_q$ , set

$$X_k(r, z, t) := \left( \frac{Y^r(d^k r, d^k z, t)}{R_k(t)}, \frac{Y^z(d^k r, d^k z, t)}{H_k(t)} \right).$$

Since  $\tilde{x}_k(0) = 1$ , we have  $R_k(0) = H_k(0) = d^k$ , hence

$$X_k(r, z, 0) = (r, z).$$

Moreover, since  $Y$  is continuous and  $R_k, H_k$  are continuous and strictly positive on  $[0, T_0]$ , the map  $(r, z, t) \mapsto X_k(r, z, t)$  is continuous on  $\text{supp } \phi_q \times [0, T_0]$ .

Just by using the definition of  $X_k$  and  $W_k$ , we claim that the Cauchy formula (67) holds pointwise in the present contradiction setting as well:

$$\frac{W_k(X_k(r, z, t), t)}{X_k^r(r, z, t)} = \frac{\phi_q(r, z)}{r}, \quad (r, z) \in \text{supp } \phi_q, \quad t \in [0, T_0]. \quad (117)$$

*Proof of the Cauchy formula (117).* By (22),

$$\frac{R'_k(t)}{R_k(t)} = \frac{x'_k(t)}{x_k(t)}, \quad \frac{H'_k(t)}{H_k(t)} = -2 \frac{x'_k(t)}{x_k(t)}.$$

Therefore, differentiating the definition of  $X_k$  in time (for a.e.  $t$ ), we obtain

$$\partial_t X_k^r(r, z, t) = \frac{u^r(R_k(t)X_k^r(r, z, t), H_k(t)X_k^z(r, z, t), t)}{R_k(t)} - X_k^r(r, z, t) \frac{x'_k(t)}{x_k(t)} = V_k^r(X_k(r, z, t), t),$$

and similarly

$$\partial_t X_k^z(r, z, t) = \frac{u^z(R_k(t)X_k^r(r, z, t), H_k(t)X_k^z(r, z, t), t)}{H_k(t)} + 2X_k^z(r, z, t) \frac{x'_k(t)}{x_k(t)} = V_k^z(X_k(r, z, t), t).$$

Hence  $X_k$  is precisely the flow map associated with  $V_k$ .

Finally, fix  $(r, z) \in \text{supp } \phi_q$  and set

$$a := (d^k r, d^k z).$$

By the definition of  $\omega_k$  through the global flow  $Y$ ,

$$\omega_k(Y(a, t), t) = Y^r(a, t) \frac{\omega_{0,k}(a)}{r_a}.$$

Since

$$\omega_{0,k}(a) = x_k(0)\phi_q(r, z), \quad r_a = d^k r, \quad Y^r(a, t) = R_k(t)X_k^r(r, z, t) = d^k \frac{x_k(t)}{x_k(0)} X_k^r(r, z, t),$$

we obtain

$$\omega_k(Y(a, t), t) = x_k(t) X_k^r(r, z, t) \frac{\phi_q(r, z)}{r}.$$

On the other hand, by the definition of  $W_k$ ,

$$\omega_k(Y(a, t), t) = \omega_k(R_k(t)X_k^r(r, z, t), H_k(t)X_k^z(r, z, t), t) = x_k(t) W_k(X_k(r, z, t), t).$$

Therefore, one can obtain the pointwise Cauchy formula (117), and it finishes the proof of (117).  $\square$

**Hierarchy of index thresholds.** Throughout the proof, we introduce several integer thresholds depending on  $(A, q)$ :

$$m_0(A, q), \quad m_{\text{cone}}(A, q), \quad m_{\text{tail}}(A, q), \quad m_1(A, q), \quad m_2(A, q).$$

For clarity, we summarize their roles and dependencies.

- (i)  $m_0(A, q)$  ensures scale separation for the first  $M$  rings (Lemma 3.8). In particular, for all  $M \geq m_0(A, q)$ , the supports  $\{\text{supp } \omega_k\}_{k=1}^M$  are pairwise disjoint and satisfy the geometric separation bounds (91)–(92). See (118) and the paragraph following Proposition 4.5.
- (ii)  $m_{\text{cone}}(A, q) \geq m_0(A, q)$  guarantees that all trajectories starting from  $\text{supp } \omega_0^{(\infty)}$  remain in the cone region  $Lr \geq |z|$  on  $[0, T_B(A, M)]$  for  $M \geq m_{\text{cone}}(A, q)$ . This allows us to use Proposition 2.1 uniformly in time with the factor  $|x|/r_x$  bounded by  $\sqrt{1+L^2}$ . See (122).
- (iii)  $m_{\text{tail}}(A, q) \geq m_{\text{cone}}(A, q)$  ensures strict separation between the head ( $k \leq M$ ) and the tail ( $k > M$ ), namely

$$\frac{r_{M,-}(t)}{R_{\text{tail}}(t)} \geq 4 \quad \text{for all } t \in [0, T_B(A, M)],$$

which yields the uniform distance bound (125) and allows us to control the tail contribution. See (124).

- (iv)  $m_1(A, q) \geq m_{\text{tail}}(A, q)$  is chosen large enough so that

$$C_E \bar{A} (1 + \log(\bar{A}/\varepsilon) + \log M) T_B(A, M) \ll 1,$$

which enables the bootstrap improvement and yields  $T_B(A, M) = T_N(A, M)$ . See (128).

- (v)  $m_2(A, q) \geq m_1(A, q)$  is chosen so that the norm-inflation time satisfies

$$T_N(A, M) < T_0$$

for all  $M \geq m_2(A, q)$ . This ensures that the ODE norm inflation occurs within the prescribed time interval and allows us to evaluate the solution at  $t = T_N(A, M)$ .

In particular, for all  $M \geq m_2(A, q)$ , all the above properties hold simultaneously.

**Step 1: Finite–ring bootstrap (tail handled by the contradiction hypothesis).**

For any integer  $M \geq 2$ , define  $T_N(A, M)$  and  $T_B(A, M)$  by

$$T_N(A, M) := \sup \left\{ t \in [0, T_0] : \max_{1 \leq k \leq M} x_k(t) \leq \bar{A} \right\}$$

$$T_B(A, M) := \sup \{ T \in [0, T_N(A, M)] : F_M(t) \leq \mu \text{ all } t \in [0, T] \}.$$

where the bootstrap functional  $F_M(t)$  is defined in (65). Since  $M$  is finite and the function  $(r, z, t) \mapsto X_k(r, z, t)$  is continuous,  $F_M(t)$  is continuous and  $F_M(0) = 0$ , hence  $T_B(A, M) > 0$ .

By the definition,  $T_B(A, M) \leq T_N(A, M)$ , hence  $x_k(t) \leq \bar{A}$  on  $[0, T_B(A, M)]$ .

Before we state the main goal of Step 1, by using the bootstrap bounds on  $[0, T_B(A, M)]$  and the fact that  $x_k(t) \leq \bar{A}$  on  $[0, T_B(A, M)]$ , we prove confinement and scale-separation for the head rings in the same way as in the proof for norm inflation.

**Proposition 4.5** (Finite-head reduction for the first  $M$  rings). *The following statements hold on  $[0, T_B(A, M)]$  for the first  $M$  rings.*

- (i) *For every  $1 \leq k \leq M$ , the Cauchy formula (117) holds and*

$$(1 - \mu) \|\phi_q\|_{L^\infty(\mathbb{R}^3)} \leq \|W_k(\cdot, \cdot, t)\|_{L^\infty(\mathbb{R}^3)} \leq (1 + \mu) \|\phi_q\|_{L^\infty(\mathbb{R}^3)},$$

$$\|\omega_k(\cdot, t)\|_{L^\infty(\mathbb{R}^3)} \leq (1 + \mu) x_k(t) \|\phi_q\|_{L^\infty(\mathbb{R}^3)} \leq (1 + \mu) \bar{A} \|\phi_q\|_{L^\infty(\mathbb{R}^3)}.$$

- (ii) For every  $2 \leq k \leq M$ , the amplitudes satisfy the same weak ODE inequalities as in (71). Consequently, repeating the proof of Proposition 3.6 with  $T_B := T_B(A, M)$  gives

$$T_B(A, M) \leq \frac{C(q, A)}{M^{\beta_q}}.$$

- (iii) The confinement and scale-separation conclusions of Lemmas 3.7 and 3.8 hold for  $1 \leq k \leq M$  on  $[0, T_B(A, M)]$ . In particular, if the following inequality holds:

$$d e^{C_{\text{sep}} \bar{A} T_B(A, M)} \leq \frac{r_-}{2r_+}. \quad (118)$$

then (91) and (92) are valid for the first  $M$  rings on  $[0, T_B(A, M)]$ .

Since  $T_B(A, M) \rightarrow 0$  as  $M \rightarrow \infty$ , there exists a large integer  $m_0(A, q)$  such that for all  $M \geq m_0(A, q)$ , the inequality (118) holds. Hence by Proposition 4.5, (91), (92) hold for all  $M \geq m_0(A, q)$ .

*Proof of Proposition 4.5.* The pointwise Cauchy formula (117) was established above directly from the global flow map  $Y$  and the definition of  $\omega_k$ ; in particular, it remains valid in the contradiction setting and does not rely on Lemma 3.1. Combining (117) with the bootstrap bound  $F_M(t) \leq \mu$  gives the  $L^\infty$  bounds in part (i).

Next fix  $2 \leq k \leq M$ . The ODE

$$x'_k(t) = x_k(t) \partial_r u_-^r(0, 0, t)$$

depends only on the rings with indices  $j < k \leq M$ . Therefore the proofs of Lemma 3.2 and the weak ODE bounds (71) in Section 3.4 apply without change to the family  $\{\omega_j\}_{j=1}^M$  on  $[0, T_B(A, M)]$ . Since  $T_B(A, M) \leq T_N(A, M)$ , we have  $x_k(t) \leq \bar{A}$  for all  $1 \leq k \leq M$  and  $0 \leq t \leq T_B(A, M)$ . Thus, because it only uses the first  $k - 1$  rings and the finite-head bootstrap  $F_M \leq \mu$ , the proof of Proposition 3.6 yields the bound in (ii).

Finally, Lemma 3.7 depends only on the bootstrap control of  $X_k$ , and Lemma 3.8 uses Lemma 3.7, the ODE (60), and the bound  $x_k(t) \leq \bar{A}$  on  $[0, T_B(A, M)]$ . Hence the same proofs give (iii) for the first  $M$  rings. It finishes the proof of Proposition 4.5.  $\square$

The goal of Step 1 is to prove, using a bootstrap argument, that for large  $M$ ,

$$T_B(A, M) = T_N(A, M). \quad (119)$$

Assume for contradiction that  $T_B(A, M) < T_N(A, M)$ .

For a bootstrap argument, for large integers  $M$ , which are at least bigger than  $m_0(A, q)$ , we control the rescaled velocities  $V_k = (V_k^r, V_k^z)$  (defined in (63)) on  $\text{supp } W_k(\cdot, \cdot, t)$  for  $1 \leq k \leq M$  and  $0 \leq t \leq T_B(A, M)$ . Decompose the vorticity  $\omega^{(\infty)}$  into *head* ( $k \leq M$ ) and *tail* ( $k > M$ ):

$$\omega^{(\infty)} = \omega^{(\leq M)} + \omega^{(>M)}, \quad \omega^{(\leq M)} := \sum_{j=1}^M \omega_j, \quad \omega^{(>M)} := \sum_{j=M+1}^{\infty} \omega_j,$$

and decompose  $u^{(\infty)} = u^{(\leq M)} + u^{(>M)}$  accordingly. Let  $V_{k,(\leq M)} = (V_{k,(\leq M)}^r, V_{k,(\leq M)}^z)$  denote the rescaled velocity built from  $u^{(\leq M)}$  by the same formula as in (63). Then for  $1 \leq k \leq M$

$$V_k^r(r, z, t) = V_{k,(\leq M)}^r(r, z, t) + \frac{u^{(>M),r}(R_k(t)r, H_k(t)z, t)}{R_k(t)}$$

and we make a corresponding decomposition for  $V_k^z$ . We divide estimates of  $V_k$  into three parts: (a) head contribution  $V_{k,(\leq M)}$ ; (b) tail contribution  $u^{(>M)}$ ; (c) Conclusion from (a) and (b).

*Step 1-(a): Estimate the head contribution  $V_{k,(\leq M)}^r, V_{k,(\leq M)}^z$*

For the head vorticity  $\omega^{(\leq M)}$ , using Proposition 4.5(i), (iii) together with Proposition 2.1, one can argue in the same way as Lemma 3.9 to obtain that for all  $M \geq m_0(A, q)$ ,

$$\sup_{(r,z),t,k} \left( \left| \frac{V_{k,(\leq M)}^r(r, z, t)}{r} \right| + \left| \frac{V_{k,(\leq M)}^z(r, z, t)}{z} \right| \right) \leq C_E(q) \bar{A} \left( 1 + \log \left( \frac{\bar{A}}{\varepsilon} \right) + \log M \right), \quad (120)$$

where the supremum is taken over all  $x, t, k$  such that

$$1 \leq k \leq M, \quad 0 \leq t \leq T_B(A, M), \quad (r, z) \in \text{supp } W_k(\cdot, t).$$

*Step 1-(b): Estimate the tail contribution  $u^{(>M),r}, u^{(>M),z}$*

In this part, we use Proposition 2.1. Under the flow, the odd-symmetry of  $\omega^{(\infty)}$  in  $z$  is preserved. Therefore, the odd-symmetry assumption of Proposition 2.1 is satisfied for  $\omega^{(\infty)}(\cdot, t)$  for all  $t > 0$ . In addition, as we are considering a Yudovich-type weak solution  $\omega^{(\infty)} \in L_t^\infty(L^1 \cap L^\infty)$ , all the assumptions of Proposition 2.1 are satisfied.

By the construction of the initial data (14) and the profile support condition (77), we know that  $\text{supp } \omega_0^{(\infty)} \cap \{z > 0\}$  is strictly contained in the cone  $z \leq L_{q,+}r$ , where  $L_{q,+} = \frac{1+\eta}{1-\eta} L_q$ .

Now, we want to prove that for all  $t \in [0, T_B(A, M)]$

$$2L_{q,+}r \geq |z| > 0 \quad \text{for all } (r, z) \in \cup_{j=1}^\infty \text{supp } \omega_j(\cdot, \cdot, t), \quad (121)$$

for a sufficiently large  $M \geq m_{\text{cone}}(A, q)$  (defined in (122) below), which will allow us to estimate the factor  $|x|/r_x$  in the  $Q(r_x)$ -estimates of Proposition 2.1 by  $\sqrt{1 + 4L_{q,+}^2}$  for all time  $t \in [0, T_B(A, M)]$ .

**Proof of the cone condition** (121). This proof is motivated by the proof of Lemma 3.1 in [KJ22]. At time  $t = 0$ , we have  $Y^z(x, 0)/Y^r(x, 0) \leq L_{q,+}$  for all  $x \in \text{supp } \omega_0^{(\infty)} \cap \{z > 0\}$ .

We analyze the evolution of the ratio  $Y^z(x, t)/Y^r(x, t)$  for a Lagrangian trajectory  $Y(x, t)$  starting at  $x \in \text{supp } \omega_0^{(\infty)} \cap \{z > 0\}$ . Consider the intermediate region  $\mathcal{R} := \{(r, z) : L_{q,+} \leq z/r \leq 2L_{q,+}\}$ . While the trajectory  $Y(x, t)$  is in the region  $\mathcal{R}$ , we can bound the factor  $|x|/r_x$  by a constant,  $\sqrt{1 + 4L_{q,+}^2}$ , when applying the  $Q(r_x)$ -estimate of Proposition 2.1 since  $2L_{q,+}r \geq z > 0$ . The contradiction hypothesis yields  $\|\omega^{(\infty)}(\cdot, t)\|_{L^\infty(\mathbb{R}^3)} \leq A_\infty \leq \bar{A}$ . Because  $-z_y \omega^{(\infty)}(y, t) \geq 0$  everywhere (due to odd symmetry and non-positivity on the upper half-plane), the integral term in Proposition 2.1 is non-negative. Therefore, Proposition 2.1 implies that whenever  $Y(x, t)$  is in  $\mathcal{R}$ ,

$$\frac{u^{(\infty),r}(Y, t)}{Y^r} \geq -C \sqrt{1 + 4L_{q,+}^2} \|\omega^{(\infty)}(\cdot, t)\|_{L^\infty} \geq -C \sqrt{1 + 4L_{q,+}^2} \bar{A}.$$

Similarly, by an analogous application of Proposition 2.1 for the vertical component  $u^{(\infty),z}$ , the rescaled velocity satisfies an upper bound:

$$\frac{u^{(\infty),z}(Y, t)}{Y^z} \leq C \left( 1 + \left| \log \frac{Y^r}{Y^z} \right| \right) \|\omega^{(\infty)}(\cdot, t)\|_{L^\infty} \leq C(1 + |\log(2L_{q,+})|) \bar{A},$$

for an absolute constant  $C > 0$ , bounding the logarithmic term since  $Y^r/Y^z \in [1/(2L_{q,+}), 1/L_{q,+}]$  in the region  $\mathcal{R}$ .

Using these inequalities, we monitor the aspect ratio of the trajectory inside  $\mathcal{R}$ :

$$\begin{aligned} \frac{d}{dt} \log \frac{Y^z(x, t)}{Y^r(x, t)} &= \frac{u^{(\infty), z}(Y(x, t), t)}{Y^z(x, t)} - \frac{u^{(\infty), r}(Y(x, t), t)}{Y^r(x, t)} \\ &\leq \left(1 + |\log(4L_{q,+})| + \sqrt{1 + 4L_{q,+}^2}\right) \bar{A} = C(q) \bar{A} \end{aligned}$$

where the constant  $C$  ultimately depends on  $q$  and fixed background parameters, but independent of  $M, t, k$ .

Suppose that a trajectory  $Y(x, t)$  enters the region  $\mathcal{R}$  at some time  $t = T_{\mathcal{R}} \leq T_B(A, M)$ . Until it escapes the region  $\mathcal{R}$ , the trajectory complies with the above differential inequality. Integrating from  $T_{\mathcal{R}}$  to  $t \leq T_B(A, M)$ , we obtain:

$$\begin{aligned} \log \frac{Y^z(x, t)}{Y^r(x, t)} &\leq \log \frac{Y^z(T_{\mathcal{R}}, x)}{Y^r(T_{\mathcal{R}}, x)} + C(q) \bar{A}(t - T_{\mathcal{R}}) \\ &\leq \log L_{q,+} + C(q) \bar{A} T_B(A, M). \end{aligned}$$

Since  $T_B(A, M) \rightarrow 0$  as  $M \rightarrow \infty$  by Proposition 4.5, there exists a large integer  $m_{\text{cone}}(A, q) \geq m_0(A, q)$  such that all  $M \geq m_{\text{cone}}(A, q)$  satisfy

$$C(q) \bar{A} T_B(A, M) \leq \log \frac{3}{2}. \quad (122)$$

Under this condition, it follows that

$$\log \frac{Y^z(x, t)}{Y^r(x, t)} \leq \log(L_{q,+}) + \log\left(\frac{3}{2}\right) = \log\left(\frac{3}{2} L_{q,+}\right).$$

From this, we conclude that  $Y^z(x, t)/Y^r(x, t) \leq \frac{3}{2} L_{q,+}$ , meaning the trajectory  $Y(x, t)$  can never reach the boundary  $z = 2L_{q,+}r$  for all  $t \in [0, T_B(A, M)]$ . Since  $Y^z(x, t) > 0$  is also strictly preserved by the flow (as the  $z = 0$  plane is invariant due to odd symmetry), the condition  $2L_{q,+}r \geq |z| > 0$  holds for all  $x \in \cup_{j=1}^{\infty} \text{supp } \omega_j(\cdot, t)$ . This completes the proof of the cone condition (121).  $\square$

Thanks to (121), we can apply the  $Q(r_x)$ -estimates of Proposition 2.1 to  $\omega^{(\infty)}(\cdot, \cdot, t)$  with the factor  $|x|/r_x$  bounded by  $\sqrt{1 + 4L_{q,+}^2}$ , for all  $t \in [0, T_B(A, M)]$  for all  $M \geq m_{\text{cone}}(A, q)$ . Set

$$K_{\text{tail}} := \overline{\bigcup_{j=M+1}^{\infty} \text{supp } \omega_{0,j}} = \left( \bigcup_{j=M+1}^{\infty} \text{supp } \omega_{0,j} \right) \cup \{0\},$$

and define the outer radial boundary of the tail  $R_{\text{tail}}(t)$  and the inner radial boundary of the head  $r_{M,-}(t)$  by

$$r_{M,-}(t) := \min_{x \in \text{supp } \omega_{0,M}} Y^r(x, t), \quad R_{\text{tail}}(t) := \max_{x \in K_{\text{tail}}} Y^r(x, t).$$

We claim that the head and the tail rings are separated. More precisely, there exists a large  $m_{\text{tail}}(A, q) \geq m_{\text{cone}}(A, q)$  such that all  $M \geq m_{\text{tail}}(A, q)$  satisfy

$$\frac{r_{M,-}(t)}{R_{\text{tail}}(t)} \geq 4 \quad \text{for all } t \in [0, T_B(A, M)]. \quad (123)$$

**Proof of the tail scale separation bound (123).** We use a bootstrap argument. Define

$$T_B^* := \sup \left\{ T \in [0, T_B(A, M)] : \frac{r_{M,-}(t)}{R_{\text{tail}}(t)} \geq 4 \quad \text{for all } t \in [0, T] \right\}.$$

At  $t = 0$ , the separation between the  $M$ -th ring and the tail is exactly:

$$\frac{r_{M,-}(0)}{R_{\text{tail}}(0)} \geq \frac{(1-\eta)d^M}{(1+\eta)d^{M+1}} = \frac{1-\eta}{1+\eta} \frac{1}{d} = \frac{3/4}{5/4}(100) = 60.$$

Under the contradiction hypothesis, the velocity field  $u^{(\infty)}$  is also globally bounded, that is,  $u^{(\infty)} \in L^\infty(0, T_0; L^\infty(\mathbb{R}^3))$ , hence the flow map  $Y^r(x, t)$  is *uniformly* Lipschitz continuous in time, that is,  $|Y^r(x, t) - Y^r(x, s)| \leq C|t - s|$  for all  $t, s \in [0, T_0]$  and  $x \in \mathbb{R}^3$  where the constant  $C$  is independent of  $t, s, x$ . Consequently, both  $t \mapsto r_{M,-}(t)$  and  $t \mapsto R_{\text{tail}}(t)$  are continuous as extrema over compact sets. Hence  $T_B^* > 0$ .

Fix  $M \geq \max\{m_0(A, q), m_{\text{cone}}(A, q)\}$ . Since  $u$  is uniformly bounded and uniformly log-Lipschitz in space on  $[0, T_0]$  (see (108)), and since  $Y$  is continuous on compact sets, the map

$$g(x, t) := u^{(\infty),r}(Y(x, t), t)$$

is bounded. Using log-Lipschitzness of  $u^{(\infty)}$  and Hölder estimate (109) of  $Y$ , it follows that  $g$  admits a modulus of continuity in  $x$ , uniform in  $t$ , on both compact sets

$$K_M := \text{supp } \omega_{0,M}, \quad K_{\text{tail}}$$

using the uniform Hölder continuity of  $Y$  (109) on the relevant compact sets. More precisely,  $g$  admits the following modulus of continuity:

$$|g(x, t) - g(y, t)| \leq C|x - y|^\gamma \log(2 + C|x - y|^{-\gamma}) =: \rho(|x - y|).$$

Hence Lemma 4.4 applies with  $K = K_M$  and  $K = K_{\text{tail}}$  and shows that  $r_{M,-}$  and  $R_{\text{tail}}$  are Lipschitz on  $[0, T_0]$ , and for a.e.  $t \in (0, T_0)$ ,

$$r'_{M,-}(t) = \min_{x \in \mathcal{A}_M(t)} u^{(\infty),r}(Y(x, t), t), \quad R'_{\text{tail}}(t) = \max_{x \in \mathcal{M}_{\text{tail}}(t)} u^{(\infty),r}(Y(x, t), t),$$

where

$$\mathcal{A}_M(t) := \text{argmin}_{x \in K_M} Y^r(x, t), \quad \mathcal{M}_{\text{tail}}(t) := \text{argmax}_{x \in K_{\text{tail}}} Y^r(x, t).$$

In particular, for a.e. such  $t$ , there exist  $x_t \in \mathcal{A}_M(t)$  and  $x'_t \in \mathcal{M}_{\text{tail}}(t)$  such that

$$r'_{M,-}(t) = u^r(Y(x_t, t), t), \quad R'_{\text{tail}}(t) = u^r(Y(x'_t, t), t).$$

Therefore,

$$\frac{d}{dt} \log \frac{r_{M,-}(t)}{R_{\text{tail}}(t)} = \frac{u^{(\infty),r}(Y(x_t, t), t)}{r_{M,-}(t)} - \frac{u^{(\infty),r}(Y(x'_t, t), t)}{R_{\text{tail}}(t)} \quad \text{for a.e. } t \in (0, T_0).$$

From this point on, all differential inequalities are understood for a.e.  $t$ , and are then integrated in time.

Setting  $Y = Y(x_t, t)$ ,  $Y' = Y(x'_t, t)$ , (hence  $Y^{rr} = R_{\text{tail}}(t)$ ) we evaluate the contraction via the  $Q(r_x)$ -estimates of Proposition 2.1:

$$\frac{d}{dt} \log R_{\text{tail}}(t) - \frac{d}{dt} \log r_{M,-}(t) \leq \frac{3}{8\pi} \int_{Q(Y^{rr}) \setminus Q(Y^r)} \frac{r_y z_y}{|y|^5} (-\omega^{(\infty)}(t, y)) dy + 2C_L \bar{A}, \quad \text{a.e. } t \in [0, T_B^*].$$

The domain of integration is  $\{y \in \mathbb{R}^3 : 2Y^{rr} \leq r_y < 2Y^r\}$ . We check its boundaries:

- **Upper boundary:** By Lemma 3.7 and (91), it holds

$$2Y^r \leq 2R_M(t) r_+ \leq R_{M-1}(t) r_- \leq r_{M-1,-}(t).$$

Thus, the domain strictly avoids rings 1 through  $M - 1$ .

- **Lower boundary:** Because  $Y^{r'}$  represents the outer boundary of the tail,  $2Y^{r'} > R_{\text{tail}}(t)$ . Thus, the domain strictly overshoots the entire tail mass.

Consequently, the integration domain intersects no ring except possibly the  $M$ -th ring. Therefore, its contribution is bounded by the integral over  $\text{supp } \omega_M(\cdot, t)$ . We bound the integral using exact volume conservation  $|\text{supp } \omega_M(\cdot, t)| = |\text{supp } \omega_{0,M}| = C(q) d^{3M}$ :

$$\frac{d}{dt} \log \frac{r_{M,-}(t)}{R_{\text{tail}}(t)} \geq -C(q) \bar{A} \int_{\text{supp } \omega_M(\cdot, t)} \frac{1}{|y|^3} dy - 2C_L \bar{A}.$$

The singular integral is therefore uniformly bounded:

$$\int_{\text{supp } \omega_M(\cdot, t)} \frac{1}{|y|^3} dy \leq \frac{|\text{supp } \omega_M(\cdot, t)|}{r_{M,-}(t)^3} \leq C(q) \frac{d^{3M}}{R_M(t)^3} \leq C(q).$$

Therefore,

$$\frac{d}{dt} \log \frac{r_{M,-}(t)}{R_{\text{tail}}(t)} \geq -C(q) \bar{A}.$$

Integrating this inequality from  $t = 0$  yields

$$\frac{r_{M,-}(t)}{R_{\text{tail}}(t)} \geq \frac{r_{M,-}(0)}{R_{\text{tail}}(0)} e^{-C(q) \bar{A} t} \geq \frac{1 - \eta}{1 + \eta} \frac{1}{d} e^{-C(q) \bar{A} t}.$$

Since  $T_B(A, M) \rightarrow 0$  as  $M \rightarrow \infty$ , there exists a large integer  $m_{\text{tail}}(A, q) \geq m_{\text{cone}}(A, q)$  such that all  $M \geq m_{\text{tail}}(A, q)$  satisfy

$$\frac{1 - \eta}{1 + \eta} \frac{1}{d} e^{-C(q) \bar{A} T_B(A, M)} = 60 e^{-C(q) \bar{A} T_B(A, M)} > 4. \quad (124)$$

Then for  $M \geq m_{\text{tail}}(A, q)$ , the bootstrap condition strictly improves on  $[0, T_B^*]$ , hence it forces  $T_B^* = T_B(A, M)$ . It finishes the proof of the tail scale separation bound (123).  $\square$

*Completion of Step 1-(b).* Using the strict scale separation (123), we can establish a uniform distance bound between the  $k$ -th ring and any tail ring  $j > M$ , allowing us to rigorously bound the tail velocity contribution.

Fix  $k \in \{1, \dots, M\}$  and  $t \in [0, T_B(A, M)]$ . Let  $x \in \text{supp } \omega_k(\cdot, t)$  and  $y \in \text{supp } \omega_j(\cdot, t)$  for some  $j > M$ . The 3D Euclidean distance is bounded below by the radial distance:

$$|x - y| \geq |r_x - r_y|.$$

For  $M \geq \max\{m_{\text{tail}}(A, q), m_0(A, q)\}$ , by using (123), since  $j > M \geq k$ , the  $j$ -th ring is strictly localized closer to the  $z$ -axis than the  $k$ -th ring:

$$r_y \leq \sup_{\xi \in \text{supp } \omega_{0,j}} Y^r(\xi, t) \leq R_{\text{tail}}(t) \leq \frac{1}{2} r_{M,-}(t) \leq \frac{1}{2} \inf_{\xi \in \text{supp } \omega_{0,k}} Y^r(\xi, t) \leq \frac{1}{2} r_x.$$

This guarantees a uniform lower bound on the distance:

$$|x - y| \geq r_x - \frac{1}{2} r_x = \frac{1}{2} r_x \geq \frac{1}{2} R_k(t) r_-. \quad (125)$$

where we used the finite-ring bootstrap Lemma 3.7, which ensures  $r_x = R_k(t) r$  with  $r \geq r_-$ .

Next, we estimate the velocity  $u_j(x, t)$  induced by the  $j$ -th ring. Because the velocity field is divergence-free, the physical volume of the  $j$ -th ring is exactly conserved over time. From the initial data (14), its volume is strictly determined by the initial geometric scale  $d^j$ :

$$|\text{supp } \omega_j(\cdot, t)| = |\text{supp } \omega_{0,j}| = C(q) (d^j)^3.$$

Using the Biot–Savart law, the contradiction hypothesis  $\|\omega_j(\cdot, t)\|_{L^\infty} \leq A_\infty \leq \bar{A}$ , and our uniform distance bound (125), we obtain:

$$|u_j(x, t)| \leq C_{\text{BS}} \int_{\text{supp } \omega_j(\cdot, t)} \frac{|\omega_j(y, t)|}{|x - y|^2} dy \leq \frac{C_{\text{BS}}}{\left(\frac{1}{2}r_- - R_k(t)\right)^2} \|\omega_j\|_{L^\infty} |\text{supp } \omega_j| \leq C(q) \bar{A} \frac{d^{3j}}{R_k(t)^2}. \quad (126)$$

We now bound the rescaled velocity contributions on the support of the  $k$ -th ring. For the radial component, we divide (126) by  $R_k(t)r$ . Using  $r \geq r_-$  and the fact that amplitudes do not decrease ( $R_k(t) = d^k \tilde{x}_k(t) \geq d^k$ ), we get:

$$\frac{|u_j^r(x, t)|}{R_k(t)r} \leq \frac{C(q)\bar{A}}{R_k(t)^3 r_-} d^{3j} \leq C(q)\bar{A} \frac{d^{3j}}{(d^k)^3} = C(q)\bar{A} (d^3)^{j-k}.$$

For the vertical component, we divide (126) by  $H_k(t)z$ . By definition (22), we have the exact geometric relation  $R_k(t)^2 H_k(t) = (d^k \tilde{x}_k(t))^2 (d^k / \tilde{x}_k(t)^2) = d^{3k}$ . Since  $|z| \geq z_-$ , this yields:

$$\left| \frac{u_j^z(x, t)}{H_k(t)z} \right| \leq \frac{C(q)\bar{A}}{R_k(t)^2 H_k(t) z_-} d^{3j} = C(q)\bar{A} \frac{d^{3j}}{d^{3k}} = C(q)\bar{A} (d^3)^{j-k}.$$

Because the base of the exponent  $d^3 = 10^{-6} < 1$ , summing these contributions over all tail rings  $j > M$  results in a rapidly converging geometric series:

$$\frac{|u^{(>M),r}(x, t)|}{R_k(t)r} + \frac{|u^{(>M),z}(x, t)|}{H_k(t)|z|} \leq C(q)\bar{A} \sum_{j=M+1}^{\infty} (d^3)^{j-k} \leq C(q)\bar{A} \frac{d^3}{1 - d^3}.$$

We conclude that the tail contribution is uniformly bounded by the target amplitude: for all  $M \geq m_{\text{tail}}(A, q)$ ,

$$\sup_{(r,z),t,k} \left( \left| \frac{u^{(>M),r}(R_k(t)r, H_k(t)z, t)}{R_k(t)r} \right| + \left| \frac{u^{(>M),z}(R_k(t)r, H_k(t)z, t)}{H_k(t)z} \right| \right) \leq C(q)\bar{A}, \quad (127)$$

where the supremum is taken over all  $x, t, k$  from the same set as (120).

*Step 1-(c): Conclusion from (a) and (b).* Combining (120) and (127), we can conclude that for all  $M \geq \max\{m_{\text{tail}}(A, q), m_0(A, q)\}$ ,

$$\sup_{(r,z),t,k} \left( \left| \frac{V_k^r(r, z, t)}{r} \right| + \left| \frac{V_k^z(r, z, t)}{z} \right| \right) \leq C_E(q)\bar{A} \left( 1 + \log \left( \frac{\bar{A}}{\varepsilon} \right) + \log M \right)$$

where the supremum is taken from the same set as in (120).

To complete bootstrap improvement, we argue in the same way as in Proposition 3.10. Recall  $T_B(A, M) \lesssim M^{-\beta_q} \rightarrow 0$  as  $M \rightarrow \infty$ . As the algebraic decay  $M^{-\beta_q}$  wins over the logarithmic growth  $\log M$ , there exists a large integer  $m_1(A, q) \geq m_{\text{tail}}(A, q)$  such that for any  $M \geq m_1(A, q)$ ,

$$C_E \bar{A} \left( 1 + \log \left( \frac{\bar{A}}{\varepsilon} \right) + \log M \right) T_B(A, M) \leq \min \left\{ \log \left( 1 + \frac{\mu}{2} \right), \log \left( \frac{1}{1 - \mu/2} \right) \right\}. \quad (128)$$

Therefore, we can obtain the improved bounds  $1 - \mu/2 \leq X_k^r/r \leq 1 + \mu/2$  and  $1 - \mu/2 \leq X_k^z/z \leq 1 + \mu/2$  on  $\text{supp } \phi_q$  for all  $0 \leq t \leq T_B(A, M)$  and all  $1 \leq k \leq M$  when  $M \geq m_1(A, q)$ . This contradicts maximality of  $T_B(A, M)$ , using the continuity of  $F_M$  and the fact that  $T_B(A, M) > 0$ . Hence (119) holds, that is,  $T_B(A, M) = T_N(A, M)$ , and it completes Step 1.

**Step 2: ODE norm inflation yields a contradiction.** Recall on  $[0, T_B(A, M)]$ , we can obtain

$$\|W_k(\cdot, \cdot, t)\|_{L^\infty(\mathbb{R}^3)} \geq (1 - \mu) \|\phi_q\|_{L^\infty(\mathbb{R}^3)} \quad (1 \leq k \leq M, 0 \leq t \leq T_B(A, M)). \quad (129)$$

In addition, the amplitudes  $\{x_k(t)\}_{k=1}^M$  satisfy the same weak ODE inequalities (71) as in Sections 3.3–3.4. By Proposition 4.5 and the choice of  $\alpha_q$  in (104), we have  $T_B(A, M) \rightarrow 0$  as  $M \rightarrow \infty$ . For  $M \geq m_1(A, q)$ , Step 1 yields  $T_B(A, M) = T_N(A, M)$ . There exists  $m_2(A, q) \geq m_1(A, q)$  such that

$$\frac{C(q, A)}{M^{\beta_q}} < T_0 \quad \text{for all } M \geq m_2(A, q)$$

where  $C(q, A)$  is the constant in (88). Since Proposition 4.5 gives  $T_B(A, M) \leq C(q, A)M^{-\beta_q}$ , it follows that  $T_N(A, M) = T_B(A, M) < T_0$ , which implies

$$\sup_{1 \leq k \leq M} x_k(T_N(A, M)) = \bar{A}.$$

Since each  $\omega_k(\cdot, t) \leq 0$  on  $\{z > 0\}$ , the functions  $-\omega_k(\cdot, t)$  are nonnegative there. Hence

$$-\omega^{(\infty)}(\cdot, t) = \sum_j (-\omega_j(\cdot, t)) \geq -\omega_k(\cdot, t) \quad \text{on } \{z > 0\}.$$

Therefore

$$\|\omega^{(\infty)}(\cdot, t)\|_{L^\infty} \geq \|\omega_k(\cdot, t)\|_{L^\infty}.$$

Evaluating at  $t = T_N(A, M)$  and using (129), we obtain

$$\begin{aligned} \left\| \omega^{(\infty)}(T_N(A, M)) \right\|_{L^\infty(\mathbb{R}^3)} &\geq \sup_{1 \leq k \leq M} \left\| \omega_k(T_N(A, M)) \right\|_{L^\infty(\mathbb{R}^3)} \\ &= \sup_{1 \leq k \leq M} x_k(T_N(A, M)) \left\| W_k(T_N(A, M)) \right\|_{L^\infty(\mathbb{R}^3)} \\ &\geq (1 - \mu) \|\phi_q\|_{L^\infty} \sup_{1 \leq k \leq M} x_k(T_N(A, M)) \\ &= (1 - \mu) \|\phi_q\|_{L^\infty} \bar{A} = \|\phi_q\|_{L^\infty} A \geq A > A_\infty. \end{aligned}$$

In fact,

$$\|\omega^{(\infty)}(t)\|_{L^\infty(\mathbb{R}^3)} > A_\infty,$$

for a.e.  $t \in [T_N(A, M) - \tau, T_N(A, M)]$ , for some sufficiently small  $\tau > 0$ , contradicting the definition of  $A_\infty$ . In other words, this contradicts the assumed existence of an essentially bounded vorticity solution on  $[0, T_0]$ . Therefore, no such  $T_0 > 0$  exists, proving Theorem 1.2-(1).  $\square$

**4.3. Proof of Theorem 1.2-(2).** This subsection proves Theorem 1.2-(2). In fact, the argument below yields a single global-in-time distributional solution; Theorem 1.2-(2) then follows by restricting that solution to an arbitrary finite time interval.

We first show that a subsequential limit of the smooth finite-ring solutions from Section 3 gives rise to a distributional solution on an arbitrary finite time interval.

**Proposition 4.6** (Finite-ring approximation of a distributional solution). *Let*

$$\omega_0^{(\infty)} = \sum_{k=1}^{\infty} \omega_{0,k}$$

be the infinite-ring initial data from (14) with  $\alpha = \alpha_q$  and  $\phi = \phi_q$ , and for each  $m \geq 1$  let

$$\omega_0^{(m)} := \sum_{k=1}^m \omega_{0,k}.$$

Let  $(u^{(m)}, \omega^{(m)})$  be the unique global smooth axisymmetric no-swirl solution of (2) with the initial condition  $\omega^{(m)}|_{t=0} = \omega_0^{(m)}$ , and set

$$\xi^{(m)} := \frac{\omega^{(m)}}{r}, \quad \xi_0^{(m)} := \frac{\omega_0^{(m)}}{r}.$$

Then, for every  $T > 0$ , there exist a subsequence  $m_j \rightarrow \infty$  and axisymmetric functions

$$u^{(\infty)} \in L^\infty(0, T; L^2(\mathbb{R}^3)) \cap L^\infty(0, T; H_{\text{loc}}^1(\mathbb{R}^3)), \quad \xi^{(\infty)} \in L^\infty(0, T; L_{\text{loc}}^2(\mathbb{R}^3)),$$

such that, writing  $\omega^{(\infty)} := r\xi^{(\infty)}$ ,

$$\begin{aligned} u^{(m_j)} &\overset{*}{\rightharpoonup} u^{(\infty)} \quad \text{in } L^\infty(0, T; L^2(\mathbb{R}^3)), \\ u^{(m_j)} &\rightarrow u^{(\infty)} \quad \text{strongly in } L^2((0, T) \times B_R) \quad \text{for every } R > 0, \\ \xi^{(m_j)} &\overset{*}{\rightharpoonup} \xi^{(\infty)} \quad \text{in } L^\infty(0, T; L^2(B_R)) \quad \text{for every } R > 0. \end{aligned}$$

Moreover,  $(u^{(\infty)}, \omega^{(\infty)})$  is an (axisymmetric no-swirl) distributional solution of (18) on  $(0, T)$  with the initial data  $\omega_0^{(\infty)}$  in the sense of Definition 1.1.

**Remark 4.1.** Proposition 4.6 pertains to a sequential limit of our finite-ring approximations. If one only cares about the existence of a distributional solution with our initial data in the sense of Definition 1.1, without keeping track of the finite-ring approximations, then this can also be obtained from [NS22, Theorems 1–2].

*Proof of Proposition 4.6.* Set

$$\xi_{0,k} := \frac{\omega_{0,k}}{r}, \quad \xi_0^{(m)} := \sum_{k=1}^m \xi_{0,k}, \quad \xi_0^{(\infty)} := \sum_{k=1}^{\infty} \xi_{0,k}.$$

Since the ring supports are pairwise disjoint, the scaling computations from Section 3.1 give, for  $p = 1, 2$ ,

$$\|\omega_{0,k}\|_{L^p(\mathbb{R}^3)}^p = \frac{\varepsilon^p}{k^{\alpha p}} d^{3k} \|\phi_q\|_{L^p(\mathbb{R}^3)}^p,$$

and

$$\|\xi_{0,k}\|_{L^p(\mathbb{R}^3)}^p = \frac{\varepsilon^p}{k^{\alpha p}} d^{(3-p)k} \left\| \frac{\phi_q}{r} \right\|_{L^p(\mathbb{R}^3)}^p.$$

Here  $\phi_q/r \in L^p(\mathbb{R}^3)$  because  $\phi_q$  is supported away from the symmetry axis. Consequently,

$$\sup_{m \geq 1} \left\| \omega_0^{(m)} \right\|_{L^1 \cap L^2(\mathbb{R}^3)} < \infty, \quad \xi_0^{(\infty)} \in L^1 \cap L^2(\mathbb{R}^3).$$

Moreover,

$$\left\| \xi_0^{(\infty)} - \xi_0^{(m)} \right\|_{L^1(\mathbb{R}^3)} \leq C\varepsilon \sum_{k=m+1}^{\infty} \frac{d^{2k}}{k^\alpha} \rightarrow 0 \quad \text{as } m \rightarrow \infty.$$

Finally, by the Lorentz estimate already proved in Section 3.1,

$$\sup_{m \geq 1} \left\| \xi_0^{(m)} \right\|_{L^{3,q}(\mathbb{R}^3)} < \infty.$$

Thus

$$\sup_{m \geq 1} \left\| \omega_0^{(m)} \right\|_{L^1 \cap L^2(\mathbb{R}^3)} < \infty, \quad \sup_{m \geq 1} \left\| \xi_0^{(m)} \right\|_{L^{3,q}(\mathbb{R}^3)} < \infty. \quad (130)$$

From the more general form of the Biot–Savart law (3), we obtain

$$\left| u_0^{(m)}(x) \right| \lesssim \int_{\mathbb{R}^3} \frac{|\omega_0^{(m)}(y)|}{|x-y|^2} dy.$$

Write

$$K_1(x) := |x|^{-2} \mathbf{1}_{\{|x| \leq 1\}}, \quad K_2(x) := |x|^{-2} \mathbf{1}_{\{|x| > 1\}}.$$

Then  $K_1 \in L^1(\mathbb{R}^3)$  and  $K_2 \in L^\infty(\mathbb{R}^3) \cap L^2(\mathbb{R}^3)$ . Young’s inequality yields

$$\left\| u_0^{(m)} \right\|_{L^2} \lesssim \|K_1\|_{L^1} \left\| \omega_0^{(m)} \right\|_{L^2} + \|K_2\|_{L^2} \left\| \omega_0^{(m)} \right\|_{L^1}.$$

Hence, using (130),

$$\sup_{m \geq 1} \left\| u_0^{(m)} \right\|_{L^2(\mathbb{R}^3)} < \infty.$$

Since  $(u^{(m)}, \omega^{(m)})$  is a smooth Euler solution, energy is conserved, so

$$\sup_{m \geq 1} \left\| u^{(m)} \right\|_{L^\infty(0, T; L^2(\mathbb{R}^3))} < \infty. \quad (131)$$

Moreover,  $\xi^{(m)} = \omega^{(m)}/r$  solves

$$\partial_t \xi^{(m)} + u^{(m)} \cdot \nabla \xi^{(m)} = 0$$

and is transported by the smooth volume-preserving flow associated with  $u^{(m)}$ . Hence its Lorentz norm is conserved:

$$\left\| \xi^{(m)}(t) \right\|_{L^{3,q}(\mathbb{R}^3)} = \left\| \xi_0^{(m)} \right\|_{L^{3,q}(\mathbb{R}^3)} \leq C \quad (0 \leq t \leq T),$$

with  $C$  independent of  $m$ .

Fix  $R > 0$ . Since  $B_{2R}$  has finite measure and  $L^{3,q}(B_{2R}) \hookrightarrow L^2(B_{2R})$ , it follows that

$$\sup_{m \geq 1} \sup_{0 \leq t \leq T} \left\| \xi^{(m)}(t) \right\|_{L^2(B_{2R})} \leq C(R). \quad (132)$$

Because  $\omega^{(m)} = r\xi^{(m)}$ , we also have

$$\sup_{m \geq 1} \sup_{0 \leq t \leq T} \left\| \omega^{(m)}(t) \right\|_{L^2(B_{2R})} \leq C(R). \quad (133)$$

Choose  $\chi_R \in C_c^\infty(B_{2R})$  such that  $\chi_R \equiv 1$  on  $B_R$ . The standard div–curl estimate on  $\mathbb{R}^3$  gives

$$\begin{aligned} & \left\| \chi_R u^{(m)}(t) \right\|_{H^1(\mathbb{R}^3)} \\ & \leq C \left( \left\| \chi_R u^{(m)}(t) \right\|_{L^2(\mathbb{R}^3)} + \left\| \operatorname{div} \left( \chi_R u^{(m)}(t) \right) \right\|_{L^2(\mathbb{R}^3)} + \left\| \operatorname{curl} \left( \chi_R u^{(m)}(t) \right) \right\|_{L^2(\mathbb{R}^3)} \right). \end{aligned}$$

Since

$$\operatorname{div} \left( \chi_R u^{(m)} \right) = \nabla \chi_R \cdot u^{(m)}, \quad \operatorname{curl} \left( \chi_R u^{(m)} \right) = \chi_R \omega^{(m)} e_\theta + \nabla \chi_R \times u^{(m)},$$

the bounds (131) and (133) imply

$$\sup_{m \geq 1} \left\| u^{(m)} \right\|_{L^\infty(0, T; H^1(B_R))} \leq C(R). \quad (134)$$

Next, since  $u^{(m)}$  is a smooth Euler solution, applying the Leray projector  $\mathbb{P}$  gives

$$\partial_t u^{(m)} = -\mathbb{P} \operatorname{div}(u^{(m)} \otimes u^{(m)}).$$

For every  $\Phi \in H^3(\mathbb{R}^3)$ ,

$$\begin{aligned} \left| \left\langle \operatorname{div}(u^{(m)} \otimes u^{(m)}), \Phi \right\rangle \right| &= \left| \int_{\mathbb{R}^3} (u^{(m)} \otimes u^{(m)}) : \nabla \Phi \, dx \right| \leq \|u^{(m)}\|_{L^2}^2 \|\nabla \Phi\|_{L^\infty} \\ &\leq C \|u^{(m)}\|_{L^2}^2 \|\Phi\|_{H^3}. \end{aligned}$$

Hence

$$\sup_{m \geq 1} \left\| \partial_t u^{(m)} \right\|_{L^\infty(0, T; H^{-3}(\mathbb{R}^3))} \leq C.$$

Since multiplication by  $\chi_R$  is bounded on  $H^{-3}(\mathbb{R}^3)$ ,

$$\sup_{m \geq 1} \left\| \partial_t (\chi_R u^{(m)}) \right\|_{L^\infty(0, T; H^{-3}(\mathbb{R}^3))} \leq C(R).$$

Hence, by the Aubin–Lions lemma,  $\{\chi_R u^{(m)}\}_{m \geq 1}$  is relatively compact in  $L^2((0, T); L^2(\mathbb{R}^3))$ . Combining this with (132), (131), (134), and Banach–Alaoglu, and then using a diagonal argument over  $R \in \mathbb{N}$ , we obtain a subsequence, still denoted by  $m$ , and functions

$$u^{(\infty)} \in L^\infty(0, T; L^2(\mathbb{R}^3)) \cap L^\infty(0, T; H_{\text{loc}}^1(\mathbb{R}^3)), \quad \xi^{(\infty)} \in L^\infty(0, T; L_{\text{loc}}^2(\mathbb{R}^3)),$$

such that

$$\begin{aligned} u^{(m)} &\overset{*}{\rightharpoonup} u^{(\infty)} \quad \text{in } L^\infty(0, T; L^2(\mathbb{R}^3)), \\ u^{(m)} &\rightarrow u^{(\infty)} \quad \text{strongly in } L^2((0, T) \times B_R) \quad \text{for every } R > 0, \end{aligned}$$

and

$$\xi^{(m)} \overset{*}{\rightharpoonup} \xi^{(\infty)} \quad \text{in } L^\infty(0, T; L^2(B_R)) \quad \text{for every } R > 0.$$

Since the class of axisymmetric no-swirl vector fields is closed under local  $L^2$ -convergence,  $u^{(\infty)}$  is still axisymmetric without swirl. Similarly, since each  $\xi^{(m)}$  is axisymmetric and the class of axisymmetric scalar functions is closed under weak convergence in  $L_{\text{loc}}^2$ , the limit  $\xi^{(\infty)}$  is axisymmetric. Set  $\omega^{(\infty)} := r\xi^{(\infty)}$ . Then, for every  $R > 0$ ,

$$\omega^{(m)} = r\xi^{(m)} \overset{*}{\rightharpoonup} \omega^{(\infty)} \quad \text{in } L^\infty(0, T; L^2(B_R)).$$

We now pass to the limit in the transport identity. For each  $m$ , smoothness of  $(u^{(m)}, \omega^{(m)})$  gives

$$\int_0^T \int_{\mathbb{R}^3} \xi^{(m)}(x, t) (\partial_t \psi(x, t) + u^{(m)}(x, t) \cdot \nabla \psi(x, t)) \, dx \, dt + \int_{\mathbb{R}^3} \xi_0^{(m)}(x) \psi(x, 0) \, dx = 0$$

for every  $\psi \in C_c^\infty(\mathbb{R}^3 \times [0, T])$ . Fix such a  $\psi$ , and choose  $R > 0$  so that  $\operatorname{supp} \psi \subset B_R \times [0, T]$ . The terms involving  $\partial_t \psi$  and the initial data pass to the limit by the weak-\* convergence of  $\xi^{(m)}$  in  $L^\infty(0, T; L^2(B_R))$  and the strong convergence  $\xi_0^{(m)} \rightarrow \xi_0^{(\infty)}$  in  $L^1(\mathbb{R}^3)$ . For the nonlinear term, write

$$\int_0^T \int_{B_R} \xi^{(m)} u^{(m)} \cdot \nabla \psi - \int_0^T \int_{B_R} \xi^{(\infty)} u^{(\infty)} \cdot \nabla \psi = I_m + J_m,$$

where

$$I_m := \int_0^T \int_{B_R} \xi^{(m)} (u^{(m)} - u^{(\infty)}) \cdot \nabla \psi, \quad J_m := \int_0^T \int_{B_R} (\xi^{(m)} - \xi^{(\infty)}) u^{(\infty)} \cdot \nabla \psi.$$

Since  $\xi^{(m)}$  is uniformly bounded in  $L^2((0, T) \times B_R)$  and  $u^{(m)} \rightarrow u$  strongly in  $L^2((0, T) \times B_R)$ , we have  $I_m \rightarrow 0$ . Also  $u \cdot \nabla \psi \in L^1(0, T; L^2(B_R))$ , so the weak-\* convergence of  $\xi^{(m)}$  implies  $J_m \rightarrow 0$ . Hence

$$\int_0^T \int_{\mathbb{R}^3} \xi^{(\infty)}(x, t) (\partial_t \psi(x, t) + u^{(\infty)}(x, t) \cdot \nabla \psi(x, t)) dx dt + \int_{\mathbb{R}^3} \xi_0^{(\infty)}(x) \psi(x, 0) dx = 0.$$

Equivalently,

$$\int_0^T \int_{\mathbb{R}^3} \frac{\omega^{(\infty)}(x, t)}{r} (\partial_t \psi(x, t) + u^{(\infty)}(x, t) \cdot \nabla \psi(x, t)) dx dt + \int_{\mathbb{R}^3} \frac{\omega_0^{(\infty)}(x)}{r} \psi(x, 0) dx = 0.$$

It remains to verify the curl and divergence conditions. For each  $m$ ,

$$\operatorname{div} u^{(m)} = 0, \quad \operatorname{curl} u^{(m)} = \omega^{(m)} e_\theta = (-x_2 \xi^{(m)}, x_1 \xi^{(m)}, 0)$$

in distributions. Passing to the limit using the strong local  $L^2$  convergence of  $u^{(m)}$  and the weak-\* convergence of  $\xi^{(m)}$  on every ball gives

$$\operatorname{div} u^{(\infty)} = 0, \quad \operatorname{curl} u^{(\infty)} = \omega^{(\infty)} e_\theta$$

in  $\mathcal{D}'((0, T) \times \mathbb{R}^3)$ .

Finally, for every  $T' < T$  and  $R > 0$ , the bounds

$$u^{(\infty)} \in L^\infty(0, T; L^2(\mathbb{R}^3)), \quad \xi^{(\infty)} \in L^\infty(0, T; L^2(B_R))$$

imply

$$\xi^{(\infty)} \in L^1((0, T') \times B_R), \quad u^{(\infty)} \xi^{(\infty)} \in L^1((0, T') \times B_R).$$

Since the time slice  $\{0\} \times \mathbb{R}^3$  has measure zero, this gives

$$\xi^{(\infty)} \in L^1_{\text{loc}}([0, T] \times \mathbb{R}^3), \quad u^{(\infty)} \xi^{(\infty)} \in L^1_{\text{loc}}([0, T] \times \mathbb{R}^3).$$

Thus all conditions in Definition 1.1 are satisfied, and  $(u^{(\infty)}, \omega^{(\infty)})$  is a distributional solution of (18) on  $(0, T)$  with initial data  $\omega_0^{(\infty)}$ .  $\square$

**Corollary 4.7** (Diagonal extraction: a single global distributional solution). *There exist a subsequence  $m_j \rightarrow \infty$  and axisymmetric functions*

$$u^{(\infty)} \in L^\infty_{\text{loc}}([0, \infty); L^2(\mathbb{R}^3)) \cap L^\infty_{\text{loc}}([0, \infty); H^1_{\text{loc}}(\mathbb{R}^3)), \quad \xi^{(\infty)} \in L^\infty_{\text{loc}}([0, \infty); L^2_{\text{loc}}(\mathbb{R}^3)),$$

such that, writing  $\omega^{(\infty)} := r \xi^{(\infty)}$ , the following holds: for every  $T > 0$ , as  $j \rightarrow \infty$ ,

$$\begin{aligned} u^{(m_j)} &\xrightarrow{*} u^{(\infty)} \quad \text{in } L^\infty((0, T); L^2(\mathbb{R}^3)), \\ u^{(m_j)} &\rightarrow u^{(\infty)} \quad \text{strongly in } L^2((0, T) \times B_R) \quad \text{for every } R > 0, \\ \xi^{(m_j)} &\xrightarrow{*} \xi^{(\infty)} \quad \text{in } L^\infty((0, T); L^2(B_R)) \quad \text{for every } R > 0, \end{aligned}$$

and  $(u^{(\infty)}, \omega^{(\infty)})$  is an (axisymmetric no-swirl) distributional solution of (18) on  $(0, \infty)$  with initial data  $\omega_0^{(\infty)}$  in the sense of Definition 1.1.

*Proof.* For  $N = 1$ , apply Proposition 4.6 with  $T = 1$ . This gives a subsequence  $\{m_j^{(1)}\}_{j \geq 1}$  and a limit  $(u^{[1]}, \xi^{[1]})$  on  $(0, 1)$ .

Assume by induction that, for some  $N \geq 2$ , we have already chosen a subsequence  $\{m_j^{(N-1)}\}_{j \geq 1}$  of positive integers such that the corresponding finite-ring solutions converge on  $(0, N-1)$ . Relabel

this subsequence as a sequence and apply Proposition 4.6 with  $T = N$ . We obtain a further subsequence  $\{m_j^{(N)}\}_{j \geq 1} \subset \{m_j^{(N-1)}\}_{j \geq 1}$  and a limit  $(u^{[N]}, \xi^{[N]})$  on  $(0, N)$ .

Thus we have constructed nested subsequences

$$\{m_j^{(1)}\} \supset \{m_j^{(2)}\} \supset \cdots.$$

Define the diagonal subsequence

$$m_j := m_j^{(j)}.$$

Fix  $N \in \mathbb{N}$ . Then for every  $j \geq N$ , the index  $m_j$  belongs to  $\{m_\ell^{(N)}\}_{\ell \geq 1}$ , because the subsequences are nested. Therefore  $\{m_j\}_{j \geq N}$  is a subsequence of  $\{m_\ell^{(N)}\}_{\ell \geq 1}$ , and so the diagonal subsequence converges on  $(0, N)$  to  $(u^{[N]}, \xi^{[N]})$  with the same properties as in Proposition 4.6.

We now check compatibility on overlaps. Since  $\{m_j^{(N+1)}\}_{j \geq 1} \subset \{m_j^{(N)}\}_{j \geq 1}$ , the sequence  $\{u^{(m_j^{(N+1)})}\}_{j \geq 1}$  converges on  $(0, N)$  both to  $u^{[N]}$  and to  $u^{[N+1]} \upharpoonright_{(0, N)}$  in the strong topology  $L^2((0, N) \times B_R)$  for every  $R > 0$ . By uniqueness of strong limits,

$$u^{[N+1]} = u^{[N]} \quad \text{a.e. on } (0, N) \times B_R$$

for every  $R > 0$ , hence a.e. on  $(0, N) \times \mathbb{R}^3$ . Likewise,  $\xi^{[N+1]} = \xi^{[N]}$  a.e. on  $(0, N) \times B_R$  for every  $R > 0$ , by uniqueness of the weak-\* limit in  $L^\infty((0, N); L^2(B_R))$ .

Therefore the local limits patch together. Define

$$u^{(\infty)} := u^{[N]}, \quad \xi^{(\infty)} := \xi^{[N]} \quad \text{on } (0, N) \times \mathbb{R}^3.$$

This is well-defined by the compatibility just proved, and the stated local-in-time bounds follow from the bounds on each finite interval  $(0, N)$ . Finally, for any  $T > 0$ , choose  $N \in \mathbb{N}$  with  $N > T$ . Since  $(u^{[N]}, r\xi^{[N]})$  is a distributional solution on  $(0, N)$ , its restriction to  $(0, T)$  gives the desired statement.  $\square$

**Proposition 4.8** (Bounded infinite-ring limits are Yudovich-type). *Let  $(u^{(\infty)}, \omega^{(\infty)})$  be the global distributional solution furnished by Corollary 4.7. Set  $\xi^{(\infty)} = \omega^{(\infty)}/r$ . Assume in addition that for some  $T \in (0, \infty)$ ,*

$$\omega^{(\infty)} \in L^\infty((0, T) \times \mathbb{R}^3).$$

Then

$$\omega^{(\infty)} \in L^\infty(0, T; L^1 \cap L^\infty(\mathbb{R}^3)).$$

In particular,  $(u^{(\infty)}, \omega^{(\infty)})$  is a Yudovich-type weak solution on  $(0, T)$ .

*Proof of Proposition 4.8.* By Corollary 4.7, we already know that

$$u^{(\infty)} \in L^\infty(0, T; L^2(\mathbb{R}^3)) \cap L^\infty(0, T; H_{\text{loc}}^1(\mathbb{R}^3)), \quad \xi^{(\infty)} \in L^\infty(0, T; L_{\text{loc}}^2(\mathbb{R}^3)),$$

and that  $(u^{(\infty)}, \omega^{(\infty)})$  satisfies the distributional transport identity for  $\xi^{(\infty)} = \omega^{(\infty)}/r$ .

Since  $\omega^{(\infty)} := \omega^{(\infty)} e_\theta \in L^\infty((0, T) \times \mathbb{R}^3)$  and

$$\text{curl } u^{(\infty)} = \omega^{(\infty)}, \quad \text{div } u^{(\infty)} = 0$$

in distributions, we can apply Lemma 4.3 to obtain a unique flow map  $Y$ , together with the Cauchy formula (111) and the transported representative (110).

Since  $Y_t$  is measure-preserving,

$$\left\| \xi^{(\infty)}(t) \right\|_{L^1 \cap L^2(\mathbb{R}^3)} = \left\| \xi_0^{(\infty)} \right\|_{L^1 \cap L^2(\mathbb{R}^3)} \quad \text{for every } t \in [0, T].$$

Also, by Lemma 4.3,  $u^{(\infty)} \in L^\infty((0, T) \times \mathbb{R}^3)$ , so trajectories move at uniformly bounded speed. Since  $\xi_0^{(\infty)}$  has compact support, there exists  $R_* > 0$  such that

$$Y_t \left( \text{supp } \xi_0^{(\infty)} \right) \subset B_{R_*} \quad \text{for all } t \in [0, T].$$

Therefore,

$$\left\| \omega^{(\infty)}(t) \right\|_{L^1(\mathbb{R}^3)} = \left\| r \xi^{(\infty)}(t) \right\|_{L^1(\mathbb{R}^3)} \leq R_* \left\| \xi^{(\infty)}(t) \right\|_{L^1(\mathbb{R}^3)} = R_* \left\| \xi_0^{(\infty)} \right\|_{L^1(\mathbb{R}^3)}$$

for every  $t \in [0, T]$ . Hence

$$\omega^{(\infty)} \in L^\infty(0, T; L^1 \cap L^\infty(\mathbb{R}^3)).$$

Since  $\text{div } u^{(\infty)} = 0$ ,  $\text{curl } u^{(\infty)} = \omega^{(\infty)} e_\theta$  in distributions, and  $u^{(\infty)} \in L^\infty(0, T; L^2(\mathbb{R}^3))$ , the standard Biot–Savart representation identifies  $u^{(\infty)}$  with the velocity induced by  $\omega^{(\infty)}$ . Thus  $(u^{(\infty)}, \omega^{(\infty)})$  is a Yudovich-type weak solution on  $(0, T)$ .  $\square$

**Remark 4.2.** *In Proposition 4.8, we upgrade the distributional solution furnished by Corollary 4.7 to a Yudovich-type weak solution provided the distributional solution is uniformly bounded. One may not upgrade any uniformly bounded distributional solution to a Yudovich-type weak solution. In that case, the corresponding velocity field  $u$  may not be uniformly bounded. Then the associated flow map might escape to infinity in finite time.*

*Proof of Theorem 1.2-(2).* Let  $\omega_0^{(\infty)}$  be the same initial data as in the first paragraph of the proof for non-existence (§ 4.2). Let  $(u^{(\infty)}, \omega^{(\infty)})$  be the global distributional solution furnished by Corollary 4.7. We claim that

$$\omega^{(\infty)} \notin L^\infty((0, T) \times \mathbb{R}^3) \quad \text{for every } T > 0.$$

Indeed, if this were false, then for some  $T > 0$  we would have

$$\omega^{(\infty)} \in L^\infty((0, T) \times \mathbb{R}^3).$$

Applying Proposition 4.8 to the restriction of  $(u^{(\infty)}, \omega^{(\infty)})$  to  $[0, T]$ , we would obtain

$$\omega^{(\infty)} \in L^\infty(0, T; L^1 \cap L^\infty(\mathbb{R}^3)),$$

so that  $(u^{(\infty)}, \omega^{(\infty)})$  is a Yudovich-type weak solution on  $(0, T)$ . This contradicts Theorem 1.2-(1). Therefore the claim is proved, and Theorem 1.2-(2) follows.  $\square$

## APPENDIX A. PROOF OF THE DANSKIN-TYPE LEMMA AND THE CAUCHY FORMULA

This appendix is devoted to prove the Danskin-type Lemma 4.4 and the Cauchy formula (110). For the Cauchy formula, we first state a proposition before proving it.

For both the lemma and the proposition, our proofs are standard, but we could not find a reference that fits our situation. Hence, we prove them here in this appendix for completeness.

*Proof of Lemma 4.4.* Let

$$M := \sup_{x \in K, 0 < t < T_0} |g(x, t)|.$$

For every  $x \in K$  and every  $0 \leq s \leq t \leq T_0$ ,

$$|Y^r(x, t) - Y^r(x, s)| \leq \int_s^t |g(x, \tau)| d\tau \leq M|t - s|.$$

Hence

$$|R_K(t) - R_K(s)| \leq \sup_{x \in K} |Y^r(x, t) - Y^r(x, s)| \leq M|t - s|,$$

and similarly

$$|r_K(t) - r_K(s)| \leq \sup_{x \in K} |Y^r(x, t) - Y^r(x, s)| \leq M|t - s|.$$

Thus  $R_K$  and  $r_K$  are Lipschitz.

Choose a countable dense set  $\{x_n\}_{n \geq 1} \subset K$ . Let  $E_0 \subset (0, T_0)$  be a full-measure set on which both  $R_K$  and  $r_K$  are differentiable. For each  $n \geq 1$ , let  $E_n \subset (0, T_0)$  be a full-measure set of right Lebesgue points of the function  $t \mapsto g(x_n, t)$ , namely

$$\lim_{h \downarrow 0} \frac{1}{h} \int_t^{t+h} g(x_n, s) ds = g(x_n, t) \quad \text{for every } t \in E_n.$$

Set

$$E := E_0 \cap E_g \cap \bigcap_{n=1}^{\infty} E_n.$$

Then  $E$  still has full measure.

We claim that for every  $t \in E$  and every  $x \in K$ ,

$$\lim_{h \downarrow 0} \frac{1}{h} \int_t^{t+h} g(x, s) ds = g(x, t).$$

Indeed, fix  $t \in E$  and  $x \in K$ , and choose  $x_{n_j} \rightarrow x$ . Then

$$\begin{aligned} \left| \frac{1}{h} \int_t^{t+h} g(x, s) ds - g(x, t) \right| &\leq \frac{1}{h} \int_t^{t+h} |g(x, s) - g(x_{n_j}, s)| ds \\ &\quad + \left| \frac{1}{h} \int_t^{t+h} g(x_{n_j}, s) ds - g(x_{n_j}, t) \right| \\ &\quad + |g(x_{n_j}, t) - g(x, t)| \\ &\leq 2\rho(|x - x_{n_j}|) + \left| \frac{1}{h} \int_t^{t+h} g(x_{n_j}, s) ds - g(x_{n_j}, t) \right|. \end{aligned}$$

First let  $h \downarrow 0$ , using that  $t \in E_{n_j}$ , and then let  $j \rightarrow \infty$ . This proves the claim.

Now fix  $t \in E$ . Since  $Y^r(\cdot, t)$  is continuous on the compact set  $K$ , the sets  $\mathcal{M}_K(t)$  and  $\mathcal{A}_K(t)$  are nonempty compact. Since  $g(\cdot, t)$  is continuous on  $K$ , the extrema of  $g(\cdot, t)$  over these sets are attained.

We first prove the formula for  $R'_K(t)$ . Let  $x \in \mathcal{M}_K(t)$ . Then for every  $h > 0$  small enough,

$$R_K(t+h) \geq Y^r(x, t+h),$$

hence

$$\frac{R_K(t+h) - R_K(t)}{h} \geq \frac{Y^r(x, t+h) - Y^r(x, t)}{h} = \frac{1}{h} \int_t^{t+h} g(x, s) ds.$$

Letting  $h \downarrow 0$  and using the claim above, we obtain

$$\liminf_{h \downarrow 0} \frac{R_K(t+h) - R_K(t)}{h} \geq g(x, t).$$

Since this holds for every  $x \in \mathcal{M}_K(t)$ ,

$$\liminf_{h \downarrow 0} \frac{R_K(t+h) - R_K(t)}{h} \geq \max_{x \in \mathcal{M}_K(t)} g(x, t).$$

For the reverse inequality, for each  $h > 0$  choose  $x_h \in \mathcal{M}_K(t+h)$ , so that

$$R_K(t+h) = Y^r(x_h, t+h).$$

By compactness of  $K$ , along any sequence  $h_j \downarrow 0$  we may pass to a subsequence, still denoted  $h_j$ , such that  $x_{h_j} \rightarrow x_* \in K$ . Since

$$Y^r(x_{h_j}, t+h_j) = R_K(t+h_j),$$

continuity of  $Y^r$  and of  $R_K$  yields

$$Y^r(x_*, t) = R_K(t),$$

so  $x_* \in \mathcal{M}_K(t)$ . Moreover,

$$\begin{aligned} \frac{R_K(t+h_j) - R_K(t)}{h_j} &= \frac{Y^r(x_{h_j}, t+h_j) - R_K(t)}{h_j} \\ &\leq \frac{Y^r(x_{h_j}, t+h_j) - Y^r(x_{h_j}, t)}{h_j} = \frac{1}{h_j} \int_t^{t+h_j} g(x_{h_j}, s) ds. \end{aligned}$$

Therefore,

$$\begin{aligned} \left| \frac{1}{h_j} \int_t^{t+h_j} g(x_{h_j}, s) ds - g(x_*, t) \right| &\leq \frac{1}{h_j} \int_t^{t+h_j} |g(x_{h_j}, s) - g(x_*, s)| ds \\ &\quad + \left| \frac{1}{h_j} \int_t^{t+h_j} g(x_*, s) ds - g(x_*, t) \right| \\ &\leq \rho(|x_{h_j} - x_*|) + \left| \frac{1}{h_j} \int_t^{t+h_j} g(x_*, s) ds - g(x_*, t) \right|. \end{aligned}$$

Letting  $j \rightarrow \infty$  and using the claim again, we obtain

$$\limsup_{h \downarrow 0} \frac{R_K(t+h) - R_K(t)}{h} \leq g(x_*, t) \leq \max_{x \in \mathcal{M}_K(t)} g(x, t).$$

Combining the lower and upper bounds, and using that  $R_K$  is differentiable at  $t$ , we conclude

$$R'_K(t) = \max_{x \in \mathcal{M}_K(t)} g(x, t)$$

since the right derivative of  $R_K$  equals to the derivative.

Finally, apply the already proved formula to the function  $-Y^r$ . Since

$$-r_K(t) = \max_{x \in K} (-Y^r(x, t)),$$

and the corresponding derivative is  $-g$ , we get

$$-r'_K(t) = \max_{x \in \mathcal{A}_K(t)} (-g(x, t)) = - \min_{x \in \mathcal{A}_K(t)} g(x, t),$$

that is,

$$r'_K(t) = \min_{x \in \mathcal{A}_K(t)} g(x, t).$$

This completes the proof of Lemma 4.4. □

Now we state the Cauchy formula under assumptions that fit our situation.

**Proposition A.1** (Cauchy formula of the transport equation along a given flow). *Let  $T_0 > 0$ . Let*

$$u \in L^\infty((0, T_0) \times \mathbb{R}^3)$$

*be divergence-free, and assume that there exists a flow map*

$$Y : \mathbb{R}^3 \times [0, T_0] \rightarrow \mathbb{R}^3$$

*such that:*

(i) *for every  $a \in \mathbb{R}^3$ , the map  $t \mapsto Y(a, t)$  is absolutely continuous and*

$$\partial_t Y(a, t) = u(Y(a, t), t) \quad \text{for a.e. } t \in (0, T_0), \quad Y(a, 0) = a;$$

(ii) *for every  $t \in [0, T_0]$ , the map  $Y_t := Y(\cdot, t)$  is a measure-preserving homeomorphism of  $\mathbb{R}^3$  onto itself;*

(iii) *there exists  $\gamma \in (0, 1]$  such that for every compact set  $K \subset \mathbb{R}^3$ ,*

$$\sup_{t \in [0, T_0]} \left( [Y_t]_{C^\gamma(K)} + [Y_t^{-1}]_{C^\gamma(K)} \right) < \infty.$$

*Let  $\xi_0 \in L^1(\mathbb{R}^3)$ , and let*

$$\xi \in L^1_{\text{loc}}([0, T_0) \times \mathbb{R}^3), \quad u\xi \in L^1_{\text{loc}}([0, T_0) \times \mathbb{R}^3)$$

*satisfy*

$$\int_0^{T_0} \int_{\mathbb{R}^3} \xi(x, t) (\partial_t \psi(x, t) + u(x, t) \cdot \nabla \psi(x, t)) dx dt + \int_{\mathbb{R}^3} \xi_0(x) \psi(x, 0) dx = 0 \quad (135)$$

*for every  $\psi \in C_c^\infty(\mathbb{R}^3 \times [0, T_0])$ .*

*Assume in addition that there exists a constant  $C_u > 0$  such that*

$$|u(x, t) - u(y, t)| \leq C_u |x - y| \log \left( 2 + \frac{1}{|x - y|} \right) \quad (136)$$

*for all  $x, y \in \mathbb{R}^3$  and for a.e.  $t \in (0, T_0)$ .*

*Then*

$$\xi(x, t) = \xi_0(Y_t^{-1}(x)) \quad \text{for a.e. } (x, t) \in \mathbb{R}^3 \times (0, T_0).$$

*Proof.* Define

$$\tilde{\xi}(x, t) := \xi_0(Y_t^{-1}(x)).$$

Since each  $Y_t$  is measure-preserving,

$$\|\tilde{\xi}(t)\|_{L^1(\mathbb{R}^3)} = \|\xi_0\|_{L^1(\mathbb{R}^3)} \quad \text{for every } t \in [0, T_0],$$

hence

$$\tilde{\xi} \in L^\infty(0, T_0; L^1(\mathbb{R}^3)) \subset L^1_{\text{loc}}((0, T_0) \times \mathbb{R}^3).$$

Fix  $\eta \in C_c^\infty(\mathbb{R}^3)$  and  $\chi \in C_c^\infty(0, T_0)$ . Set

$$K := \text{supp } \eta, \quad M := \|u\|_{L^\infty((0, T_0) \times \mathbb{R}^3)}.$$

Define

$$K_* := \{x \in \mathbb{R}^3 : \text{dist}(x, K) \leq MT_0\}, \quad K_{**} := \{x \in \mathbb{R}^3 : \text{dist}(x, K) \leq 2MT_0\}.$$

For  $(x, t) \in \mathbb{R}^3 \times [0, T_0]$ , define

$$\Phi(x, t) := \int_t^{T_0} \chi(\tau) \eta(Y_\tau(Y_t^{-1}(x))) d\tau.$$

We first record some elementary properties of  $\Phi$ .

*Step 1: support and Hölder regularity of  $\Phi$ .* If  $\Phi(x, t) \neq 0$ , then there exists  $\tau \in \text{supp } \chi$  such that  $Y_\tau(Y_t^{-1}(x)) \in K$ . Writing  $a := Y_t^{-1}(x)$  and using the flow equation,

$$|x - Y_\tau(a)| = |Y_t(a) - Y_\tau(a)| \leq M|t - \tau| \leq MT_0,$$

hence  $x \in K_*$ . Therefore

$$\text{supp } \Phi(\cdot, t) \subset K_* \quad \text{for every } t \in [0, T_0].$$

Next, if  $x \in K_*$  and  $a = Y_t^{-1}(x)$ , then

$$\text{dist}(a, K) \leq \text{dist}(a, x) + \text{dist}(x, K) \leq 2MT_0,$$

so

$$Y_t^{-1}(K_*) \subset K_{**} \quad \text{for every } t \in [0, T_0].$$

By assumption (iii), there exists  $\beta := \gamma^2 \in (0, 1]$  and a constant  $C > 0$  depending only on  $K_*$ ,  $K_{**}$  such that for all  $t, \tau \in [0, T_0]$ ,

$$|Y_\tau(Y_t^{-1}(x_1)) - Y_\tau(Y_t^{-1}(x_2))| \leq C|x_1 - x_2|^\beta, \quad x_1, x_2 \in K_*.$$

Hence

$$[\eta \circ Y_\tau \circ Y_t^{-1}]_{C^\beta(K_*)} \leq C\|\nabla\eta\|_{L^\infty},$$

uniformly in  $t, \tau \in [0, T_0]$ . It follows that

$$\sup_{t \in [0, T_0]} [\Phi(\cdot, t)]_{C^\beta(K_*)} \leq C\|\chi\|_{L^1(0, T_0)}\|\nabla\eta\|_{L^\infty}. \quad (137)$$

Since  $\text{supp } \Phi(\cdot, t) \subset K_*$  and  $K_*$  is closed, we have  $\Phi(\cdot, t) = 0$  on  $\mathbb{R}^3 \setminus K_*$ . By continuity, it also follows that  $\Phi(\cdot, t) = 0$  on  $\partial K_*$ . Consequently,

$$[\Phi(\cdot, t)]_{C^\beta(\mathbb{R}^3)} \leq [\Phi(\cdot, t)]_{C^\beta(K_*)}.$$

Indeed, if  $x, y \in K_*$  or  $x, y \notin K_*$ , the claim is immediate. If  $x \in K_*$  and  $y \notin K_*$ , choose  $z \in [x, y] \cap \partial K_*$  where  $[x, y]$  denotes the straight line segment connecting  $x$  to  $y$ . Then  $\Phi(z, t) = \Phi(y, t) = 0$ , so

$$|\Phi(x, t) - \Phi(y, t)| = |\Phi(x, t) - \Phi(z, t)| \leq [\Phi(\cdot, t)]_{C^\beta(K_*)} |x - z|^\beta \leq [\Phi(\cdot, t)]_{C^\beta(K_*)} |x - y|^\beta.$$

The case  $x \notin K_*$  and  $y \in K_*$  is symmetric. Combining this with (137), we obtain

$$\sup_{t \in [0, T_0]} [\Phi(\cdot, t)]_{C^\beta(\mathbb{R}^3)} \leq C\|\chi\|_{L^1(0, T_0)}\|\nabla\eta\|_{L^\infty}. \quad (138)$$

*Step 2:  $\Phi$  solves a backward transport equation.* Let  $\varphi \in C_c^\infty(\mathbb{R}^3 \times (0, T_0))$ . By the change of variables  $x = Y_t(a)$  and the measure-preserving property of  $Y_t$ ,

$$\begin{aligned} \int_0^{T_0} \int_{\mathbb{R}^3} \Phi(x, t) (\partial_t \varphi(x, t) + u(x, t) \cdot \nabla \varphi(x, t)) dx dt \\ = \int_{\mathbb{R}^3} \int_0^{T_0} \left( \int_t^{T_0} \chi(\tau) \eta(Y_\tau(a)) d\tau \right) \frac{d}{dt} \varphi(Y_t(a), t) dt da. \end{aligned}$$

Set

$$G_a(t) := \int_t^{T_0} \chi(\tau) \eta(Y_\tau(a)) d\tau.$$

Since  $G_a$  is absolutely continuous and

$$G'_a(t) = -\chi(t)\eta(Y_t(a)) \quad \text{for a.e. } t,$$

integration by parts in  $t$  gives

$$\begin{aligned} \int_0^{T_0} \int_{\mathbb{R}^3} \Phi(x, t) (\partial_t \varphi(x, t) + u(x, t) \cdot \nabla \varphi(x, t)) dx dt &= - \int_{\mathbb{R}^3} \int_0^{T_0} G'_a(t) \varphi(Y_t(a), t) dt da \\ &= \int_{\mathbb{R}^3} \int_0^{T_0} \chi(t) \eta(Y_t(a)) \varphi(Y_t(a), t) dt da \\ &= \int_0^{T_0} \int_{\mathbb{R}^3} \chi(t) \eta(x) \varphi(x, t) dx dt. \end{aligned}$$

Therefore, in distributions on  $(0, T_0) \times \mathbb{R}^3$ ,

$$\partial_t \Phi + u \cdot \nabla \Phi = -\chi(t)\eta(x). \quad (139)$$

*Step 3: spatial mollification and commutator.* Let  $\rho \in C_c^\infty(\mathbb{R}^3)$  be a standard nonnegative mollifier supported in  $B_1(0)$  with  $\int \rho = 1$ , and set

$$\rho_\varepsilon(x) := \varepsilon^{-3} \rho(x/\varepsilon), \quad \Phi_\varepsilon := \rho_\varepsilon * \Phi, \quad \eta_\varepsilon := \rho_\varepsilon * \eta.$$

Then  $\Phi_\varepsilon$  is smooth in  $x$ , compactly supported in  $K_* + B_\varepsilon$ , and from (139),

$$\partial_t \Phi_\varepsilon + \rho_\varepsilon * (u \cdot \nabla \Phi) = -\chi(t)\eta_\varepsilon.$$

Hence

$$\partial_t \Phi_\varepsilon + u \cdot \nabla \Phi_\varepsilon = -\chi(t)\eta_\varepsilon + R_\varepsilon, \quad (140)$$

where

$$R_\varepsilon := u \cdot \nabla \Phi_\varepsilon - \rho_\varepsilon * (u \cdot \nabla \Phi).$$

Using  $\operatorname{div} u = 0$ , we may rewrite  $R_\varepsilon$  as

$$R_\varepsilon(x, t) = \int_{\mathbb{R}^3} \nabla \rho_\varepsilon(y) \cdot (u(x, t) - u(x - y, t)) (\Phi(x - y, t) - \Phi(x, t)) dy.$$

Indeed, the term containing  $\Phi(x, t)$  alone vanishes because

$$\int_{\mathbb{R}^3} \nabla \rho_\varepsilon(y) \cdot (u(x, t) - u(x - y, t)) dy = - \int_{\mathbb{R}^3} \rho_\varepsilon(y) \operatorname{div} u(x - y, t) dy = 0.$$

If  $x \notin K_* + \overline{B}_\varepsilon$ , then  $\operatorname{dist}(x, K_*) > \varepsilon$ . Since  $\operatorname{supp} \nabla \rho_\varepsilon \subset B_\varepsilon(0)$ , for every  $y \in \operatorname{supp} \nabla \rho_\varepsilon$  we have

$$\operatorname{dist}(x - y, K_*) \geq \operatorname{dist}(x, K_*) - |y| > 0.$$

Hence  $\Phi(x, t) = \Phi(x - y, t) = 0$ , and therefore  $R_\varepsilon(x, t) = 0$ . Thus

$$\operatorname{supp} R_\varepsilon(\cdot, t) \subset K_* + \overline{B}_\varepsilon \quad \text{for every } t \in [0, T_0]. \quad (141)$$

Using (136) and (138), we obtain for all  $(x, t) \in \mathbb{R}^3 \times (0, T_0)$

$$\begin{aligned} |R_\varepsilon(x, t)| &\leq C[\Phi(\cdot, t)]_{C^\beta(\mathbb{R}^3)} \int_{\mathbb{R}^3} |\nabla \rho_\varepsilon(y)| |y|^\beta |u(x, t) - u(x - y, t)| dy \\ &\leq C \int_{|y| < \varepsilon} |\nabla \rho_\varepsilon(y)| |y|^{1+\beta} \log\left(2 + \frac{1}{|y|}\right) dy \\ &\leq C \varepsilon^\beta \log\left(2 + \frac{1}{\varepsilon}\right). \end{aligned}$$

Therefore

$$\|R_\varepsilon\|_{L^\infty((0,T_0)\times\mathbb{R}^3)} \longrightarrow 0 \quad \text{as } \varepsilon \rightarrow 0. \quad (142)$$

*Step 4: testing the weak formulation with  $\Phi_\varepsilon$ .* Since  $\chi \in C_c^\infty(0, T_0)$ , there exists  $\delta_0 \in (0, T_0)$  such that

$$\chi(t) = 0 \quad \text{for } t \in [T_0 - \delta_0, T_0].$$

Hence, by the definition of  $\Phi$ ,

$$\Phi(x, t) = 0 \quad \text{for all } (x, t) \in \mathbb{R}^3 \times [T_0 - \delta_0, T_0],$$

and therefore the same holds for  $\Phi_\varepsilon$ .

Also, (140) yields

$$\partial_t \Phi_\varepsilon = -u \cdot \nabla \Phi_\varepsilon - \chi(t)\eta_\varepsilon + R_\varepsilon \in L^\infty((0, T_0) \times \mathbb{R}^3),$$

so  $\Phi_\varepsilon$  is compactly supported and belongs to  $W^{1,\infty}(\mathbb{R}^3 \times [0, T_0])$ .

Choose  $\theta \in C_c^\infty((-1, 1))$  such that

$$\theta \equiv 1 \quad \text{on } [-\frac{1}{2}, \frac{1}{2}],$$

and define  $\tilde{\Phi}_\varepsilon$  on  $\mathbb{R}^3 \times \mathbb{R}$  by

$$\tilde{\Phi}_\varepsilon(x, t) := \begin{cases} \theta(t)\Phi_\varepsilon(x, 0), & t < 0, \\ \Phi_\varepsilon(x, t), & 0 \leq t \leq T_0, \\ 0, & t > T_0. \end{cases}$$

Then  $\tilde{\Phi}_\varepsilon \in W^{1,\infty}(\mathbb{R}^3 \times \mathbb{R})$  and has compact support.

Let  $\vartheta \in C_c^\infty(\mathbb{R}^4)$  be a standard mollifier, and set

$$\vartheta_\sigma(z) := \sigma^{-4}\vartheta(z/\sigma), \quad \Psi_{\varepsilon,\sigma} := \vartheta_\sigma * \tilde{\Phi}_\varepsilon.$$

For  $0 < \sigma < \delta_0/4$ , the restriction of  $\Psi_{\varepsilon,\sigma}$  to  $\mathbb{R}^3 \times [0, T_0]$  belongs to  $C_c^\infty(\mathbb{R}^3 \times [0, T_0])$ .

Moreover, as  $\sigma \rightarrow 0$ ,

$$\begin{aligned} \Psi_{\varepsilon,\sigma} &\rightarrow \Phi_\varepsilon \quad \text{uniformly on } \mathbb{R}^3 \times [0, T_0], \\ \partial_t \Psi_{\varepsilon,\sigma} &\rightarrow \partial_t \Phi_\varepsilon, \quad \nabla \Psi_{\varepsilon,\sigma} \rightarrow \nabla \Phi_\varepsilon \quad \text{a.e. on } \mathbb{R}^3 \times (0, T_0), \end{aligned}$$

and

$$\Psi_{\varepsilon,\sigma}(\cdot, 0) \rightarrow \Phi_\varepsilon(\cdot, 0) \quad \text{uniformly on } \mathbb{R}^3.$$

These functions are uniformly bounded, and their supports are contained in one fixed compact subset of  $\mathbb{R}^3 \times [0, T_0]$ ; likewise,  $\Psi_{\varepsilon,\sigma}(\cdot, 0)$  are supported in one fixed compact subset of  $\mathbb{R}^3$ .

Testing (135) with  $\Psi_{\varepsilon,\sigma}$  and passing to the limit  $\sigma \rightarrow 0$  by dominated convergence, using  $\xi, u\xi \in L^1_{\text{loc}}$  and  $\xi_0 \in L^1$ , we obtain

$$0 = \int_0^{T_0} \int_{\mathbb{R}^3} \xi (\partial_t \Phi_\varepsilon + u \cdot \nabla \Phi_\varepsilon) dx dt + \int_{\mathbb{R}^3} \xi_0(x) \Phi_\varepsilon(x, 0) dx.$$

Using (140),

$$\int_0^{T_0} \int_{\mathbb{R}^3} \xi(x, t) \chi(t) \eta_\varepsilon(x) dx dt = \int_0^{T_0} \int_{\mathbb{R}^3} \xi(x, t) R_\varepsilon(x, t) dx dt + \int_{\mathbb{R}^3} \xi_0(x) \Phi_\varepsilon(x, 0) dx. \quad (143)$$

*Step 5: passage to the limit.* Because  $\eta_\varepsilon \rightarrow \eta$  uniformly and  $\text{supp } \eta_\varepsilon$  stays inside a fixed compact set, while  $\xi \in L^1_{\text{loc}}$ , the left-hand side of (143) converges to

$$\int_0^{T_0} \int_{\mathbb{R}^3} \xi(x, t) \chi(t) \eta(x) dx dt.$$

Also, by (141), for  $0 < \varepsilon < 1$  we have

$$\text{supp } R_\varepsilon(\cdot, t) \subset K_* + \bar{B}_1 \quad \text{for every } t \in [0, T_0].$$

Hence, using (142) and  $\xi \in L^1_{\text{loc}}$ , we obtain

$$\left| \int_0^{T_0} \int_{\mathbb{R}^3} \xi(x, t) R_\varepsilon(x, t) dx dt \right| \leq \|R_\varepsilon\|_{L^\infty((0, T_0) \times \mathbb{R}^3)} \int_0^{T_0} \int_{K_* + \bar{B}_1} |\xi(x, t)| dx dt \rightarrow 0.$$

Finally, since  $\Phi(\cdot, 0)$  is compactly supported and Hölder continuous,  $\Phi_\varepsilon(\cdot, 0) \rightarrow \Phi(\cdot, 0)$  uniformly, hence

$$\begin{aligned} \int_{\mathbb{R}^3} \xi_0(x) \Phi_\varepsilon(x, 0) dx &\longrightarrow \int_{\mathbb{R}^3} \xi_0(a) \Phi(a, 0) da \\ &= \int_{\mathbb{R}^3} \xi_0(a) \int_0^{T_0} \chi(\tau) \eta(Y_\tau(a)) d\tau da \\ &= \int_0^{T_0} \chi(\tau) \int_{\mathbb{R}^3} \xi_0(a) \eta(Y_\tau(a)) da d\tau = \int_0^{T_0} \chi(\tau) \int_{\mathbb{R}^3} \tilde{\xi}(x, \tau) \eta(x) dx d\tau, \end{aligned}$$

where in the last step we used the change of variables  $x = Y_\tau(a)$  and the measure-preserving property of  $Y_\tau$ .

Passing to the limit  $\varepsilon \rightarrow 0$  in (143), we obtain

$$\int_0^{T_0} \int_{\mathbb{R}^3} \xi(x, t) \chi(t) \eta(x) dx dt = \int_0^{T_0} \int_{\mathbb{R}^3} \tilde{\xi}(x, t) \chi(t) \eta(x) dx dt.$$

Since  $\chi \in C_c^\infty(0, T_0)$  and  $\eta \in C_c^\infty(\mathbb{R}^3)$  are arbitrary, it follows that

$$\xi = \tilde{\xi} \quad \text{in } \mathcal{D}'((0, T_0) \times \mathbb{R}^3),$$

hence a.e. on  $(0, T_0) \times \mathbb{R}^3$  because both functions are locally integrable. This proves

$$\xi(x, t) = \xi_0(Y_t^{-1}(x)) \quad \text{for a.e. } (x, t) \in \mathbb{R}^3 \times (0, T_0),$$

and completes the proof.  $\square$

## APPENDIX B. ODE MODELS

This appendix records the two auxiliary ODE analyses announced in § 1.8. We retain the notation introduced there and only recall the definitions needed below. These propositions are not used in the proof of the main theorems; they serve only as to explain motivations behind the localized model. This appendix provides rigorous justifications of the heuristic discussion in § 1.8.2 and § 1.8.3.

**B.1. Sharp Dichotomy for the Flattened-Coefficient ODEs.** We consider the flattened model (27) from § 1.8.2: for  $k \geq 2$  with  $x_k^{\text{flat}}(0) =: x_k^0 = \frac{\varepsilon}{k^\alpha}$ .

**Proposition B.1.** *Fix  $0 < \alpha < 1$  and  $0 < \varepsilon \leq 1$ . Then the unique positive solution of (27) with  $x_k^{\text{flat}}(0) =: x_k^0 = \frac{\varepsilon}{k^\alpha}$  satisfies:*

- (1) *If  $\alpha < \frac{2}{7}$ , then for every fixed  $t > 0$ , it holds  $x_k^{\text{flat}}(t) \rightarrow \infty$  as  $k \rightarrow \infty$ .*
- (2) *If  $\alpha > \frac{2}{7}$ , then for every fixed  $t > 0$ , it holds  $x_k^{\text{flat}}(t) \rightarrow 0$  as  $k \rightarrow \infty$ .*

*At the borderline  $\alpha = \frac{2}{7}$ , the family  $\{x_k^{\text{flat}}(t)\}_{k \geq 1}$  stays uniformly bounded for each fixed  $t > 0$ .*

*Proof.* Since the system is triangular and the right-hand side in (27) depends only on the lower modes, one constructs the solution inductively in  $k$ . Moreover,  $x_k^{\text{flat}}(t)$  is positive and nondecreasing for every  $k$ .

Using the definition of  $\Gamma_j^{\text{flat}}$  together with  $\frac{d}{dt} \log x_k^{\text{flat}}(t) = S_{k-1}^{\text{flat}}(t)$ , it holds

$$(\Gamma_j^{\text{flat}})'(t) = -3\Gamma_j^{\text{flat}}(t)S_{j-1}^{\text{flat}}(t). \quad (144)$$

**Step 1: depletion identities.** Differentiating  $b_j^{\text{flat}}$  and using  $\frac{d}{dt} \log x_k^{\text{flat}}(t) = S_{k-1}^{\text{flat}}(t)$ , and (144), we obtain

$$(b_j^{\text{flat}})'(t) = -5b_j^{\text{flat}}(t)S_{j-1}^{\text{flat}}(t) \quad (j \geq 1). \quad (145)$$

Here,  $S_0^{\text{flat}} \equiv 0$ . Summing over  $1 \leq j \leq k$  gives the equation (28) of  $S_k^{\text{flat}}$ . We now use the elementary identity  $S_j^{\text{flat}} = S_{j-1}^{\text{flat}} + b_j^{\text{flat}}$ , which yields

$$(S_j^{\text{flat}})^2 - (S_{j-1}^{\text{flat}})^2 = 2b_j^{\text{flat}}S_{j-1}^{\text{flat}} + (b_j^{\text{flat}})^2.$$

Summing this relation over  $1 \leq j \leq k$ , we obtain

$$2 \sum_{j=1}^k b_j^{\text{flat}}(t) S_{j-1}^{\text{flat}}(t) = (S_k^{\text{flat}}(t))^2 - \sum_{j=1}^k (b_j^{\text{flat}}(t))^2.$$

Inserting this into the equation (28) of  $S_k^{\text{flat}}$ , we arrive at (29).

**Step 2: norm inflation when  $\alpha < \frac{2}{7}$ .** Since  $\sum_{j=1}^k (b_j^{\text{flat}})^2 \geq 0$ , (29) implies

$$(S_k^{\text{flat}})'(t) \geq -\frac{5}{2}(S_k^{\text{flat}}(t))^2.$$

By comparison with the scalar ODE  $U' = -\frac{5}{2}U^2$ , we obtain

$$S_k^{\text{flat}}(t) \geq \frac{1}{\frac{5}{2}t + \frac{1}{S_k^{\text{flat}}(0)}} \quad \text{for all } t \geq 0.$$

Integrating in time yields

$$\int_0^t S_k^{\text{flat}}(s) ds \geq \frac{2}{5} \log \left( 1 + \frac{5}{2} t S_k^{\text{flat}}(0) \right). \quad (146)$$

At time  $t = 0$  we have  $\Gamma_j^{\text{flat}}(0) = 1$ , hence  $b_j^{\text{flat}}(0) = x_j^0 = \frac{\varepsilon}{j^\alpha}$  and  $S_k^{\text{flat}}(0) = \varepsilon \sum_{j=1}^k \frac{1}{j^\alpha}$ . By the integral test, for  $k \geq 2$ ,

$$\frac{\varepsilon}{1-\alpha} (k^{1-\alpha} - 1) \leq S_k^{\text{flat}}(0) \leq \varepsilon + \frac{\varepsilon}{1-\alpha} (k^{1-\alpha} - 1) \leq C(\alpha) \varepsilon k^{1-\alpha}. \quad (147)$$

Using (27), (146), and the lower bound in (147), we get

$$\begin{aligned} x_k^{\text{flat}}(t) &= x_k^0 \exp\left(\int_0^t S_{k-1}^{\text{flat}}(s) ds\right) \\ &\geq \frac{\varepsilon}{k^\alpha} \left(1 + \frac{5}{2} t S_{k-1}^{\text{flat}}(0)\right)^{2/5} \geq C(\varepsilon, t, \alpha) k^{-\alpha} (k-1)^{\frac{2}{5}(1-\alpha)}. \end{aligned}$$

Therefore, if  $\frac{2}{5}(1-\alpha) > \alpha$ , equivalently  $\alpha < \frac{2}{7}$ , then  $x_k^{\text{flat}}(t) \rightarrow \infty$  as  $k \rightarrow \infty$  for every fixed  $t > 0$ .

**Step 3: decay when  $\alpha > \frac{2}{7}$ .** From (145) and  $S_{j-1}^{\text{flat}} \geq 0$ , we have  $(b_j^{\text{flat}})'(t) \leq 0$ . Hence  $0 < b_j^{\text{flat}}(t) \leq b_j^{\text{flat}}(0) = \frac{\varepsilon}{j^\alpha} \leq \varepsilon \leq 1$ . In particular,

$$\sum_{j=1}^k (b_j^{\text{flat}}(t))^2 \leq \sum_{j=1}^k b_j^{\text{flat}}(t) = S_k^{\text{flat}}(t).$$

Using this in (29), we obtain

$$(S_k^{\text{flat}})'(t) \leq -\frac{5}{2} \left( (S_k^{\text{flat}}(t))^2 - S_k^{\text{flat}}(t) \right).$$

Let  $U_k$  solve  $U_k'(t) = -\frac{5}{2}(U_k(t)^2 - U_k(t))$  with  $U_k(0) = S_k^{\text{flat}}(0)$ . By scalar comparison,

$$S_k^{\text{flat}}(t) \leq U_k(t) \quad \text{for all } t \geq 0.$$

The explicit solution is

$$U_k(t) = \frac{1}{1 - \left(1 - \frac{1}{S_k^{\text{flat}}(0)}\right) e^{-5t/2}},$$

and therefore

$$\int_0^t S_k^{\text{flat}}(s) ds \leq \int_0^t U_k(s) ds = \frac{2}{5} \log\left(1 + (e^{5t/2} - 1) S_k^{\text{flat}}(0)\right).$$

Using again (27) and (147), we conclude

$$\begin{aligned} x_k^{\text{flat}}(t) &= x_k^0 \exp\left(\int_0^t S_{k-1}^{\text{flat}}(s) ds\right) \\ &\leq \frac{\varepsilon}{k^\alpha} \left(1 + (e^{5t/2} - 1) S_{k-1}^{\text{flat}}(0)\right)^{2/5} \leq C(\varepsilon, t, \alpha) k^{-\alpha} (k-1)^{\frac{2}{5}(1-\alpha)}. \end{aligned} \quad (148)$$

Thus, if  $\alpha > \frac{2}{7}$ , then  $\frac{2}{5}(1-\alpha) - \alpha < 0$ , and therefore  $x_k^{\text{flat}}(t) \rightarrow 0$  as  $k \rightarrow \infty$  for every fixed  $t > 0$ .

At the borderline  $\alpha = \frac{2}{7}$ , the bound (148) show that  $x_k^{\text{flat}}(t)$  stays uniformly bounded in  $k$  for each fixed  $t > 0$ .  $\square$

**B.2. Frozen-Profile ODEs.** We now treat the frozen-profile model (25) from § 1.8.3. Recall that  $\Lambda_{\text{froz}} : (0, 1] \rightarrow (0, \infty)$  is the frozen Biot–Savart coefficient introduced there; in particular,  $\Lambda_{\text{froz}}$  is  $C^1$ , positive, and non-increasing. We consider the frozen model (25) with  $x_k^{\text{froz}}(0) =: x_k^0 = \frac{\varepsilon}{k^\alpha}$ ,  $k \geq 2$  and  $x_1^{\text{froz}}(t) \equiv x_1^0 = \varepsilon$ .

Recall the logarithmic-derivative correction  $Q_{\text{froz}}(\Gamma)$  defined in (33), and we denote its supremum by  $Q_* := \sup_{\Gamma \in (0,1]} Q_{\text{froz}}(\Gamma) \in [0, \infty]$ .

**Proposition B.2.** *Fix  $\varepsilon > 0$  and  $0 < \alpha < 1$ . Then the unique positive solution of (25) with  $x_k^{\text{froz}}(0) = \frac{\varepsilon}{k^\alpha}$ ,  $k \geq 2$  and  $x_1^{\text{froz}}(t) \equiv \varepsilon$  satisfies:*

- (1) *If  $\alpha < \frac{2}{7}$ , then for every fixed  $t > 0$ ,  $x_k^{\text{froz}}(t) \rightarrow \infty$  as  $k \rightarrow \infty$ .*

(2) Assume in addition that  $Q_* < 5$ . Then, for every fixed  $t > 0$ ,

$$x_k^{\text{froz}}(t) \leq \frac{C(\varepsilon, t, \alpha, Q_*, \Lambda_{\text{froz}}(1))}{k^\alpha} (k-1)^{\frac{2}{5-Q_*}(1-\alpha)}. \quad (149)$$

In particular, if  $\alpha > \frac{2}{7-Q_*}$ , then  $x_k^{\text{froz}}(t) \rightarrow 0$  as  $k \rightarrow \infty$ .

**Remark B.1** (How the profile geometry enters the decay threshold). *The quantity  $Q_*$  depends only on the frozen coefficient  $\Lambda_{\text{froz}}$ , hence only on the frozen profile geometry from § 1.8.3. In the localized regime discussed there, the logarithmic-derivative bounds for  $\Lambda_{\text{froz}}$  show that  $Q_*$  can be made arbitrarily small by choosing the frozen profile support inside a cone of sufficiently small slope. Indeed, arguing in a similar way as in the proof of Lemma 3.4, one can obtain*

$$Q_{\text{froz}}(\Gamma) \leq 15 \frac{(\Gamma L_+)^2}{1 + (\Gamma L_+)^2} \leq 15 \frac{L_+^2}{1 + L_+^2}, \quad L_+ := \sup_{(r,z) \in \text{supp } \phi} \frac{|z|}{r}.$$

Thus, for any fixed  $\alpha > \frac{2}{7}$ , one can choose the frozen profile geometry so that  $\alpha > \frac{2}{7-Q_*}$  and therefore the decay conclusion in part (2) applies.

*Proof.* As in the flattened case, the system is triangular and therefore has a unique global positive solution.

Define  $S_0^{\text{froz}}(t) := 0$ . Using the definition of  $S_k^{\text{froz}}$ , the frozen model equation (25) becomes  $\frac{d}{dt} \log x_k^{\text{froz}}(t) = S_{k-1}^{\text{froz}}(t)$  for  $k \geq 2$ . Also,  $(\Gamma_j^{\text{froz}})'(t) = -3 \Gamma_j^{\text{froz}}(t) S_{j-1}^{\text{froz}}(t)$ . Differentiating  $b_j^{\text{froz}}$  yields (33) for  $j \geq 1$ . (The case  $j = 1$  is harmless because  $S_0^{\text{froz}} \equiv 0$ .) As before,

$$\sum_{j=1}^k b_j^{\text{froz}}(t) S_{j-1}^{\text{froz}}(t) = \frac{1}{2} \left( (S_k^{\text{froz}}(t))^2 - \sum_{j=1}^k (b_j^{\text{froz}}(t))^2 \right). \quad (150)$$

**Step 1: norm inflation when  $\alpha < \frac{2}{7}$ .** Since  $Q_{\text{froz}}(\Gamma) \geq 0$ , from (33) we get

$$(b_j^{\text{froz}})'(t) \geq -5 b_j^{\text{froz}}(t) S_{j-1}^{\text{froz}}(t).$$

Summing over  $1 \leq j \leq k$  and using (150), we obtain

$$(S_k^{\text{froz}})'(t) \geq -\frac{5}{2} \left( (S_k^{\text{froz}}(t))^2 - \sum_{j=1}^k (b_j^{\text{froz}}(t))^2 \right) \geq -\frac{5}{2} (S_k^{\text{froz}}(t))^2.$$

The rest of Step 1 proceeds in the same way as in Step 2 of Proposition B.1 for the flat model. Therefore, exactly as in the proof of Proposition B.1,

$$\int_0^t S_k^{\text{froz}}(s) ds \geq \frac{2}{5} \log \left( 1 + \frac{5}{2} t S_k^{\text{froz}}(0) \right). \quad (151)$$

Since  $\Gamma_j^{\text{froz}}(0) = 1$ , it holds  $b_j^{\text{froz}}(0) = \Lambda_{\text{froz}}(1) x_j^0 = \Lambda_{\text{froz}}(1) \frac{\varepsilon}{j^\alpha}$ , and hence

$$S_k^{\text{froz}}(0) = \Lambda_{\text{froz}}(1) \varepsilon \sum_{j=1}^k \frac{1}{j^\alpha} \geq C(\Lambda_{\text{froz}}(1), \varepsilon, \alpha) k^{1-\alpha}.$$

Using  $\frac{d}{dt} \log x_k^{\text{froz}}(t) = S_{k-1}^{\text{froz}}(t)$  and (151), we obtain

$$x_k^{\text{froz}}(t) \geq C(\Lambda_{\text{froz}}(1), \varepsilon, t, \alpha) k^{-\alpha} (k-1)^{\frac{2}{5}(1-\alpha)}.$$

Thus, if  $\alpha < \frac{2}{7}$ , then  $x_k^{\text{froz}}(t) \rightarrow \infty$  as  $k \rightarrow \infty$  for every fixed  $t > 0$ .

**Step 2: decay when  $\alpha > \frac{2}{7-Q_*}$ .** Assume now that  $Q_* < 5$ . Then (33) gives

$$(b_j^{\text{froz}})'(t) \leq -(5 - Q_*) b_j^{\text{froz}}(t) S_{j-1}^{\text{froz}}(t) \leq 0. \quad (152)$$

Therefore,

$$0 \leq b_j^{\text{froz}}(t) \leq b_j^{\text{froz}}(0) = \Lambda_{\text{froz}}(1) \frac{\varepsilon}{j^\alpha} \leq \Lambda_{\text{froz}}(1) \varepsilon =: \Lambda^*$$

In particular,

$$\sum_{j=1}^k (b_j^{\text{froz}}(t))^2 \leq \Lambda^* \sum_{j=1}^k b_j^{\text{froz}}(t) = \Lambda^* S_k^{\text{froz}}(t).$$

Using (152) and (150), we get

$$(S_k^{\text{froz}})'(t) \leq -\frac{5 - Q_*}{2} \left( (S_k^{\text{froz}}(t))^2 - \Lambda^* S_k^{\text{froz}}(t) \right).$$

Let  $U_k$  solve

$$U_k'(t) = -\frac{5 - Q_*}{2} (U_k(t)^2 - \Lambda^* U_k(t)), \quad U_k(0) = S_k^{\text{froz}}(0).$$

By scalar comparison,  $S_k^{\text{froz}}(t) \leq U_k(t)$  for all  $t \geq 0$ . The explicit formula for  $U_k$  is

$$U_k(t) = \frac{\Lambda^*}{1 - \left(1 - \frac{\Lambda^*}{S_k^{\text{froz}}(0)}\right) e^{-(5-Q_*)\Lambda^*t/2}},$$

and therefore

$$\int_0^t S_k^{\text{froz}}(s) ds \leq \frac{2}{5 - Q_*} \log \left( 1 + \frac{e^{(5-Q_*)\Lambda^*t/2} - 1}{\Lambda^*} S_k^{\text{froz}}(0) \right).$$

Using

$$S_{k-1}^{\text{froz}}(0) = \Lambda_{\text{froz}}(1) \varepsilon \sum_{j=1}^{k-1} j^{-\alpha} \leq C(\Lambda_{\text{froz}}(1), \varepsilon, \alpha) (k-1)^{1-\alpha},$$

together with  $\frac{d}{dt} \log x_k^{\text{froz}}(t) = S_{k-1}^{\text{froz}}(t)$ , we obtain

$$x_k^{\text{froz}}(t) = x_k^0 \exp \left( \int_0^t S_{k-1}^{\text{froz}}(s) ds \right) \leq \frac{\varepsilon}{k^\alpha} \left( 1 + \frac{e^{(5-Q_*)\Lambda^*t/2} - 1}{\Lambda^*} S_{k-1}^{\text{froz}}(0) \right)^{\frac{2}{5-Q_*}},$$

which yields (149). Finally, if  $\frac{2}{5-Q_*}(1-\alpha) < \alpha$ , or equivalently  $\alpha > \frac{2}{7-Q_*}$ , then the right-hand side of (149) tends to zero as  $k \rightarrow \infty$ .  $\square$

## APPENDIX C. LIST OF NOTATION

For the convenience of the reader, we collect here the main notation that recurs throughout the paper. This appendix is intended as a global lookup table for symbols used repeatedly in the statements and main proofs. Proof-local symbols and locally introduced constants are usually not listed here.

- **Biot–Savart law and sign convention.** We define vorticity by  $\text{curl } u = \omega$  in the general case and  $\text{curl } u = \omega e_\theta$  in the axisymmetric, no-swirl case. This determines the signs in the Biot–Savart law as indicated in (3) and (5), and we will use these definitions and the Biot–Savart laws with these signs. For the correct sign of the general Biot–Savart law, see [EGP18, the first page] and [Tsa18, Equation (1.44)].

On the other hand, if one defines vorticity with the minus sign, that is,  $\text{curl } u = -\omega$  in the general case and  $\text{curl } u = -\omega e_\theta$  in the axisymmetric, no-swirl case. Then it will lead to an extra minus sign in the Biot–Savart law. This convention is used for example in [KJ22, Equations (1.3), (1.5), (1.6)].

The displayed Biot–Savart formulas in [CMZ25, Equation (3)], [MB01, Equations (2.94), (2.95)], [BV22, Equation (1.53)], and [Dan07a, p. 477] use the cross-product order  $(x - y) \times \omega(y)$ . This is the negative of the convention used in the present paper. Consequently, those displayed Biot–Savart formulas correspond to the replacement  $\omega_{\text{ref}} = -\omega$  when compared with the present convention.

- **Outer-region notation for Proposition 2.1** (Section 2).
  - $Q(\rho) := \{y \in \mathbb{R}^3 : r_y \geq 2\rho\}$ : the outer region with radial cutoff  $\rho$  in Proposition 2.1.
- **Physical variables and coordinates.**
  - $u = u^r e_r + u^z e_z$ : the axisymmetric no-swirl velocity field.
  - $\text{curl } u = \omega(r, z, t) e_\theta$ : the vorticity vector where  $\omega$  denotes the scalar angular vorticity.
  - $\xi := \omega/r$ : the relative vorticity.
  - $(r, \theta, z)$ : cylindrical coordinates in  $\mathbb{R}^3$ .
  - $(r_x, \theta_x, z_x)$ : the cylindrical coordinates of a point  $x \in \mathbb{R}^3$ .
- **Parameter hierarchy and fixed background data.**
  - $\tilde{\varepsilon} > 0, q > 1$ : the fundamental parameters.
  - $L_q, \alpha_q, \phi_q, z_{0,q}$ : quantities fixed once  $q$  is fixed.
    - \*  $L_q = z_{0,q}/r_0$  is the cone-slope parameter.
    - \*  $\alpha_q$  is the logarithmic decay exponent.
    - \*  $\phi_q$  is the fixed reference profile.
    - \*  $z_{0,q}$  is the corresponding reference height.
  - $r_0, \eta, \mu, d$ : globally fixed geometric parameters. In the paper they are taken to be
 
$$r_0 = 1, \quad \eta = \frac{1}{4}, \quad \mu = \frac{1}{20}, \quad d = 10^{-2}.$$
  - $\varepsilon = \varepsilon(\tilde{\varepsilon}, q)$ : the amplitude parameter chosen after fixing  $(\tilde{\varepsilon}, q)$  and thereafter treated as fixed.
  - $k, m, A, t, T_N, T_B$ : running parameters.
  - $k$ : the ring index; smaller  $k$  corresponds to a larger, more outer ring.
  - $m$ : the total number of rings in the finite superposition.
- **Initial data and multiring decomposition** (mainly Section 3.1 and Section 4).
  - $\omega_0^{(m)} = \sum_{k=1}^m \omega_{0,k}$ : the finite-ring initial data; in the instantaneous blow-up argument one also uses the infinite sum  $\omega_0^{(\infty)} = \sum_{k=1}^{\infty} \omega_{0,k}$ .
  - $\omega^{(m)}$ : the smooth finite-ring solution generated by  $\omega_0^{(m)}$ .
  - $\omega_k$ : the evolved  $k$ -th vortex ring.
  - $u^{(m)}$ : the velocity induced by  $\omega^{(m)}$ .
  - $u_k$ : the velocity induced by  $\omega_k$ .
  - For a fixed  $k$ ,  $\omega_- := \sum_{j=1}^{k-1} \omega_j$  and  $u_- := \sum_{j=1}^{k-1} u_j$  denote the outer-ring contributions, while  $\omega_+ := \sum_{j=k+1}^m \omega_j$  and  $u_+ := \sum_{j=k+1}^m u_j$  denote the inner-ring contributions.
  - $\xi^{(m)} := \omega^{(m)}/r, \xi_0^{(m)} := \omega_0^{(m)}/r$ : relative-vorticity variables.
- **Rescaled ring variables and local flow maps** (Section 3.1).
  - $x_k(t)$ : the amplitude factor of the  $k$ -th ring.
  - $\tilde{x}_k(t) := x_k(t)/x_k(0)$ : the normalized amplitude.

- $R_k(t) = d^k \tilde{x}_k(t)$ : the radial scale of the  $k$ -th ring.
- $H_k(t) = d^k \tilde{x}_k(t)^{-2}$ : the vertical scale of the  $k$ -th ring.
- $W_k(r, z, t)$ : the rescaled profile of the  $k$ -th ring, defined through

$$\omega_k(r, z, t) = x_k(t) W_k \left( \frac{r}{R_k(t)}, \frac{z}{H_k(t)}, t \right).$$

- $V_k = (V_k^r, V_k^z)$ : the rescaled velocity field driving  $W_k$ .
- $X_k = (X_k^r, X_k^z)$ : the flow map associated with  $V_k$  on the support of  $\phi_q$ .
- **Bootstrap quantities** (Section 3.2 and § 3.5).
  - $A > 0$ : the target amplitude for norm inflation.
  - $\bar{A} := A/(1 - \mu)$ : the renormalized target amplitude.
  - $T_N(A, m)$ : the ODE norm-inflation time, i.e. the time at which some  $x_k$  reaches  $\bar{A}$ .
  - $F_m(t)$ : the bootstrap deviation functional measuring the relative distortion of  $X_k^r/r$  and  $X_k^z/z$  on  $\text{supp } \phi_q$ .
  - $T_B(A, m)$ : the maximal time on which the bootstrap bounds  $F_m(t) \leq \mu$  hold.
- **ODE/stretching cascade notation** (Section 3.4; see also § 1.8 and Appendix B).
  - *Superscript/subscript convention*.
    - \* Superscript orig denotes quantities belonging to the *original weak ODEs*, i.e. the PDE-driven cascade with the true coefficients  $\Lambda_j(t, \Gamma)$ .
    - \* Subscript froz means that the transported profile has been *frozen* against the fixed profile  $\phi_q$ , so  $\Lambda_j(t, \Gamma)$  is replaced by  $\Lambda_{\text{froz}}(\Gamma)$  while the amplitude and aspect-ratio variables remain those of the original cascade.
    - \* Superscript loc denotes the *localized model*, where  $\Lambda_{\text{froz}}(\Gamma)$  is replaced by the explicit localized coefficient  $\Lambda_{\text{loc}}(\Gamma)$ .
    - \* In the heuristic discussion and Appendix B, superscripts such as froz, flat, and str denote the stand-alone frozen-profile, flattened-coefficient, and strong no-self-slowdown model ODEs, respectively.
  - In Section 3.4 we temporarily write  $x_k^{\text{orig}}(t) := x_k(t)$  (and similarly for the derived ODE quantities) in order to distinguish the original cascade from its simplified models. After that section, the paper returns to the shorter notation  $x_k(t)$ .
  - $\Gamma_k^{\text{orig}}(t) := \frac{H_k(t)}{R_k(t)} = \left( \frac{x_k^{\text{orig}}(0)}{x_k^{\text{orig}}(t)} \right)^3$ : the aspect ratio of the  $k$ -th ring in the original weak ODEs.
  - $K_\Gamma(r, z) := \frac{r^2 z}{(r^2 + \Gamma^2 z^2)^{5/2}}$ : the rescaled Biot–Savart kernel appearing in the ODE coefficients.
  - $\Lambda_j(t, \Gamma) := \iint K_\Gamma(r, z) (-W_j(r, z, t)) dr dz$ : the *unfrozen* Biot–Savart coefficient coming from the true transported profile  $W_j$ .
  - $\Lambda_{\text{froz}}(\Gamma) := \iint K_\Gamma(r, z) (-\phi_q(r, z)) dr dz$ : the *frozen* Biot–Savart coefficient obtained by replacing  $W_j(\cdot, \cdot, t)$  with the fixed profile  $\phi_q$ .
  - $\Lambda_{\text{loc}}(\Gamma) := \frac{r_0^2 z_0, q}{(r_0^2 + \Gamma^2 z_0, q^2)^{5/2}}$ : the explicit localized coefficient obtained from the cone localization of  $\phi_q$ .

–

$$b_j^{\text{orig}}(t) := x_j^{\text{orig}}(t) \Gamma_j^{\text{orig}}(t)^2 \Lambda_j(t, \Gamma_j^{\text{orig}}(t)),$$

$$S_k^{\text{orig}}(t) := \sum_{j=1}^k b_j^{\text{orig}}(t), \quad B_j^{\text{orig}}(t) := \int_0^t b_j^{\text{orig}}(s) ds$$

: the true outer-ring contribution, its cumulative stretching rate, and its time integral.

$$b_{\text{froz},j}^{\text{orig}}(t) := x_j^{\text{orig}}(t) \Gamma_j^{\text{orig}}(t)^2 \Lambda_{\text{froz}}(\Gamma_j^{\text{orig}}(t)) = x_j^{\text{orig}}(0) \Gamma_j^{\text{orig}}(t)^{5/3} \Lambda_{\text{froz}}(\Gamma_j^{\text{orig}}(t)),$$

$$S_{\text{froz},k}^{\text{orig}}(t) := \sum_{j=1}^k b_{\text{froz},j}^{\text{orig}}(t)$$

: the frozen-coefficient comparison quantities associated with the original cascade.

$$b_j^{\text{loc}}(t) := x_j^{\text{loc}}(t) \Gamma_j^{\text{loc}}(t)^2 \Lambda_{\text{loc}}(\Gamma_j^{\text{loc}}(t)),$$

$$S_k^{\text{loc}}(t) := \sum_{j=1}^k b_j^{\text{loc}}(t), \quad B_j^{\text{loc}}(t) := \int_0^t b_j^{\text{loc}}(s) ds$$

: the localized-model outer contribution, cumulative stretching rate, and time integral.

- $\kappa_{\text{froz}}(\Gamma) := 5 + 3\Gamma \frac{\Lambda'_{\text{froz}}(\Gamma)}{\Lambda_{\text{froz}}(\Gamma)}$ : the coefficient governing the differential equation for  $b_{\text{froz},j}^{\text{orig}}$ .
- $c_\mu := \frac{(1-\mu)^3}{(1+\mu)^5}$ ,  $C_\mu := \frac{(1+\mu)^3}{(1-\mu)^5}$ : the bootstrap comparison constants between the true and frozen outer contributions.
- $\Theta_\mu := \frac{C_\mu}{c_\mu} = \left(\frac{1+\mu}{1-\mu}\right)^8$ : the comparison ratio appearing in the frozen/unfrozen bootstrap inequalities.
- $\Psi(\zeta) := \zeta^{5/3}(1+\zeta^2)^{-5/2}$ : the one-parameter Biot–Savart profile arising after localization.
- $L_{q,-} := \frac{1-\eta}{1+\eta}L_q$ , and  $L_{q,+} := \frac{1+\eta}{1-\eta}L_q$ : lower and upper cone-slope bounds coming from the support of  $\phi_q$ .
- $\zeta_k^{\text{orig}}(t) := L_q \Gamma_k^{\text{orig}}(t)$ , and  $\zeta_k^{\text{loc}}(t) := L_q \Gamma_k^{\text{loc}}(t)$ : the cone variables in the original and localized cascades.
- $\zeta_* := \frac{1}{\sqrt{2}}$ : the threshold where  $\Psi$  changes monotonicity.
- $\zeta_\eta := \frac{1+\eta}{1-\eta} \zeta_*$ : the fixed productive threshold used in the front-migration argument.
- $J_{\zeta_\eta}^{\text{orig}}(t) := \max \left\{ 1 \leq j \leq m-1 : \zeta_j^{\text{orig}}(t) \geq \zeta_\eta \right\}$ : the front index in the original cascade.
- $t_{\zeta_\eta}^{\text{orig}} := \inf \left\{ t > 0 : \zeta_m^{\text{orig}}(t) = \zeta_\eta \right\}$ : the threshold-hitting time of the last ring.

$$\gamma_q := \frac{3\Theta_\mu}{\log(L_q/\zeta_\eta)}, \quad \beta_q := \frac{1}{1+\gamma_q} - \alpha_q = \frac{\log(L_q/\zeta_\eta)}{3\Theta_\mu + \log(L_q/\zeta_\eta)} - \alpha_q.$$

Here  $\beta_q > 0$  is the exponent giving the algebraic decay  $T_B(A, m) \lesssim m^{-\beta_q}$ .

- **Global flow and radial-extremum notation** (Section 4.1 and Appendix A).
  - $Y(a, t)$ : the global Lagrangian flow map of the bounded log-Lipschitz velocity field  $u$  obtained under the contradiction hypothesis.
  - $Y_t^{-1} = Y^{-1}(\cdot, t)$ : the inverse map of  $Y_t := Y(\cdot, t)$ .
  - $R_K(t) := \max_{x \in K} Y^r(x, t)$  and  $r_K(t) := \min_{x \in K} Y^r(x, t)$  are the outer and inner radial envelopes of  $K$  under the flow for a compact set  $K \subset \mathbb{R}^3$ .

- $\mathcal{M}_K(t) := \operatorname{argmax}_{x \in K} Y^r(x, t)$  and  $\mathcal{A}_K(t) := \operatorname{argmin}_{x \in K} Y^r(x, t)$  : the maximizing and minimizing sets used in the Danskin-type lemma.
- **Finite-head contradiction notation** (Section 4.2).
  - $\omega_0^{(\infty)} = \sum_{k=1}^{\infty} \omega_{0,k}$ : the infinite-ring initial data.
  - $\omega^{(\infty)}, u^{(\infty)}$ : the infinite-ring solution and the velocity field induced by  $\omega^{(\infty)}$ .
  - An integer  $M \geq 2$  is the finite head cutoff used in the contradiction/bootstrapped argument.
  - $\omega^{(\leq M)} := \sum_{j=1}^M \omega_j$  and  $\omega^{(>M)} := \sum_{j=M+1}^{\infty} \omega_j$  : the head and tail parts of the vorticity. The same notation is used for the corresponding velocity decomposition  $u^{(\infty)} = u^{(\leq M)} + u^{(>M)}$ .
  - $V_{k,(\leq M)}$ : the rescaled velocity built only from the head part  $u^{(\leq M)}$ .
  - $K_M := \operatorname{supp} \omega_{0,M}$  : the initial support of the  $M$ -th ring.

$$K_{\text{tail}} := \overline{\bigcup_{j=M+1}^{\infty} \operatorname{supp} \omega_{0,j}}$$

- : the initial tail set.
- $r_{M,-}(t) := \min_{x \in K_M} Y^r(x, t)$  : the inner radial boundary of the  $M$ -th head ring.
- $R_{\text{tail}}(t) := \max_{x \in K_{\text{tail}}} Y^r(x, t)$  : the outer radial boundary of the tail.
- $\mathcal{A}_M(t) := \operatorname{argmin}_{x \in K_M} Y^r(x, t)$  and  $\mathcal{M}_{\text{tail}}(t) := \operatorname{argmax}_{x \in K_{\text{tail}}} Y^r(x, t)$  : the extremizing sets used in the head-tail separation argument.

This appendix complements the notation conventions from § 1.13; generic constants and suppressed dependences are governed there.

#### ACKNOWLEDGEMENTS

The authors are grateful to In-Jee Jeong for introducing us to the ill-posedness problem beyond Danchin’s regime, and to both In-Jee Jeong and Xiaoyutao Luo for stimulating discussions.

#### REFERENCES

- [AB15] Jonas Azzam and Jacob Bedrossian. Bounded mean oscillation and the uniqueness of active scalar equations. *Trans. Amer. Math. Soc.*, 367(5):3095–3118, 2015.
- [AHK10] Hammadi Abidi, Taoufik Hmidi, and Sahbi Keraani. On the global well-posedness for the axisymmetric Euler equations. *Math. Ann.*, 347(1):15–41, 2010.
- [BL15] Jean Bourgain and Dong Li. Strong ill-posedness of the incompressible Euler equation in borderline Sobolev spaces. *Invent. Math.*, 201(1):97–157, 2015.
- [BL21] Jean Bourgain and Dong Li. Strong ill-posedness of the 3D incompressible Euler equation in borderline spaces. *Int. Math. Res. Not. IMRN*, 2021(16):12155–12264, 2021.
- [BR95] Pierre Bernhard and Alain Rapaport. On a theorem of Danskin with an application to a theorem of von Neumann–Sion. *Nonlinear Anal.*, 24(8):1163–1181, 1995.
- [BV22] Jacob Bedrossian and Vlad Vicol. *The Mathematical Analysis of the Incompressible Euler and Navier–Stokes Equations: An Introduction*, volume 225 of *Graduate Studies in Mathematics*. American Mathematical Society, Providence, RI, 2022.
- [Che95] Jean-Yves Chemin. *Fluides parfaits incompressibles*. Number 230 in Astérisque. Société Mathématique de France, Paris, 1995.
- [CLM25] Diego Córdoba, Andrés Laín-Sanclemente, and Luis Martínez-Zoroa. Finite-time singularity via multi-layer degenerate pendula for the 2D Boussinesq equation with uniform  $C^{1, \sqrt{\frac{4}{3}}-1-\varepsilon} \cap L^2$  force. *Adv. Math.*, 480:110480, 2025.

- [CM23] Diego Córdoba and Luis Martínez-Zoroa. Blow-up for the incompressible 3D-Euler equations with uniform  $C^{1, \frac{1}{2}-\varepsilon} \cap L^2$  force. arXiv:2309.08495, 2023. To appear in Duke Math. J.
- [CMZ25] Diego Córdoba, Luis Martínez-Zoroa, and Fan Zheng. Finite time singularities to the 3D incompressible Euler equations for solutions in  $C^\infty(\mathbb{R}^3 \setminus \{0\}) \cap C^{1,\alpha} \cap L^2$ . *Ann. PDE*, 11:19, 2025.
- [Dan67] John M. Danskin. The directional derivative. In *The Theory of Max-Min and its Application to Weapons Allocation Problems*, volume 5 of *Ökonometrie und Unternehmensforschung / Econometrics and Operations Research*, chapter 3, pages 19–32. Springer-Verlag, Berlin, Heidelberg, 1967.
- [Dan07a] Raphaël Danchin. Axisymmetric incompressible flows with bounded vorticity. *Russ. Math. Surv.*, 62(3):475–496, 2007.
- [Dan07b] Raphaël Danchin. On perfect fluids with bounded vorticity. *C. R. Math. Acad. Sci. Paris*, 345(7):391–394, 2007.
- [EGP18] Alberto Enciso, M. Ángeles García-Ferrero, and Daniel Peralta-Salas. The Biot–Savart operator of a bounded domain. *J. Math. Pures Appl. (9)*, 119:85–113, 2018.
- [Elg21] Tarek M. Elgindi. Finite-time singularity formation for  $C^{1,\alpha}$  solutions to the incompressible Euler equations on  $\mathbb{R}^3$ . *Ann. of Math. (2)*, 194(3):647–727, 2021.
- [EM70] David Ebin and Jerrold Marsden. Groups of diffeomorphisms and the motion of an incompressible fluid. *Ann. of Math. (2)*, 92(2):102–163, 1970.
- [Gun27] N. Gunther. On the motion of fluid in a moving container. *Izv. Akad. Nauk SSSR Ser. Fiz.-Mat.*, 20:1323–1348, 1927.
- [Kat72] Tosio Kato. Nonstationary flows of viscous and ideal fluids in  $\mathbb{R}^3$ . *J. Funct. Anal.*, 9:296–305, 1972.
- [KJ22] Junha Kim and In-Jee Jeong. A simple ill-posedness proof for incompressible Euler equations in critical Sobolev spaces. *J. Funct. Anal.*, 283:109673, 2022.
- [Lic30] Leon Lichtenstein. Über einige Existenzprobleme der Hydrodynamik homogener, unzusammendrückbarer, reibungsloser Flüssigkeiten. *Math. Z.*, 32:608–725, 1930.
- [LJ25] Deokwoo Lim and In-Jee Jeong. On the optimal rate of vortex stretching for axisymmetric Euler flows without swirl. *Arch. Ration. Mech. Anal.*, 249:32, 2025.
- [MB01] Andrew J. Majda and Andrea L. Bertozzi. *Vorticity and incompressible flow*. Cambridge Texts in Applied Mathematics. Cambridge Univ. Press, 2001.
- [NS22] Camilla Nobili and Christian Seis. Renormalization and energy conservation for axisymmetric fluid flows. *Math. Ann.*, 382:1–36, 2022.
- [Ser95] Philippe Serfati. Solutions  $C^\infty$  en temps,  $n$ -D de l'équation d'Euler incompressible. *C. R. Acad. Sci. Paris Sér. I Math.*, 320(5):555–558, 1995.
- [Shk26] Steve Shkoller. Incompressible euler blowup at the  $C^{1, \frac{1}{3}}$  threshold. arXiv:2603.10945, 2026.
- [SR01] Laure Saint-Raymond. Blow-up of solutions to the incompressible Euler equations. *J. Math. Pures Appl. (9)*, 80(6):593–617, 2001.
- [SY94] Toshikazu Shirota and Takeshi Yanagisawa. Note on global existence for the two-dimensional nonhomogeneous incompressible Euler equations. *Proc. Japan Acad. Ser. A Math. Sci.*, 70(10):299–304, 1994.
- [Tsa18] Tai-Peng Tsai. *Lectures on Navier–Stokes Equations*, volume 192 of *Graduate Studies in Mathematics*. American Mathematical Society, Providence, RI, 2018.
- [Yud63] V. I. Yudovich. Non-stationary flows of an ideal incompressible fluid. *Zh. Vychisl. Mat. Mat. Fiz.*, 3:1032–1066, 1963.

INSTITUTE FOR THEORETICAL SCIENCES, WESTLAKE INSTITUTE FOR ADVANCED STUDY, WESTLAKE UNIVERSITY, 600 DUNYU ROAD, HANGZHOU, ZHEJIANG 310024, PEOPLE'S REPUBLIC OF CHINA

*Email address:* jhbang@westlake.edu.cn

INSTITUTE FOR THEORETICAL SCIENCES, WESTLAKE UNIVERSITY, 600 DUNYU ROAD, HANGZHOU, ZHEJIANG 310024, PEOPLE'S REPUBLIC OF CHINA

*Email address:* cheskidov@westlake.edu.cn